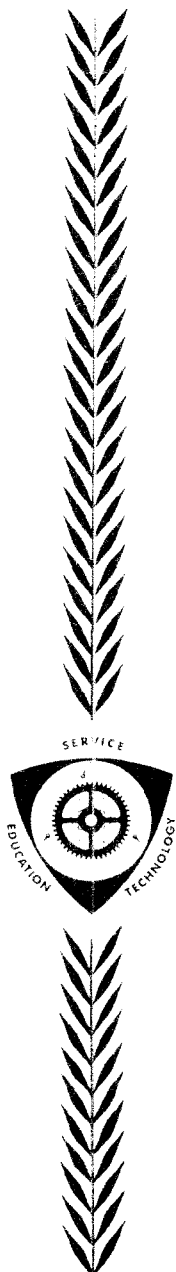


IN-1182
ENDF-116
May 1969

AN EVALUATION AND COMPILATION OF
NEPTUNIUM-237 CROSS SECTION DATA FOR
THE ENDF-B FILE



IDAHO NUCLEAR CORPORATION
NATIONAL REACTOR TESTING STATION
IDAHO FALLS, IDAHO

U. S. ATOMIC ENERGY COMMISSION

Printed in the United States of America
Available from
Clearinghouse for Federal Scientific and Technical Information
National Bureau of Standards, U. S. Department of Commerce
Springfield, Virginia 22151
Price: Printed Copy \$3.00; Microfiche \$0.65

LEGAL NOTICE

This report was prepared as an account of Government sponsored work. Neither the United States, nor the Commission, nor any person acting on behalf of the Commission:

A. Makes any warranty or representation, express or implied, with respect to the accuracy, completeness, or usefulness of the information contained in this report, or that the use of any information, apparatus, method, or process disclosed in this report may not infringe privately owned rights; or

B. Assumes any liabilities with respect to the use of, or for damages resulting from the use of any information, apparatus, method, or process disclosed in this report.

As used in the above, "person acting on behalf of the Commission" includes any employee or contractor of the Commission, or employee of such contractor, to the extent that such employee or contractor of the Commission, or employee of such contractor prepares, disseminates, or provides access to, any information pursuant to his employment or contract with the Commission, or his employment with such contractor.

IN-1182
ENDF-116
Issued: May 1969
Mathematics and Computers
TID-4500

AN EVALUATION AND COMPILATION OF
NEPTUNIUM-237 CROSS SECTION DATA FOR
THE ENDF/B FILE

J. R. Smith and K. A. Grimesey

IDAHO NUCLEAR CORPORATION

A JOINTLY OWNED SUBSIDIARY OF
AEROJET ALLIED
GENERAL CHEMICAL
CORPORATION CORPORATION



U. S. Atomic Energy Commission Research and Development Report
Issued Under Contract AT(10-1)-1230
Idaho Operations Office

ABSTRACT

This evaluation of ^{237}Np neutron cross-section data was undertaken as part of the effort by the Cross Sections Evaluation Working Group (CSEWG) to assemble the first version of the Evaluated Nuclear Data File B (ENDF/B). Graphs of calculated and experimental data from which the various files for this isotope were constructed are included along with complete documentation over the energy range from 0.00001 eV to 15 MeV.

CONTENTS

ABSTRACT.....	ii
A. INTRODUCTION.....	1
B. THERMAL REGION: BELOW 0.1 eV.....	2
C. RESOLVED RESONANCE REGION: 0.1 eV TO 36 eV.....	2
D. UNRESOLVED REGION: 36 eV TO 1200 eV.....	13
E. RESONANCE INTEGRAL.....	18
F. CONTINUUM REGION.....	22
G. FISSION CROSS SECTION.....	23
H. CAPTURE CROSS SECTION.....	24
I. ELASTIC SCATTERING CROSS SECTION.....	25
J. TOTAL CROSS SECTION.....	29
K. ELASTIC SCATTERING ANGULAR DISTRIBUTIONS.....	29
L. (n,n') INELASTIC SCATTERING CROSS SECTION.....	29
M. (n,2n) and (n,3n) CROSS SECTIONS.....	32
N. FISSION NEUTRON SPECTRUM.....	35
O. MEAN NUMBER OF NEUTRONS PER FISSION.....	36
P. FISSION PRODUCT YIELDS.....	37
Q. REFERENCES.....	38
APPENDIX A -- CROSS SECTION PLOTS.....	41

FIGURES

1. ^{237}Np total cross section in resolved range.....	3
2. Capture and fission cross sections in the unresolved range....	14
3. Total and elastic potential cross sections in the unresolved range.....	15
4. Fission and capture cross sections in the continuum region above 10 keV.....	27

5. Fission cross section above 1.0 MeV.....	28
6. (n,n') inelastic scattering cross sections.....	31
7. Temperature distributions for (n,n'), (n,2n), and (n,3n) inelastic secondaries.....	33

TABLES

I. Resolved Resonance Parameters.....	5
II. Average Parameters For The Unresolved Resonance Region.....	17
III. Measured And Calculated Resonance Integrals For ^{237}Np	21
IV. First Eleven Levels And Spin And Parity Of Levels For ^{237}Np	30
V. Measurements Of $\bar{\nu}$ For ^{237}Np	36

A. INTRODUCTION

This evaluation of ^{237}Np neutron cross-section data was undertaken as part of the effort by the Cross-Sections Evaluation Working Group (CSEWG) to assemble the first version of the Evaluated Nuclear Data File B (ENDF/B). This report presumes a degree of familiarity with the ENDF/B format, which has been described in detail by Honeck^[1].

The objective of CSEWG was to produce this first version of ENDF/B in a limited time, with a minimum of re-evaluating. This first version is accordingly often referred to as a "zeroth iterate" of the file. Emphasis was placed on utilizing existing evaluations wherever possible. No complete evaluation of ^{237}Np data was found. Two partial evaluations existed, and these were used as the basis of the present file in their respective energy regions. They are:

1. Sol Pearlstein^[2] has fit the low-energy data for several heavy nuclei. He used the "recommended" parameters from BNL-325, Supp. 2, with potential scattering and additional $1/v$ terms adjusted to give a reasonable fit to the experimental data on file. These recommended parameters are principally those of Slaughter et al.^[3] at ORNL, with less weight given to the results of Cline^[4], Adamchuk^[5], and Smith et al.^[6] The experimental points fitted were those of Smith et al. from .02 eV to 1.0 eV, and Slaughter et al. from 0.2 eV to about 36 eV. The fission fit was to the data of Leonard^[7]. The Pearlstein fit is the basis of the ENDF/B file below 36 eV.
2. D. T. Goldman^[8] estimated the capture elastic and inelastic scattering cross sections for ^{237}Np in the region 1200 eV to 10 MeV. The resonance parameters of Slaughter et al.^[3] formed the principal point of departure for these calculations. Goldman relied mainly on theoretical calculations using Hauser-Feshbach^[9] statistical theory and optical model parameters, suitably modified to include spin-orbit interactions, to extend the reaction cross sections above the energy region where detailed measurements had been made.

B. THERMAL REGION: BELOW 0.1 eV

The low-energy limit of the resolved resonance range was chosen as 0.1 eV. Below this energy the available evidence indicates that the absorption cross section is essentially $1/v$. The evidence in this case consists of the crystal spectrometer total cross section data of Smith et al.^[6], the low-energy tail of the Pearlstein fit^[2], and several measurements of the absorption cross section in reactor spectra. The data of Smith et al. are the only energy-dependent data available below 0.1 eV, and they extend only to 0.02 eV. These data show no departure from a $1/v$ dependence below 0.1 eV, though admittedly a small deviation could be masked by limitations in the counting statistics and corrections for order effects in the Bragg beam. The tabulated ENDF/B absorption cross section file, therefore, represents a $1/v$ curve normalized to 169.0 barns at 0.0253 eV. Most of this absorption is due to neutron capture, with only 19 mb attributable to fission. Of the capture, approximately 21 barns can be accounted for by the resolved resonances, with the remaining 148 barns attributed to a $1/v$ contribution from unidentified resonances. Figure 1 shows the total cross-section measurements of Smith et al. and Slaughter et al., plus the fit by Pearlstein. The ENDF/B total cross section follows the Pearlstein fit.

The spin-independent potential scattering cross section was taken as 12.0 barns. Pearlstein^[2] assumed a 13.6 barn potential scattering cross section. The lower value was chosen to smooth the transition in total cross section at 1200 eV from the calculated values, using unresolved parameters from File 2, to the Adamchuk measurements^[5]. This small adjustment should cause no undue distress in the lower energy region, particularly since the true between-resonance cross sections are probably lower than the measured values.

C. RESOLVED RESONANCE REGION: 0.1 eV TO 36 eV

The initial evaluation of Neptunium-237 took place before the publication of the resolved resonance data of D. Paya et al.^[10] late in 1966. Consequently the resolved resonance range is based on the fit by S. Pearlstein^[2] using the "recommended" parameters in BNL-325, Supp. 2, which predate the Paya data. These parameters are principally the work

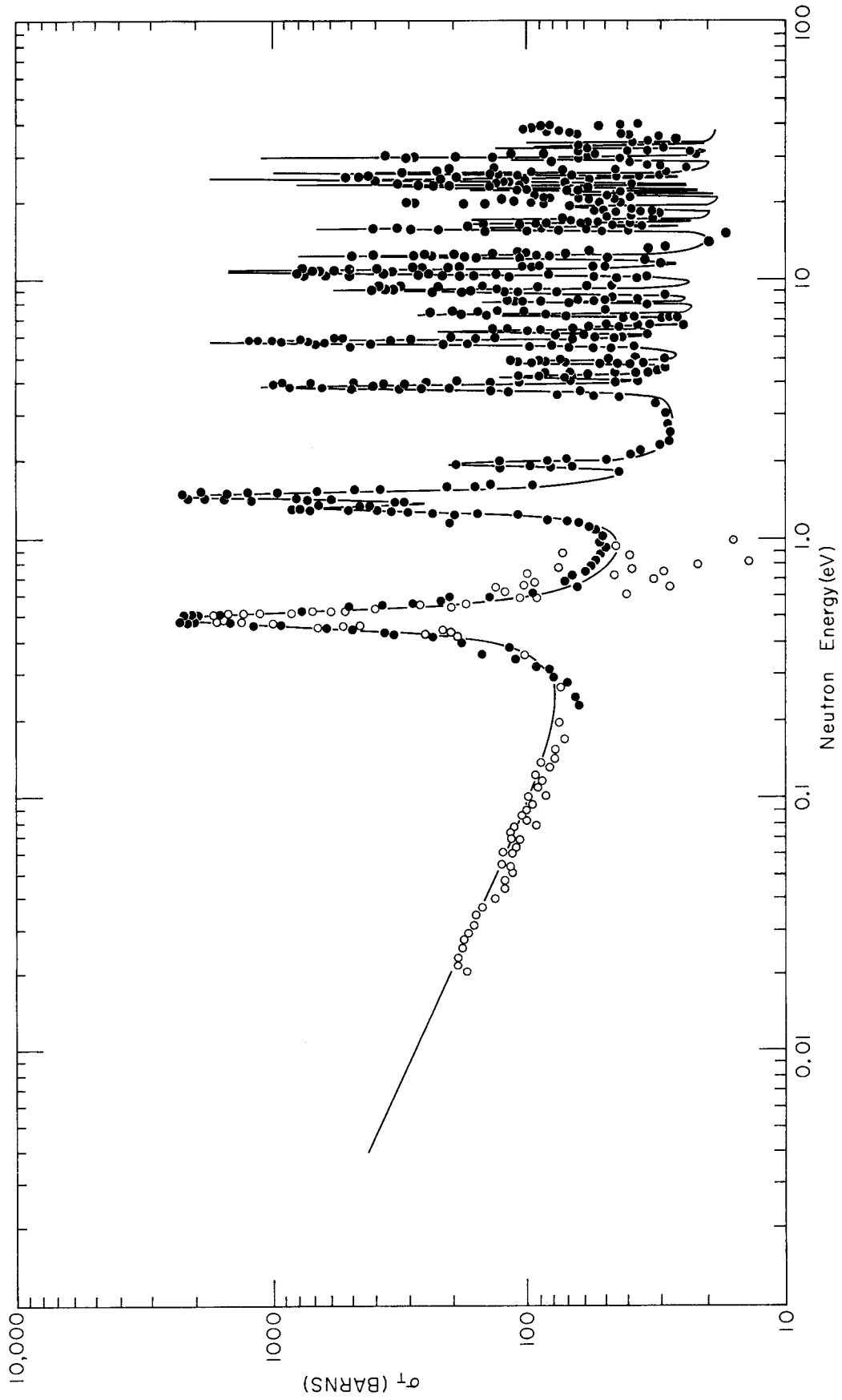


Figure 1. ^{237}Np Total Cross Section in Resolved Range

of Slaughter et al.^[3] at ORNL, with lesser weight given to the values of Cline^[4], Adamchuk^[5], and Smith et al.^[6] The fission widths were derived from Leonard's data^[7]. The "recommended" parameters from BNL-325, Supp. 2, are resolved to 36 eV and this energy was chosen as the upper cutoff of the resolved resonance region. Pearlstein's fit to these parameters for the total cross section to 36 eV is given in Figure 1. This fit is based on a potential scattering cross section of 13.6 barns. Since we recommend a 12.0 barn potential scattering cross section, the between resonance fit will be approximately 1.6 barns less than the values shown in Figure 1. No spin assignment has been made and consequently J has been set equal to I, the target nucleus spin, throughout the resolved resonance range and in the unresolved range for s wave neutrons only. Since the unresolved range ends at 1200 eV, very little, if any, contribution from p wave resonances is to be expected.

Table I contains the "recommended" resolved resonance parameters from BNL-325 along with the recent data of D. Paya et al.^[10] The most striking difference is that the Paya data show fully resolved resonances at substantially higher energy than do the older data. The generally superior resolution of the Paya data is further demonstrated by the observation of many weak levels. Enough fission widths have been determined to give a more realistic estimate of the average fission width than is afforded by the Leonard data^[7]. Radiation widths have been assigned to many levels, permitting a much better estimate of the average radiation width. The Paya parameters were not available when the ENDF/B file was first assembled. The shortage of time and the lack of pointwise data by which to compare the goodness of fit of the new parameters with the old prevented the Paya data from being fully incorporated in the resolved range on this zeroeth iterate of ENDF/B. It is anticipated that the next major re-evaluation of the ²³⁷Np file will fully incorporate the Paya data. This will permit the resolved resonance region to be extended to about 100 eV and the unresolved region to be extended to about 7 or 8 keV.

TABLE 1

RESOLVED RESONANCE PARAMETERS

A. BNL-325 Supp. 2 (ENDF/B)

B. Paya, et al.

E_0 (eV)		Γ (mV)		$2g \Gamma_n$ (mV)		Γ_γ (mV)		Γ_f (mV)	
A	B	A	B	A	B	A	B	A	B
0.489	0.489	34	34	.0325	0.0325	34		0.00075	0.00075
1.33	1.32		39.8	.031	0.0374	34		0.0027	0.0027
1.48	1.48		48.3	.125	0.145	34		0.0006	0.00075
1.97	1.97		41.2	.0150	0.0166				
3.89	3.86		41.6	0.24	0.244				0.0045
4.29	4.26		37.5	0.025	0.0264				
4.89	4.85		38.7	0.028	0.0345				
5.81	5.77		44.8	0.65	0.622				0.006
6.41	6.37		38.2	0.09	0.093				
6.73	6.67		47.9	0.013	0.012				
	7.18		35.4		0.0078				
7.46	7.42		39.9	0.131	0.146				
8.37	8.30		37.8	0.08	0.107				
9.02	8.97		38.5	0.11	0.121				
9.33	9.30		42.7	0.40	0.522				
	10.23		38.1		0.025				
	10.68		36.1		0.506				
10.84	10.84		45.4	1.3	0.88				

TABLE 1 (Cont'd)

RESOLVED RESONANCE PARAMETERS

A. BNL-325 Supp. 2 (ENDF/B)

B. Paya, et al.

E_0 (eV)		Γ (mV)		$2g \Gamma_n$ (mV)		Γ_γ (mV)		Γ_f (mV)	
A	B	A	B	A	B	A	B	A	B
11.10	11.09		43.9	1.3	0.885				
12.25	12.20		49.7	0.05	0.0624				
12.63	12.61		42.3	0.85	0.795				
	13.15				0.0197				
	15.83				0.102				
16.10	16.11		49.7	1.04	0.924				
16.88	16.88		34.6	0.25	0.243				
	17.02				0.006				
17.62	17.59		39.6	0.25	0.184				
	17.88				0.018				
	18.89				0.0366				
19.22	19.11			0.04	0.106				
19.89	19.92		35.9	0.11	0.075				
	20.39		41.7		1.13				
	21.09		35.4		0.516				
	21.35				0.0229				
22.04	22.01		41.6	0.127	1.26				
22.88	22.86		40.1	0.38	0.447				

TABLE 1 (Cont'd)

RESOLVED RESONANCE PARAMETERS

A. BNL-325 Supp. 2 (ENDF/B)

B. Paya, et al.

E_0 (eV)	Γ (mV)		$2g \Gamma_n$ (mV)		Γ_γ (mV)		Γ_f (mV)	
	A	B	A	B	A	B	A	B
23.71	23.67	41.7	2.1	1.69				
	23.97	61.0		0.171				
25.01	24.97	48.7	5.1	4.61			0.0058	
	26.17	40.1		0.239			0.066	
26.59	26.54	44.7	3.2	2.84			0.037	
	27.05			0.0247				
	28.48			0.146				
	28.92			0.11				
	29.46			0.086				
30.47	30.40	42.1	4.2	3.76			0.135	
30.73	30.72	53.5		0.327				
31.34	31.29	36.3	0.1	0.278				
	31.65			0.0478				
33.50	33.41	28.0	0.5	0.438				
34.05	33.90	66.0	0.34	0.458				
	34.67			0.184				
35.24	35.19	37.2	0.37	0.327				
	36.36	68.7		0.159				
	36.81			0.072				

TABLE 1 (Cont'd)

RESOLVED RESONANCE PARAMETERS

A. BNL-325 Supp. 2 (ENDF/B)

B. Paya, et al.

E_0 (eV)		Γ (mV)		$2g \Gamma_n$ (mV)		Γ_γ (mV)		Γ_f (mV)	
A	B	A	B	A	B	A	B	A	B
37.17	37.14		46.5	1.549	1.36				0.239
	37.86				0.064				
38.24	38.16		61.9	1.410	1.61				
39.07	38.92		57.5	1.625	1.24				0.600
39.37	39.22		47.3	.552	0.65				
	39.90		80.2		0.66				
41.41	41.34		40.0	2.252	2.26				6.35
	42.38				0.0907				0.380
	42.81				0.117				
	43.65				0.290				
	45.70		62.8		0.483				
	46.01				0.659				
46.43	46.34		46.8	2.453	3.07				
47.43	47.31		45.7	2.052	2.40				
	48.47				0.11				
	48.78				0.53				
49.90	49.80		46.4	4.380	5.09				
50.53	50.38		48.3	9.241	0.93				0.041

TABLE 1 (Cont'd)

RESOLVED RESONANCE PARAMETERS

A. BNL-325 Supp. 2 (ENDF/B)

B. Paya, et al.

E ₀ (eV)	Γ (mV)		2g Γ _n (mV)		Γ _γ (mV)		Γ _f (mV)	
	A	B	A	B	A	B	A	B
		51.89			0.091			
		52.19			0.373			
		52.62			0.703			
		53.03			0.062			
		53.86			0.387			
		54.20			0.131			
		55.01			0.317			
56.25		56.03	1.500	109.0	1.99			
		58.35			0.463			
		58.60			2.01			
59.60		59.48	1.081	45.0	2.70			
60.18		60.01	2.265	45.9	1.83			
61.13		60.92	0.985	40.6	0.523			
		61.61			2.10			
62.63		62.44	0.950	82.2	1.72			
63.01		62.89	0.984	47.2	0.276			
		63.92			0.276			
		64.94		44.7	1.01			

TABLE 1 (Cont'd.)

RESOLVED RESONANCE PARAMETERS
 A. BNL-325 Supp. 2 (ENDF/B)
 B. Paya, et al.

E_0 (eV)		Γ (mV)		$2g \Gamma_n$ (mV)		Γ_Y (mV)		Γ_f (mV)	
A	B	A	B	A	B	A	B	A	B
65.91	65.68		50.6	3.897	4.55				
	67.45		44.0		5.78				
67.72	67.93		46.0	9.710	2.93				
	68.74				0.359				
70.48	70.22		68.0	2.519	2.14				
	70.65				0.5				
	71.18				2.30				
71.50	71.44			4.904	2.68				
	73.85				0.31				
74.53	74.26			2.245	1.47				
	74.54				0.51				
	75.09				0.11				
	76.53				0.186				
	76.97				0.375				
78.62	78.33		78.8	1.773	2.45				
79.50	79.24		54.1	2.318	2.52				
	80.35				0.157				
	80.60				0.542				

TABLE 1 (Cont'd)

RESOLVED RESONANCE PARAMETERS

A. BNL-325 Supp. 2 (ENDF/B)

B. Paya, et al.

E_0 (eV)		Γ (mV)		$2g \Gamma_n$ (mV)		Γ_γ (mV)		Γ_f (mV)	
A	B	A	B	A	B	A	B	A	B
	81.59				0.42				
	82.09				0.818				
	83.39				3.11				
83.88	83.70			8.975	5.55				
	85.19		64.1		1.19				
	86.07				0.835				
86.73	86.50			7.450	5.72				
87.99	87.65		49.0	4.127	3.70				
	88.13				1.03				
	88.90				1.85				
89.73	89.43			5.873	4.29				
91.12	90.84			4.773	4.98				
	91.32				0.158				
	91.95				0.51				
	92.75				0.189				
93.52	93.36		48.8	1.934	1.8				
	94.22				0.368				
	95.37				0.358				

TABLE 1 (Cont'd)

RESOLVED RESONANCE PARAMETERS

A. BNL-325 Supp. 2 (ENDF/B)

B. Paya, et al.

E_0 (eV)		Γ (mV)		$2g \Gamma_n$ (mV)		Γ_γ (mV)		Γ_f (mV)	
A	B	A	B	A	B	A	B	A	B
	96.14				0.055				
	96.61				0.35				
97.99	97.72		65.3	1.980	3.48				
	98.46		77.4		2.38				
	98.99				0.1				
	99.49		51.7		1.94				
100.43	100.19		58.4	6.614	5.30				
101.36	101.03		62.5	6.041	5.41				
	101.62				1.23				
	101.92				1.67				
	102.15				0.30				
	103.94				1.60				
	104.68				0.34				
	105.37		79.7		2.18				
	105.89		44.4		3.29				
	107.21				0.51				

D. UNRESOLVED REGION: 36 eV TO 1200 eV

In the unresolved resonance region data are computed from average parameters deduced from parameters of resonances fully resolved at lower energy. Here again the appearance of the Paya data posed the problem as to whether or not to incorporate it in the file, which previously contained unresolved parameters deduced by Goldman from Slaughter's data. Since the unresolved parameters are few, the decision was to make the change. Consequently, the unresolved parameters in the ENDF/B file are those derived from the Paya data. A comparison of the alternative sets is shown in Table II.

The infinitely dilute capture cross section in the unresolved range from 36 eV to 1200 eV, calculated by the RAVEN code^[11] using Goldman's average parameters, exhibits approximately $1/v$ behavior as expected for s-wave neutrons and is plotted in Figure 2 as the dashed curve. The residual $1/v$ capture cross section from the thermal region of 147.0 barns at 0.0253 eV was added to the results of the unresolved calculation before it was plotted. The capture cross section below 10 keV resulting from Goldman's optical model calculation is also plotted in Figure 2. A 4.3 barn discontinuity with the unresolved results is evident at 1200 eV. If the 12 barn potential scattering cross section is added to the infinitely dilute calculation using Goldman's parameters throughout the unresolved region, the total cross section obtained is in excellent agreement with a presumed average of the Adamchuk measured data. The smooth curve through the Adamchuk measurements plotted in BNL-325, Supp. 2, is reproduced in Figure 3 and is essentially identical to the values obtained from Goldman's parameters and a 12 barn potential scattering cross section above 70 eV.

The infinitely dilute resonance calculation by RAVEN has taken proper account of Doppler broadening at room temperature and integrated averages of the fluctuation of the neutron width $\langle \Gamma_n^0 \rangle$ in the Porter Thomas distribution through the unresolved region.

Also plotted in Figure 2 and Figure 3 are the capture, fission and total cross sections between 36 eV and 1200 eV using average unresolved

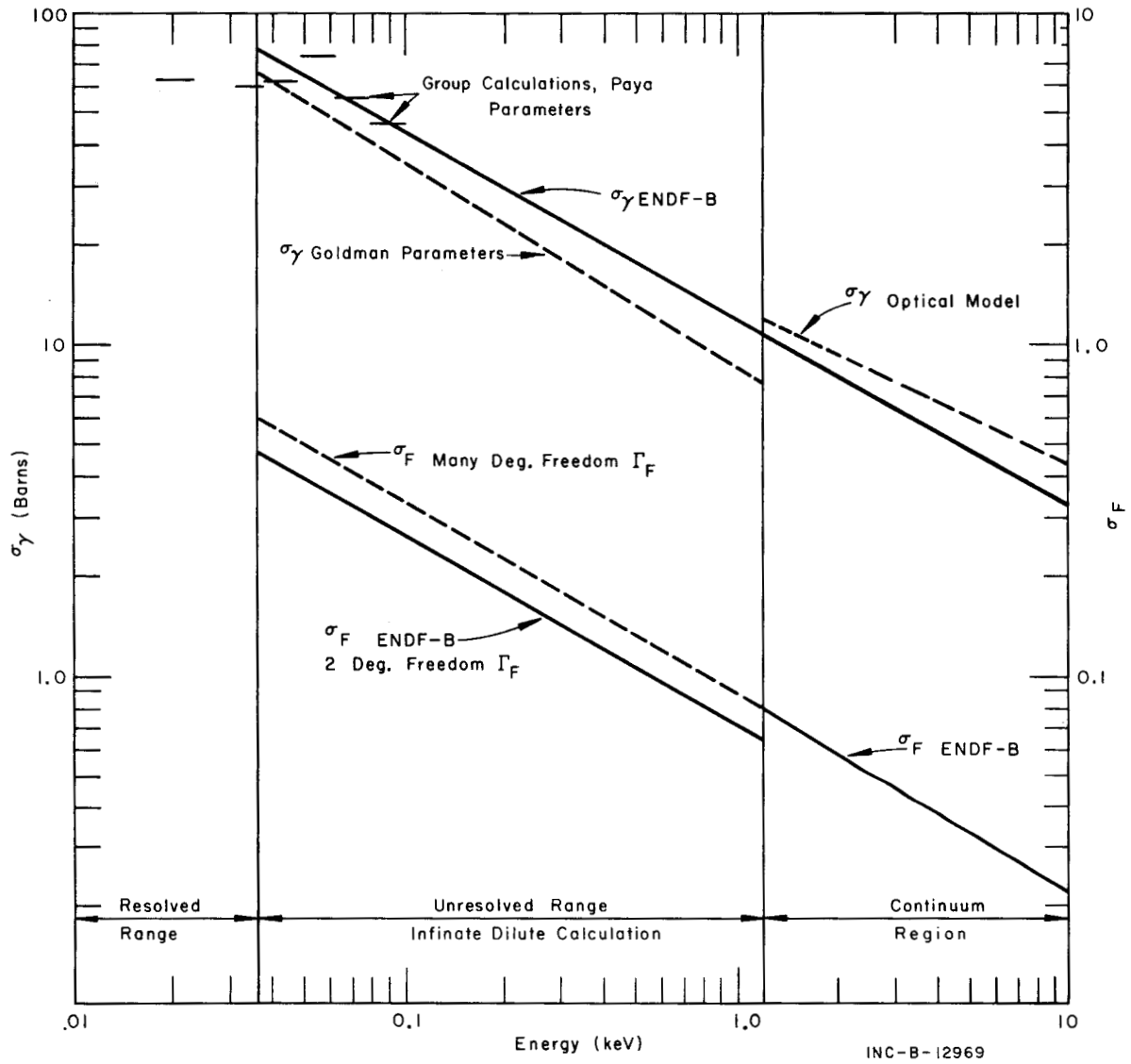


Figure 2. Capture and Fission Cross Sections in the Unresolved Range

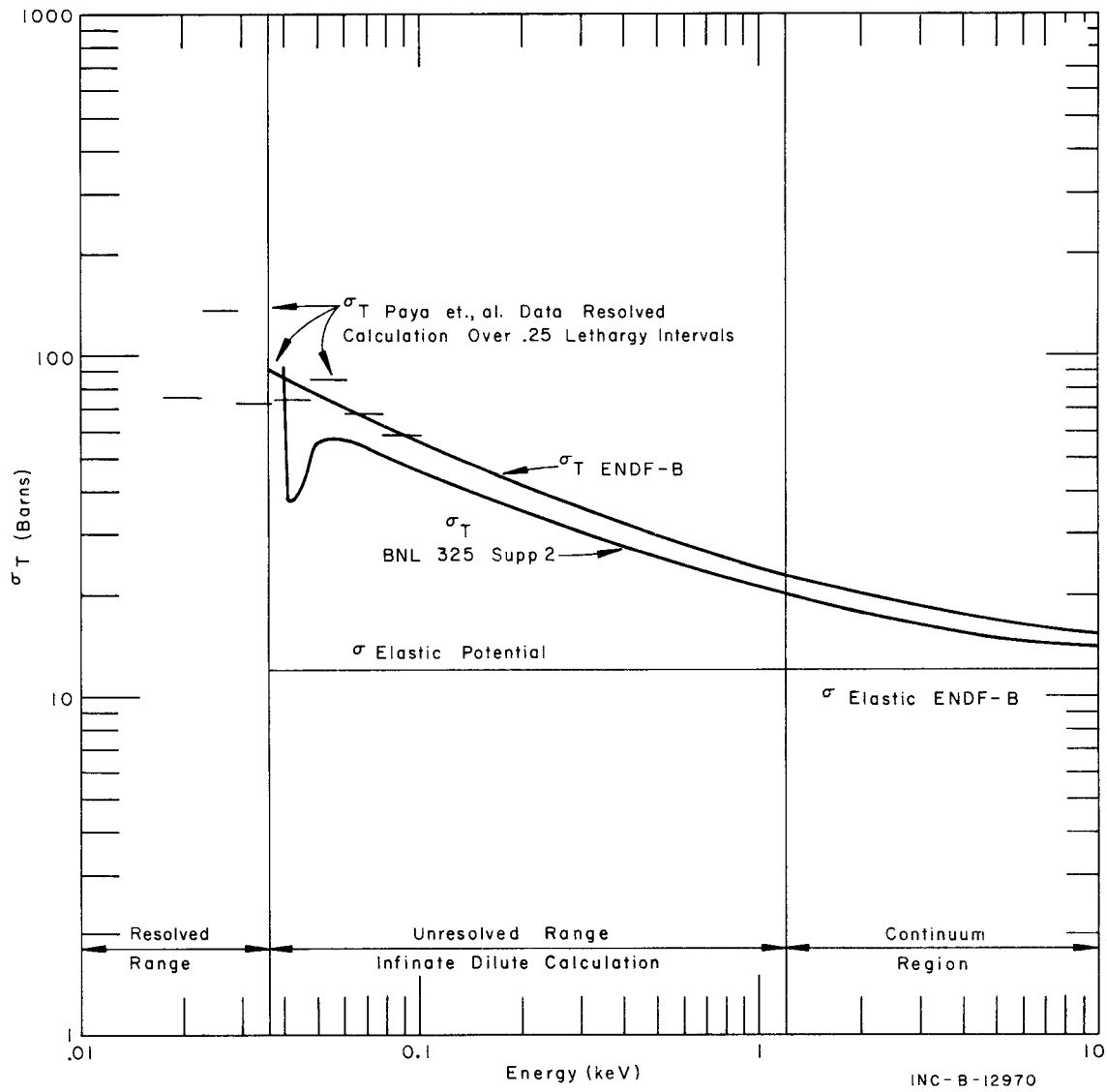


Figure 3. Total and Elastic Potential Cross Sections in the Unresolved Range

parameters based on the Paya data^[9]. As was done with the Goldman parameters, the residual $1/v$ cross section from the thermal region and a 12 barn potential scattering cross section were added to the unresolved capture cross section calculated from the Paya parameters to obtain the total cross section in Figure 3. The Paya data yield cross sections consistently higher than the Adamchuk data.

File 2 in the ENDF/B evaluation for the unresolved range contains parameters deduced from the Paya resolved parameters. From these parameters are calculated average cross sections which are shown in Figure 2 and Figure 3 and labeled ENDF/B. From 1200 eV to 10 keV, the capture and fission cross sections in File 3 are extrapolations of the Paya data in the unresolved range.

The Paya resolved resonance parameters extend into the present unresolved region to about 107 eV. To examine the low-energy fluctuation of the capture cross section in the unresolved range, an infinitely dilute resolved resonance calculation was made with the RAVEN code^[11], producing average capture cross sections over 0.25 lethargy intervals from 20 to 100 eV using the Paya resolved parameters and the residual $1/v$ capture cross section from the thermal region. The results of this calculation are plotted in Figures 2 and 3 for the capture and total cross sections, respectively. The fluctuation above 36 eV is minimal, indicating excellent agreement with the average parameters used for the whole unresolved range. The improved statistical sample that the Paya data represent as compared with the older data means that the unresolved resonance calculations can be extrapolated into the continuum region with greater confidence.

The Paya unresolved parameters are listed in Table II along with the unresolved parameters deduced by Goldman. The strength function $\langle \Gamma_n^0 \rangle / d$ is slightly larger for the Paya data but the average radiation width is 30 per cent larger. In the absence of spin assignments all resonances were considered to be of one spin state. As a result, the values $\langle d \rangle$ shown in Table II are approximately half the true spacing per spin state. Similarly, the values of $\frac{\langle \Gamma_n^0 \rangle}{\langle d \rangle}$ are approximately twice the true value $\left(\frac{\langle \Gamma_n^0 \rangle}{\langle d \rangle} \right)$ per spin state.

TABLE II

AVERAGE PARAMETERS FOR THE UNRESOLVED RESONANCE REGION

	$\langle d \rangle$ eV	$\langle \Gamma_n^0 \rangle$ mV	$\langle \Gamma_\gamma \rangle$ mV	$\langle \Gamma_F \rangle$ mV	$\langle \Gamma_n^0 \rangle / \langle d \rangle$
Paya et al.	0.76	0.166	44	0.37	0.22×10^{-3}
Goldman	1.36	0.266	34	----	0.196×10^{-3}

Three points should be discussed here which will tend to influence the interpretation of calculated cross sections in the unresolved range.

1. Multigroup cross sections in the resolved and unresolved resonance range are based on infinitely dilute integrals of the equations for the cross sections over a specified energy range. The specification of infinitely dilute integrals is not precise for the more sophisticated equations presently contained in multigroup spectrum codes. The value of the effective scattering cross section per absorber atom used in these calculations was 100,000 barns per atom. Deviations from this value by a factor of ten will produce infinitely dilute capture and fission cross sections which differ by a few per cent.
2. In the unresolved range, the average fission width for ^{237}Np of 0.37 mV was specified for two degrees of freedom in the fission width distribution in File 2. Some multigroup codes, e.g., RAVEN^[11], can not treat single level fission in the unresolved range for chi-squared distributions of n degrees of freedom. In these codes, fission is usually approximated by calculating the fission cross section within the framework of the capture cross section. This implies an infinite number of degrees of freedom in the chi-squared distribution for the fission width. In Figure 2, the curve for the fission cross section labeled Many Degrees Freedom Γ_F was based on an infinite number of degrees of freedom for the fission width distribution in the infinitely dilute calculation in the unresolved range. The curve labeled ENDF/B is for two degrees of freedom

in the fission width distribution. This calculation gives a cross section about 25 per cent lower throughout the unresolved range.

The fission cross section in the continuum region above 1200 eV is an extrapolation of the infinitely dilute cross section in the unresolved range calculated for an infinite number of degrees of freedom in the fission width distribution. Therefore, for two degrees of freedom, a discontinuity in the fission cross section of 0.015 barns will exist at 1200 eV. Since there are no experimental data between 1200 eV and 20 keV and the cross section is small in this range, we chose to ignore this discrepancy.

3. In the absence of any total cross section measurements in the MeV region, the elastic scattering cross section is only a rather gross estimate to begin with. In the unresolved range, we have set the elastic cross section equal to the potential scattering cross section of 12 barns. Some processing codes will automatically compute a compound elastic scattering contribution in the unresolved range based on the single level equations. This would presumably be added to the potential scattering cross section throughout the unresolved range. Compound elastic scattering contributions from the ^{237}Np unresolved parameters amount to from two to four barns in the unresolved range for this isotope. If a compound elastic contribution is calculated by the processing code, then a discontinuity in the elastic scattering cross section will occur at 1200 eV. A corresponding discontinuity will also exist for the total cross section if this occurs. Such a discrepancy is probably not important in this isotope for most reactor applications.

E. RESONANCE INTEGRAL

The ENDF/B format presently makes no provision for dealing with resonance integrals. The modern multi-group techniques which the file was designed to serve do not use the resonance integral in the calculation

of reaction rates. Still, the resonance integral does represent a useful concept for making rough comparisons of the relative absorption of nuclei in a slowing-down spectrum, and its measurement represents an important integral experiment against which to test the resonance parameters derived from cross-section measurements. Some discussion is therefore in order, even though for ^{237}Np this discussion could be willingly foregone. There continues to be a sharp discrepancy between the values of the resonance integral as measured in a reactor^[12,13,14,15] and the values calculated from resonance parameters^[3-6,8]. The situation is summarized in Table III, which lists the available measured and calculated values. The measured values are consistently higher than the calculated values. This unhappy situation has persisted despite the efforts of experimenters to perceive and eliminate systematic errors from their experiments. Rogers and Scoville^[15], for example, added a correction for the difference in neutron importance between 4.9 eV (the energy of the large resonance in their gold standard) and the 0.5 eV lower integral limit. Their quoted error of approximately 30 barns does not, however, include estimates of the errors involved in this correction. It may well be that the true errors in the measured and calculated resonance integrals would bridge the gap between the values if they could be properly assessed.

The calculations by the RAVEN code make use of the Chernick-Vernon equations and cross sections are calculated directly from the single level formula and suitably Doppler broadened with appropriate wing corrections applied. The unresolved resonance calculations apply Doppler broadening and also account for the statistical variation of the neutron width. The present ENDF-B parameters consign 506 barns as the contribution to the resonance integral from the resolved range above 0.5 eV, with 112 barns as the contribution from the unresolved region. The Paya resolved parameters increase the contribution to the resolved range by about 50 barns for a total of 664 barns. Thus the Paya resolved parameters will only increase the resonance integral a small fraction of the amount necessary to account for the present discrepancy between experimental and measured values.

The major difficulty with the ^{237}Np resonance integral is quite probably associated with the location of the first resonance, astride the cadmium cutoff function. This is far from the idealized case visualized when the idea of a resonance integral was conceived, and there is a question as to whether it is really proper to define a resonance integral for ^{237}Np in terms of a Cd cutoff. Measurement in a gadolinium or samarium cover might be more appropriate, even though resonance interference might be a greater problem than it is with cadmium covers.

In view of the pathological character of the ^{237}Np resonance integral, the apparent disagreement between the differential and integral experiments is not too surprising. We do not feel that the results of the resonance integral measurements challenge the validity of the resonance parameters in the ENDF file.

TABLE III

MEASURED AND CALCULATED RESONANCE INTEGRALS FOR ^{237}Np

<u>Reference</u>	<u>Measurement (barns)</u>	<u>Corrected Measurement To Infinitely Dilute</u>	<u>Calculated Value With Comments</u>
12	~800		(None)
13,14	870 ± 130	898 (c)	450,(a)(b)
15	863 ± 28	905	519,(a)(e)
8	- - - - -	---	774,(d)
Present ENDF/B Parameters		---	618,(f)
Paya Resolved Parameters, ENDF/B Unresolved Parameters		---	664,(g)

- (a) The contribution from the residual $1/v$ capture cross section of 148 barns at 0.0253 eV is not present here. The contribution this $1/v$ thermal component makes to the resonance integral between 0.5 eV and 10 keV is 66 barns.
- (b) No "wing correction" was added to the individual resolved resonance parameters. The lower energy cutoff was .132 eV instead of .5 eV.
- (c) Correction factor applied for equivalent infinitely dilute measurement using renormalization to a gold cross section of 1558 ± 40 barns.
- (d) (NR) infinite dilute resolved resonance calculation using MUFT parameters without Doppler broadening. A 0.5 eV thermal cutoff would greatly reduce this value.
- (e) BNL-325, Supp. 2, "recommended" resolved resonance parameters to 36.0 eV. Unresolved parameters from 36.0 eV to 10 keV were:
 $\langle d \rangle = 1.08$ eV, $\langle \Gamma_n^0 \rangle = 0.174$ mV, $\Gamma_\gamma = 34$ mV. The unresolved contribution was 87 barns. Calculations performed by the RAVEN code^[11].
- (f) Calculation performed by the RAVEN code^[11]. Thermal $1/v$ contribution of 66 barns included.
- (g) Paya resolved parameters to 74.4 eV, ENDF/B unresolved parameters to 1200 eV were used. Thermal $1/v$ contribution of 66 barns included.

F. CONTINUUM REGION

In the continuum region from 1200 eV to 15 MeV, the experimental data for ^{237}Np become even more sparse than in the lower energy ranges. Several experimenters have measured the fission cross section^[16-23], and Stupegia et al.^[24,25] have made measurements of the capture cross section at several energies. The only total cross section measurements reported in this region are those of Adamchuk et al.^[5] Other experimenters undoubtedly have collected data in this region in the process of measuring resonance parameters, but have not released it. This is probably due to a sample problem. The oxide samples generally used are of an optimum thickness for resonance measurements. Consequently, they are too thin for accurate determinations in low cross section regions. A more serious problem is that such oxide samples usually contain a moisture contaminant of undetermined amount. It is next to impossible to determine an accurate value for a low, unstructured cross section in the presence of a water contaminant of uncertain composition. It is suspected that Adamchuk's experiment was not completely free from these problems either. His data are, therefore, not necessarily accorded the pre-eminent status that otherwise might be owed to the sole set of published data.

The experimental data in this energy region were augmented by theoretical calculations by D. Goldman^[8], upon which the ENDF inelastic scattering cross sections are based, and by a calculation performed by S. Pearlstein of the $(n,2n)$ and $(n,3n)$ cross section using techniques he has previously described^[26].

Since the continuum region is represented in the ENDF/B file entirely by pointwise data, cross sections involved are given completely by this file. Appendix A contains computer plots of the individual cross sections which appear in the ENDF/B File 3. On the other hand, the cross sections given in File 3 for the resonance regions, both resolved and unresolved, are the smooth $1/v$ components only. For these regions the curves in Appendix A do not tell the complete story. The complete cross sections in this case are shown in Figures 1 through 3.

G. FISSION CROSS SECTION

The fission cross section of ^{237}Np features the characteristic shape of a threshold reaction near 1 MeV, but there is also an appreciable amount of subthreshold fission. Leonard^[7] found a fission cross section at 0.0253 eV of 19 mb, and also measured the fission widths of the first three resonances. Paya^[10] measured fission widths of many additional resonances and found measurable fission widths in some but not in others. Those resonances in which fission occurs seem to occur in groups. The average parameters derived from the Paya data and listed in Table II yield a cross section of 80 mb at 1200 eV. From there the cross section was extrapolated at constant logarithmic slope to tie into the experimental data.

The experimental data on fast neutron fission in ^{237}Np are the most abundant of all cross section data for this nucleus. Eight groups of experimenters have made measurements in the energy region 20 keV - 20 MeV. This plethora of data proves to be not an unmixed blessing. There is substantial disagreement among the various experimenters, first in the "threshold" region around 20 keV, but more strikingly in the region of the first plateau between 1 and 5 MeV. In the vicinity of 20 keV the results of Perkin^[19] and White^[20] lie somewhat lower than those of Gokhberg^[18]. Across the first plateau the data fall into essentially two groups, with the results of Klema^[16], Henkel^[17], and Gokhberg^[18] lying significantly lower than those of Schmitt and Murray^[21], Stein^[23], and Pankratov^[22]. In this evaluation greatest weight was given to the results of Perkin and White at low energies and to Schmitt and Murray and Stein et al. in the higher energy region. These experimenters took great care, using a variety of modern techniques, to ascertain the fission foil composition and chamber efficiency.

Figures 4 and 5 show the evaluated ENDF-B fission cross section curve threading its way amongst the experimental data points in the MeV region. The scale in Figure 4 is logarithmic, the better to illustrate the structure of the curve near threshold. Figure 5 is shown on a linear scale in order to display more clearly the results of the various measurements above 1 MeV. In the latter figure the data of

Schmitt-Murray^[21] and Stein et al.^[23] are shown normalized to different sets of evaluated data for ^{238}U and ^{235}U , respectively. The difference between points from the same experiment, normalized to different secondary standard data files, is as great as the discrepancy between the two experiments, particularly around 2.5 MeV. In the construction of the ENDF/B curve, slightly greater weight was given to the Stein data than to the Schmitt data because it was normalized to the fission cross section of ^{235}U rather than ^{238}U . Although there are disturbing disagreements between measurements for both these nuclides, the situation for ^{235}U seems somewhat less chaotic than that for ^{238}U . Thus, the present evaluation of MeV fission data for ^{237}Np leans rather heavily on evaluations of the ^{235}U fission cross section for the same energy range. Until this picture is clarified further, any evaluation of the ^{237}Np fission cross section will remain somewhat tenuous.

In summary, the ENDF/B fission cross section for ^{237}Np ties into the minimum at 30 keV in accordance with the Perkin and White points, favors the White data to 0.5 MeV, the Stein and Schmitt-Murray data across the first plateau from 1-5 MeV, and ends with the Pankratov data to the file limit at 15 MeV.

H. CAPTURE CROSS SECTION

The only MeV capture data available at the time the ENDF/B evaluations were started was the optical model calculation of D. Goldman^[8] which is plotted in Figure 4. The optical model calculation served to suggest the order of magnitude of the MeV capture cross section and exhibit the general trend.

The measurements of Stuepelia et al.^[24,25] represent the only experimental data on capture by ^{237}Np in the MeV region. As such, they formed the basis for the ENDF/B file in this region. The data are shown in Figure 4. On this log-log plot the points can be reasonably well fit with a straight line. This line has been used to extrapolate the Stuepelia data to 15 MeV to complete the capture file. The relationship is approximately

$$\sigma_c = 3.8 E^{-.65} (\text{MeV}) \quad (1)$$

This relationship seems to fit the data adequately and forms a reasonable extrapolation to the high energy end of the file. At the low energy end of the continuum region at 1200 eV, the capture cross section was normalized to 10.78 barns. This value resulted from the addition of a 10.1 barn contribution from the infinitely dilute unresolved resonance calculation at 1200 eV using the Paya parameters and a 0.68 barn contribution from the residual $1/v$ cross section extrapolated from the thermal region.

To connect the Stuepegia measurement at 0.152 MeV to the 1200 eV value, it is necessary for the curve to change slope in the interim region. The calculated curve of D. C. Stuepegia et al.^[25] shows such a change, and meets both the value indicated by Equation (1) at 0.15 MeV(13b) and an extension of the unresolved calculation to 10 keV. The Stuepegia calculations are based on the statistical model of the compound nucleus as described by Moldauer^[38-40]. It would be desirable to have additional experimental data to support the calculated curve below 0.15 MeV. Nevertheless the curve appears to give a reasonable interpolation between regions.

The extrapolation of the infinite dilute unresolved s-wave resonance calculation using the average Paya parameters in Table II gives a 10 keV value of 3.3 barns. This value was chosen as the 10 keV tie point to the Stuepegia calculations. Below 10 keV, the ENDF/B data represent an extrapolation of the infinitely dilute unresolved resonance calculation using the average Paya parameters in Table II.

I. ELASTIC SCATTERING CROSS SECTION

Between 0.1 and 36 eV, the elastic scattering cross section is determined wholly by the resonance parameters in File 2. The spin independent scattering length entered in File 2 is based on a 12.0 barn potential scattering cross section. No smooth scattering cross section appears in File 3 from 0.1 eV to 1200 eV. Depending on the reactor spectrum code which uses the unresolved data, the elastic scattering cross section in the unresolved range from 36 to 1200 eV will be 12 barns

unless approximate average compound elastic terms are accounted for by the nuclear code in the unresolved range. In this evaluation, the elastic scattering cross section was assumed to be 12.0 barns throughout the unresolved range.

No experimental data for elastic scattering exists for this isotope outside of that obtained from the resolved resonance parameters. However, there is no reason to expect that the high energy elastic scattering cross section for this isotope would exhibit properties appreciably different than any other fissionable isotope which possesses roughly the same non-elastic cross section to 15 MeV. In the keV region the 12 barn potential scattering cross section is expected to begin falling off as higher angular momentum neutrons begin to enter into the potential scattering process. At higher energies, compound elastic events will modify the general behavior depending upon the competition with other reaction cross sections.

The only measurement made which could influence the selection of an appropriate elastic cross section above 1200 eV is the total cross section measurements by Adamchuk et al.^[5] between 1200 eV and 10 keV. In the vicinity of 1200 eV, using capture and fission cross sections generated by the Paya et al.^[10] unresolved resonance parameters, a rough average of the Russian total cross section measurements would imply approximately 9 barns elastic scattering to 10 keV. Thus, if one accepts the Paya data and a 12 barn potential scattering cross section throughout the resonance region, a discontinuity of roughly 3 barns in the elastic cross section appears at 1200 eV. Pearlstein^[2] recommended a potential cross section in the resonance region of 13.6 barns for his fit. The 12 barn potential scattering cross section was selected for this evaluation as a compromise with the Russian total cross section data to 10 keV. Adding the capture and fission cross sections above 1200 eV to the 12 barn elastic scattering cross section, gives a total cross section to 10 keV which just skirts the upper bounds of Adamchuk's measurements and has been plotted in Figure 3.

Above 10 keV, the elastic cross section chosen in this evaluation as representative of the behavior expected for ^{237}Np was the elastic

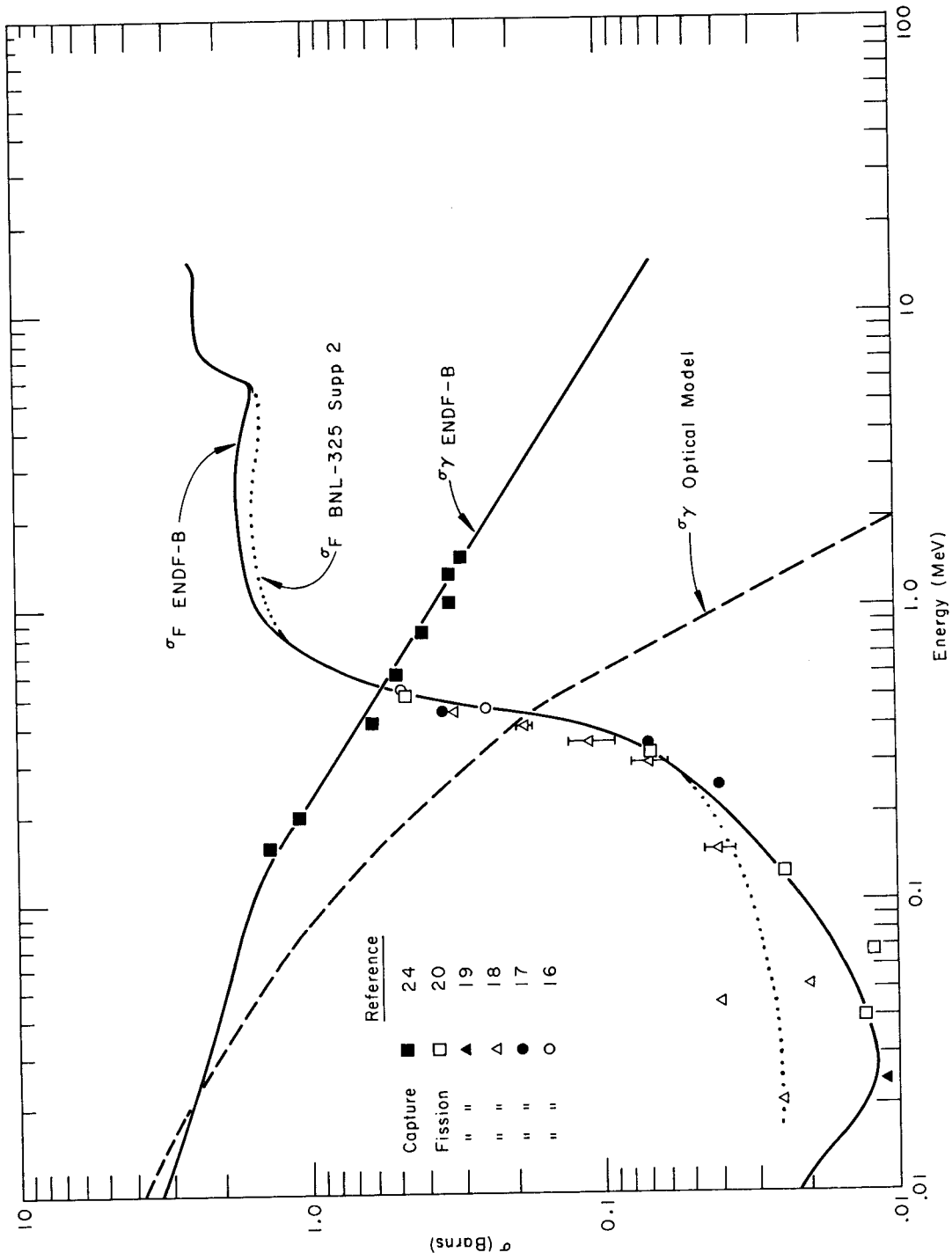
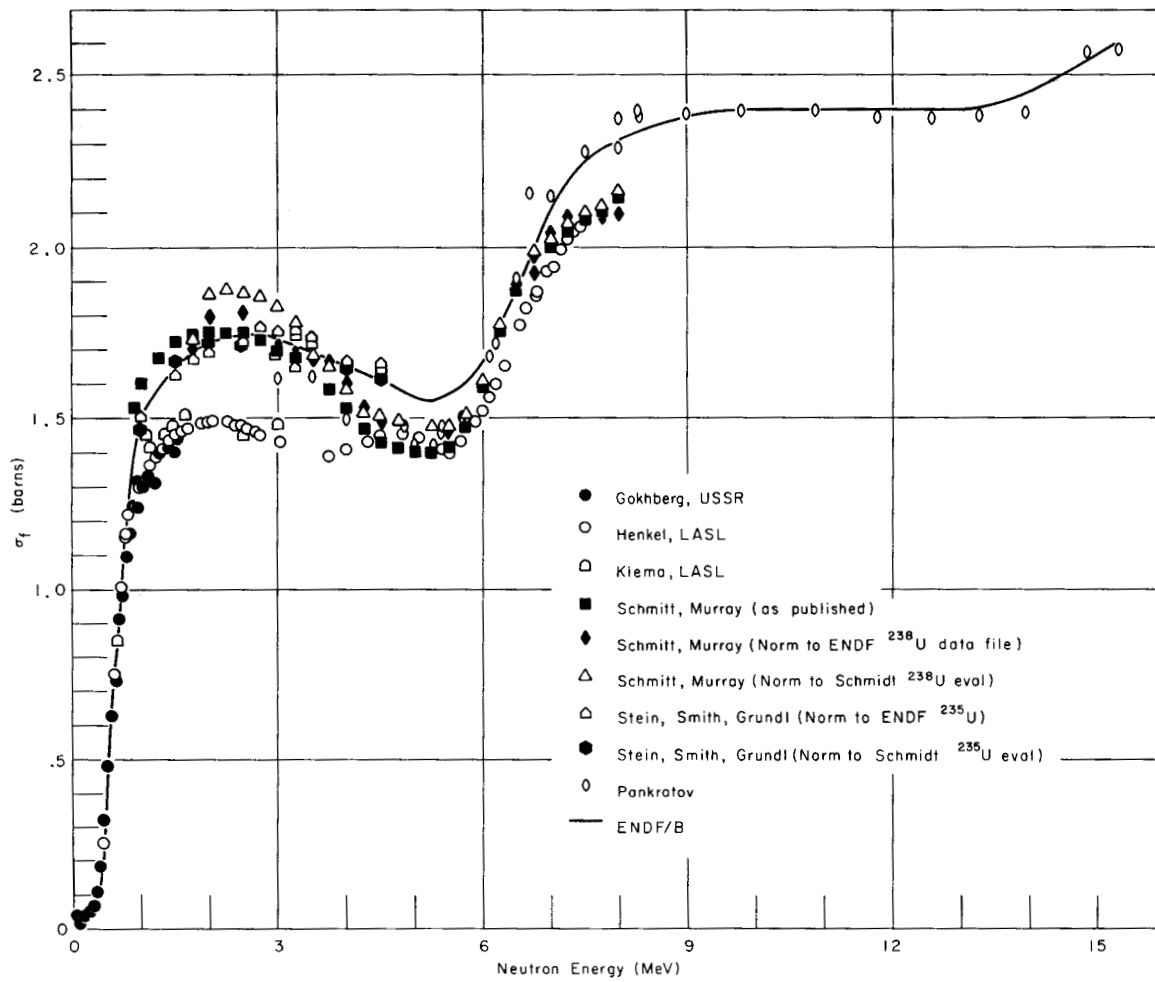


Figure 4. Fission and Capture Cross Sections in the Continuum Region Above 10 keV



INC-C-12965

Figure 5. Fission Cross Section Above 1.0 MeV

scattering cross section of ^{239}Pu according to the J. J. Schmidt evaluation^[27]. At 10 keV, the 12 barn potential scattering cross section joins smoothly to the ^{239}Pu elastic scattering cross section.

J. TOTAL CROSS SECTION

No total cross section measurements have been made for this isotope above 110 eV other than the total cross section measurements of Adamchuk to 10 keV discussed above. The total cross section contained in File 3 is the sum of the individual reaction cross sections and the elastic scattering cross section contained in this file. In the resonance region, the contribution due to the resolved and unresolved resonance parameters is not present in the plots presented in Appendix A.

K. ELASTIC SCATTERING ANGULAR DISTRIBUTIONS

File 4 contains the angular distributions recommended for this isotope in the form of a Legendre representation. No measured data exist at present for this isotope. The angular distributions in File 4 were assembled by H. Alter^[28] of Atomics International and are composed of a mixture of measured data for ^{235}U , ^{238}U , and ^{239}Pu .

L. (n,n') INELASTIC SCATTERING CROSS SECTION

Data on inelastic scattering used in this evaluation include both discrete level excitations and an evaporation spectrum continuum region. The cross sections were obtained from calculations by D. Goldman^[8]. Goldman does not present specific details of the calculation other than to state that the theoretical approach was based on a modification of the Hauser-Feshbach statistical model^[9] to include spin-orbit interactions. Excitation cross sections were calculated for the first eleven levels of ^{237}Np to 0.5 MeV. The level energies and spin and parity of these levels are given in Table IV.

TABLE IV
 FIRST ELEVEN LEVELS AND SPIN AND PARITY
 OF LEVELS FOR ^{237}Np

<u>Level Energy (MeV)</u>	<u>Spin and Parity</u>
0.0332	7/2 +
0.0596	5/2 -
0.076	9/2 +
0.103	7/2 -
0.159	9/2 -
0.224	11/2 -
0.268	3/2 -
0.305	13/2 -
0.332	1/2 +
0.369	5/2 +
0.371	3/2 +

Figure 6 contains plots of the total (n,n') cross section as calculated by Goldman to 10 MeV as well as the individual cross sections for excitation of the first eleven levels to 1.0 MeV. Goldman extrapolated the level cross sections linearly to 10 MeV to take rough account of direct interaction (n,n') events anticipated for isotopes of this mass. In this evaluation, we have chosen to ignore direct interaction effects in the MeV region and have extrapolated the level excitation cross sections from 0.5 to 1.0 MeV. The region between 0.5 and 1.0 MeV contains a combination of level excitations and evaporation spectra secondaries as illustrated in Figure 6. Above 1.0 MeV the secondary neutrons are assumed to follow a 100 per cent evaporation spectrum.

Above 0.33 MeV evaporation spectra secondaries begin to appear. The nuclear temperature $\theta(E)$ for the evaporation model was computed from [8]

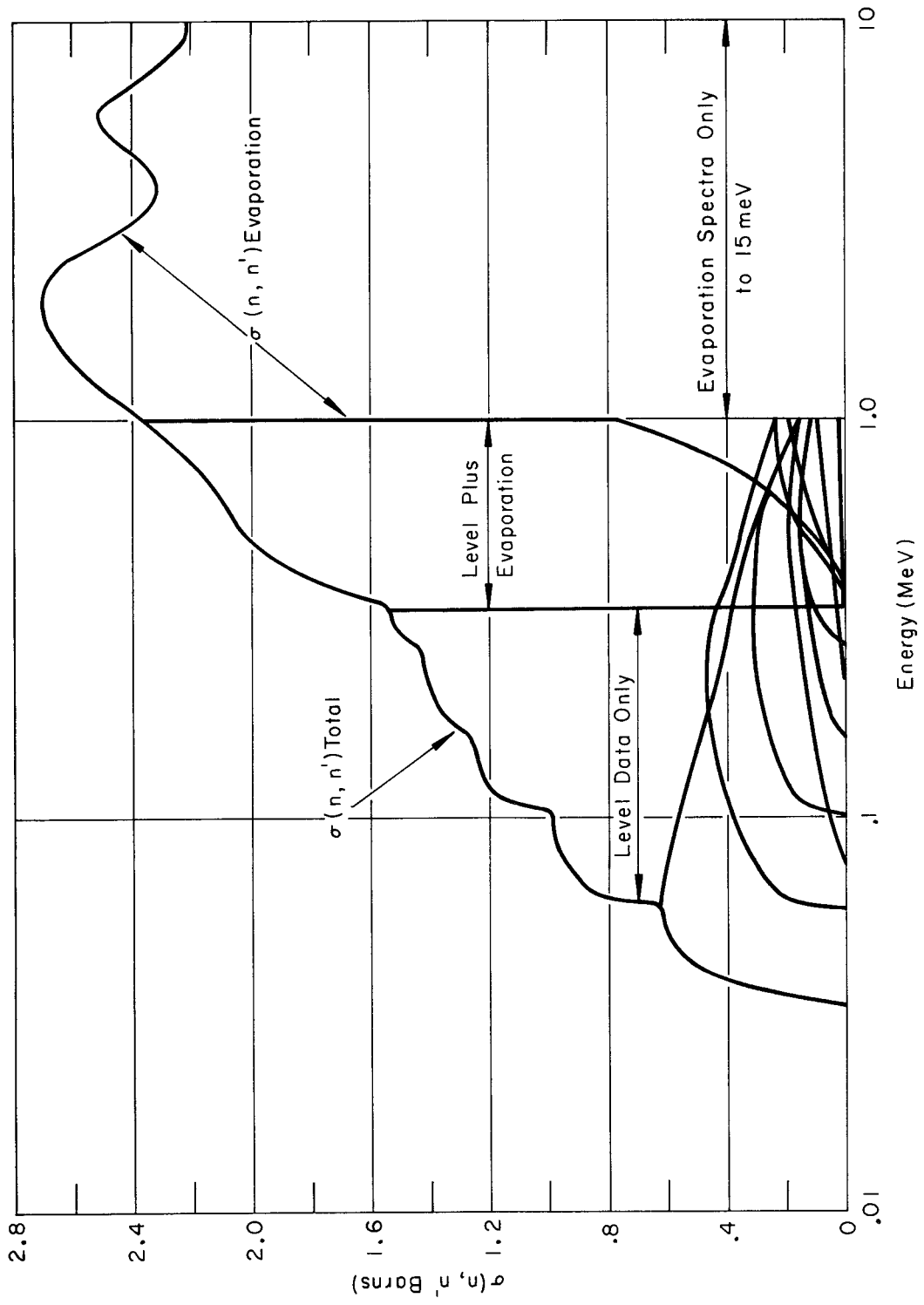


Figure 6. (n,n') Inelastic Scattering Cross Sections

$$\theta(E) = 3230 \sqrt{\frac{E(\text{MeV})}{A}} \quad (2)$$

where A is the mass of the target nucleus.

The tabulated nuclear temperature distribution has been plotted in Figure 7 along with the nuclear temperature computed for the (n,2n) and (n,3n) reactions. For LF=9 in File 5, the secondary transfer cross sections are computed from the evaporation model, using

$$\sigma(E \rightarrow E') = \sigma(E) p(E \rightarrow E') \quad (3)$$

$$p(E \rightarrow E') = \frac{E'}{\theta^2(E)} e^{-\frac{E'}{\theta(E)}} \quad (4)$$

where E is the neutron energy at which the reaction is initiated and E' is the final energy of the secondary neutrons.

In Appendix A, the excitation functions for inelastic scattering from individual levels are plotted as probabilities relative to the total (n,n') inelastic cross section. Figure 6 contains plots of the actual level cross sections in barns.

M. (n,2n) AND (n,3n) CROSS SECTIONS

(n,2n) and (n,3n) inelastic cross sections were calculated by S. Pearlstein, using his published techniques^[26]. The secondary energy distributions are described as evaporation spectra with a nuclear temperature distribution following the procedure used by Pitterle^[29] in compiling the ²⁴⁰Pu file of ENDF/B. The cross sections are plotted in Appendix A. Present restrictions on File 5 of ENDF/B do not permit the specification of independent spectra for the two or three neutrons emitted in the (n,2n) and (n,3n) reactions. The energetics of the (n,2n) reaction require that the average energy of each neutron emitted be less than that for the (n,n') reaction at a given initial energy, since the binding energy of the second neutron in the target nucleus is not available in the reaction. LeCouteur^[30] suggests that a reasonable approximation for the average energy θ_2 of each neutron emitted is

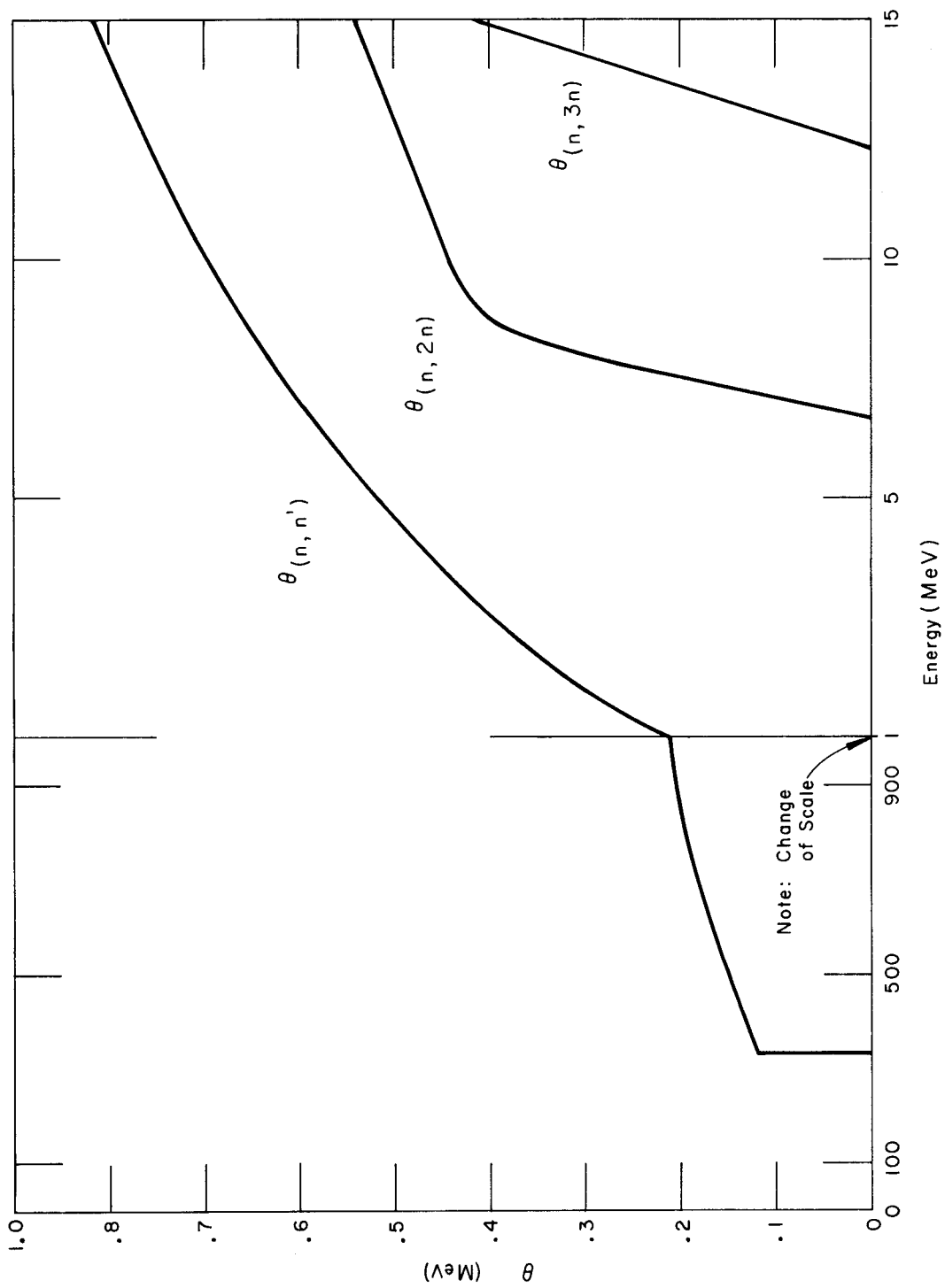


Figure 7. Temperature Distributions for (n, n') , $(n, 2n)$, and $(n, 3n)$ Inelastic Secondaries

$$\theta_2 = \frac{2}{3} \theta_1, \quad (5)$$

where θ_1 is the nuclear temperature of a neutron emitted in the (n,n') reaction given by Equation (2).

Below 8 MeV, the excess energy above the threshold of the (n,2n) reaction at 6.79 MeV is less than $2\theta_2$, the total average energy of the two neutrons emitted as given by Equation (5). In this region, between 6.79 MeV and approximately 8 MeV, Equation (5) is an oversimplification and θ_2 as given by Equation (5) is not possible. In this region, the nuclear temperature must decrease rapidly to zero at the threshold. An approximate linear fit to the value given by Equation (5) is used between 6.79 MeV and 8 MeV and joined smoothly to Equation (5) above 8 MeV. In this region, the average energy of the two neutrons emitted was taken to be one-half of the excess excitation energy above the threshold, as was done by T. A. Pitterle^[29] in the ²⁴⁰Pu evaluation for ENDF-B.

This was felt to be a reasonable assumption in this energy range since the average energy of both neutrons emitted is certainly less than the maximum energy available to them.

θ_2 to 8 MeV was then obtained from

$$2 \theta_2 = \frac{E - E_{th}}{2} = \frac{E - 6.79}{2} \text{ (MeV)}. \quad (6)$$

The resultant nuclear temperature for the (n,2n) reaction is graphed in Figure 7 as is the (n,3n) temperature also. The transfer cross sections for each of the two neutrons emitted are then given by Equations (3) and (4).

In the case of the (n,3n) reaction, a similar simplified approach was followed. Because the binding energy of two neutrons must be accounted for, the average energy available to each between the threshold and 15 MeV will be quite low. Again we followed the example of Pitterle^[29], who assumed an approximately linear behavior for the nuclear temperature, as in the energy region immediately above the threshold of the (n,2n)

reaction. The nuclear temperature should be approximately zero at the threshold of 12.234 MeV. The 15 MeV value is estimated to be 2/3 of the (n,2n) temperature plus 1/3 of the inelastic scattering temperature evaluated at the energy.

$$E = 0.8 (15 - 12.234 - 4 \theta_2) . \quad (7)$$

where θ_2 is the (n,2n) temperature at 15 MeV. The value calculated for the (n,3n) nuclear temperature at 15 MeV is 0.41 MeV.

In both the (n,2n) and (n,3n) reactions, gross approximations are involved in the specification of the evaporation model for secondary energy distribution, especially in the vicinity of the threshold of either reaction. As an example, for neutrons just above the threshold of the (n,2n) reaction, the evaporation model permits a small but finite probability that both neutrons are re-emitted near the incident energy. This situation is forbidden by the energetics of the reaction. The fact that the nuclear temperature is small in the region just above the threshold tends to reduce this probability, but still permits forbidden transitions. In the absence of discrete level excitation data for ^{235}Np and ^{236}Np , the present prescription is about as well as can be done when the evaporation model is the only alternative. It still presents serious short-comings, especially in the case of the (n,3n) reaction. However, these approximations can be partially justified in view of the fact that both the (n,2n) and (n,3n) cross sections are based on theoretical estimates to begin with.

N. FISSION NEUTRON SPECTRUM

The secondary energy distribution of fission neutrons is given as a single temperature Maxwell distribution (LF=8). The temperature corresponds to the average fission neutron energy, which can be calculated using Terrell's formula^[31]:

$$\bar{E} = 0.75 + 0.65 \sqrt{\bar{\nu} + 1} \text{ (MeV)} \quad (8)$$

To derive the nuclear temperature we use

$$\theta = \frac{2}{3} \bar{E} = 0.50 + 0.43 \sqrt{\bar{\nu} + 1} \text{ (MeV)}.$$

Using the zero energy extrapolation of the $\bar{\nu}$ value, we obtain $\theta = 1.32$ MeV.

File 1

In the General Information section, File 1, is contained some additional information not directly related to cross sections.

0. MEAN NUMBER OF NEUTRONS PER FISSION ($\bar{\nu}$)

Only a few measurements of $\bar{\nu}$ for ^{237}Np have been made and they have been in broad spectra. The measurements are summarized in Table V. Not enough data are available to allow a direct determination of the energy dependence of $\bar{\nu}$. A slope of 0.16 MeV^{-1} was assumed^[32] and passed through the average of the two measurements of Hansen^[33]. This procedure yielded the relation

$$\bar{\nu} = 2.61 + 0.16 \text{ MeV}^{-1}.$$

TABLE V
MEASUREMENTS OF $\bar{\nu}$ FOR ^{237}Np

<u>Author</u>	<u>Neutron Energy (Mean)</u>	<u>$\bar{\nu}$</u>
Kuz'minov et al. ^[34]	2.5	2.72 ± 0.15
Hansen ^[33]	1.40	2.81 ± 0.09
	1.67	2.90 ± 0.04
Lebedev et al. ^[35]	2	2.96 ± 0.05

Decay Data

Decay constants (sec^{-1}) are given for several short decay chains involving ^{237}Np and the products of $(n,2n)$, $(n,3n)$ and (n,γ) reactions.

Since no provision is made in the ENDF/B format for branching in these chains, only the principal mode of each decay appears in the file. Decay constants were calculated from half lives listed by Goldman on the well-known GE nuclide chart, vintage 1965^[36].

P. FISSION PRODUCT YIELDS

The fission yield data of Iyer et al.^[37] represents the bulk of the available data. Iyer's values are presented as relative yields. To obtain absolute yield values, the data of Iyer et al. were plotted on a linear graph. A smooth curve was drawn through the points. The area under the curve was measured with a planimeter and normalized to 200 per cent yield. The points listed in File 1 were read from this smooth curve. Because the smooth curve was followed, the ENDF/B fission yield data will not reproduce any true fluctuations in the yield, such as may be due to shell effects.

Q. REFERENCES

- [1] H. C. Honeck, BNL-8381 (1964).
- [2] S. Pearlstein, BNL-982 (1966).
- [3] G. C. Slaughter, J. A. Harvey, and R. C. Block, ORNL 3085, p 42 (1966).
- [4] J. E. Cline, E. H. Magleby, and W. H. Burgus, Bul. Am. Phys. Soc. 4, 270 (1959).
- [5] I. V. Adamchuk, S. S. Moskalev, and M. I. Pevzner, J. Nucl. Energy 13 72 (1960).
- [6] M. S. Smith et al., Phys. Rev. 107 525 (1957).
- [7] B. R. Leonard and R. H. Odegaarden, unpublished.
- [8] D. T. Goldman, Trans. Am. Nucl. Soc. 7 84, (1964).
- [9] W. Hauser, H. Feshback, Phys. Rev. 87 366 (1952).
- [10] D. Paya et al., Paper CN-23/69, Nuclear Data for Reactors, Supplement, INDC/156, IAEA, Vienna, 1967.
- [11] F. J. Wheeler, IDO-17212, (July 1966).
- [12] F. Brown and G. R. Hall, "The Thermal Neutron Capture Cross Section of Np-237", J. Inorg. and Nuclear Chem. 2, 204-8 (1956).
- [13] H. Rose, W. A. Cooper, R. B. Tattersall, "The Use of the Pile Oscillator in Thermal Reactor Problems", Proceedings of the Second International Conference on the Peaceful Uses of Atomic Energy, Vol. 1, p 16 (United Nations, Geneva, 1958).
- [14] R. B. Tattersall, H. Rose, S. K. Pattenden and D. Jowett, "Pile Oscillator Measurements of Resonance Absorption Integrals", J. Nucl. Energy, Vol. 12, pp 32-46 (1960).
- [15] J. W. Rogers and J. J. Scoville, "Resonance Absorption Integrals Measured by Reactivity Techniques", Trans. Am. Nucl. Soc. 10, 259 (1967).
- [16] E. D. Klema, Phys. Rev. 72, 88 (1947). [Los Alamos] Ionization chamber. Relative to U-235 σ_f .
- [17] R. L. Henkel, LA-1495 (1952). [Los Alamos] Spiral counter. Normalized to U-235 $\sigma_f = 1.44$ b at 1.50 MeV, from Klema, above.

- [18] B. M. Gokhberg et al., Doklady Akad. Nauk SSSR 128, 1157 (1959).
[Translation in Soviet Phys. Doklady 4, 1074 (1959)]. Ionization chamber.
- [19] Perkin, J. Nucl. En. 19, 423 (1965).
- [20] P. H. White, J. G. Hodgkinson et al., Physics and Chemistry of Fission Vol. I, p 219, International Atomic Energy Agency Solzburg, (March 1965).
- [21] Schmitt and Murray, Phys. Rev. 116, 1575 (1959).
- [22] Pankrotov, Atomnaya Energiya 14, 117 (1963).
- [23] Stein et al., Conf-660303, p 623, Washington, 1966.
- [24] D. C. Stupegia, M. Schmidt, and Curtis R. Keedy, Nuc. Sci. and Eng., 29, 218 (1967).
- [25] D. C. Stupegia et al., Paper CN-23/51, Nuclear Data for Reactors, Supplement, INDC/156, Vienna, 1967.
- [26] S. Pearlstein, Nuc. Sci. and Eng. 23, 238 (1965).
- [27] J. J. Schmidt, KFK 120, Karlsruhe.
- [28] H. Alter, Private Communication.
- [29] T. A. Pitterle, M. Yamamoto, Evaluated Neutron Cross Sections of Pu-240 For The ENDF/B File, APDA-218 (1968).
- [30] K. J. LeCouteur, Proc. Phys. Soc. A65, 718 (1952).
- [31] J. Terrell, Physics and Chemistry of Fission, Vol. 2, IAEA, (1965).
- [32] J. C. Hopkins and B. C. Diven, Nucl. Phys. 48, 433 (1963).
- [33] G. E. Hansen, Los Alamos unpublished report (1958). Quoted in R. B. Leachman, p 664, Proc. Second UN Conf. on PUAE, Geneva (1958).
- [34] B. D. Kuz'minov, L. S. Kutsaeva, and I. I. Bondarenko, Atomnaya Energiya 4, 187 (1958).
- [35] V. I. Lebedev and V. I. Kalashnikova, Atomnaya Energiya, Vol. 10, No. 4, 371 (1961).
- [36] D. T. Goldman and J. R. Stehn, Chart of the Nuclides (1965).
- [37] R. S. Iyer et al., The Physics and Chemistry of Fission, Vol. 1 p 439, IAEA, Vienna, 1965.
- [38] P. A. Moldauer, C. A. Engelbrecht, G. J. Duffy, Nearrex, A Computer Code For Nuclear Reaction Calculations, ANL-6478 (1964).

- [39] P. A. Moldauer, Rev. Mod. Phys. 36, 1079 (1964).
- [40] P. A. Moldauer, Phys. Rev. 135, B642 (1964).

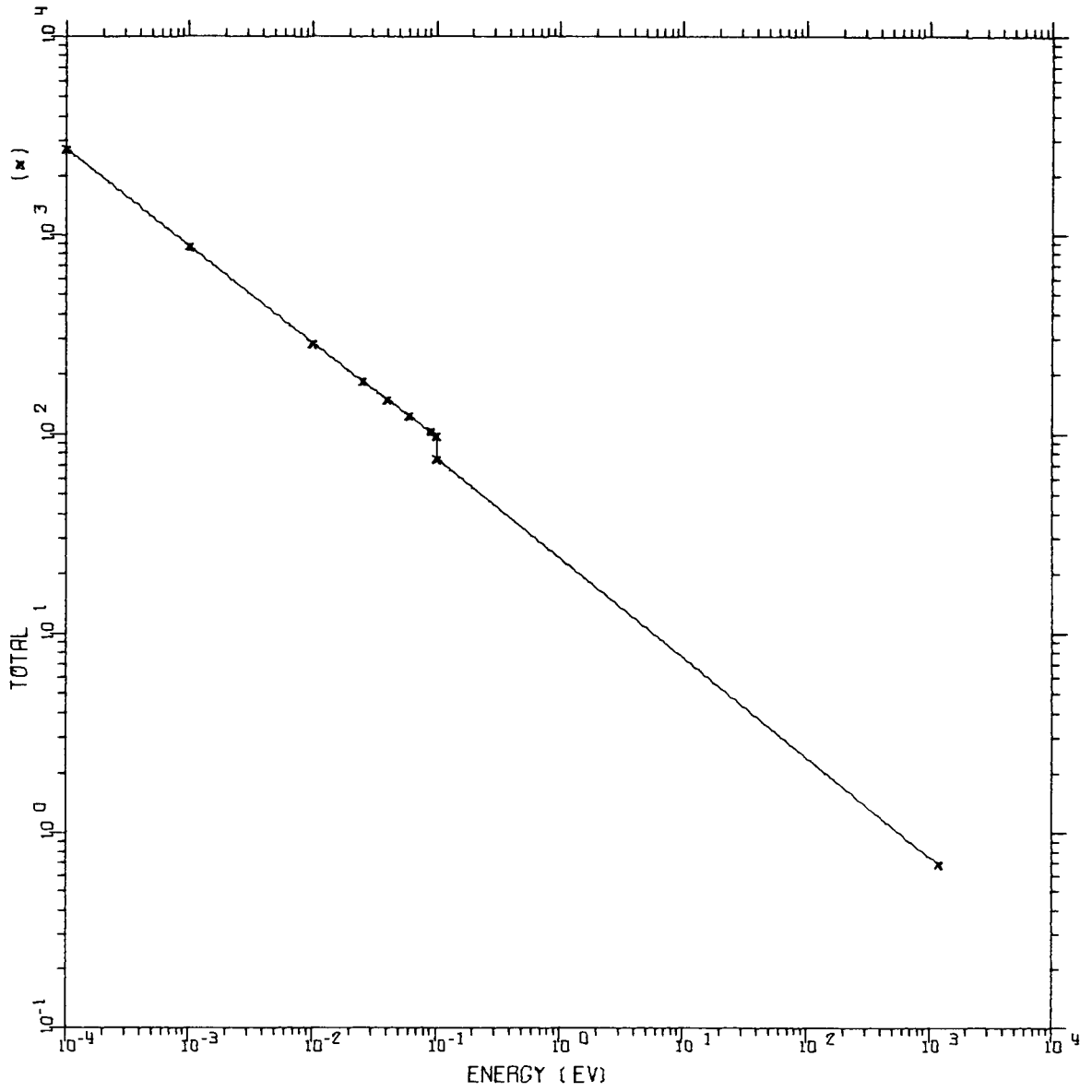
APPENDIX A

CROSS SECTION PLOTS

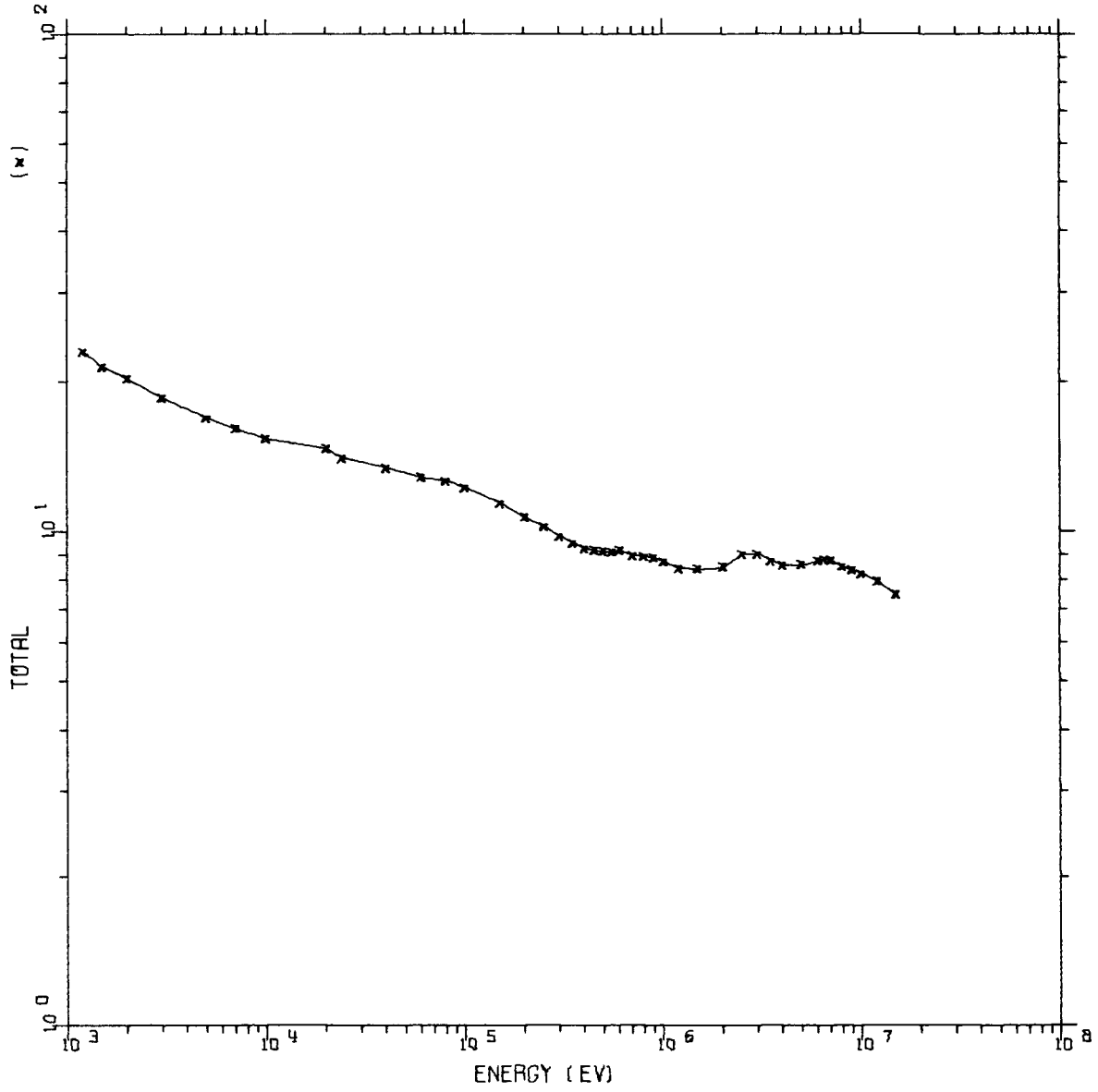
Appendix A contains computer plots of the individual cross sections which appear in ENDF/B files 3, 4 and 5. The computer plots of file 3 do not contain the resonance contributions from the resolved and unresolved resonance ranges. Therefore, discontinuities will exist in the computer plots at the extremities of these ranges.

The plots of the inelastic level cross sections are given as probabilities relative to the total (n,n') cross section. The actual level cross sections are given in Figure 6.

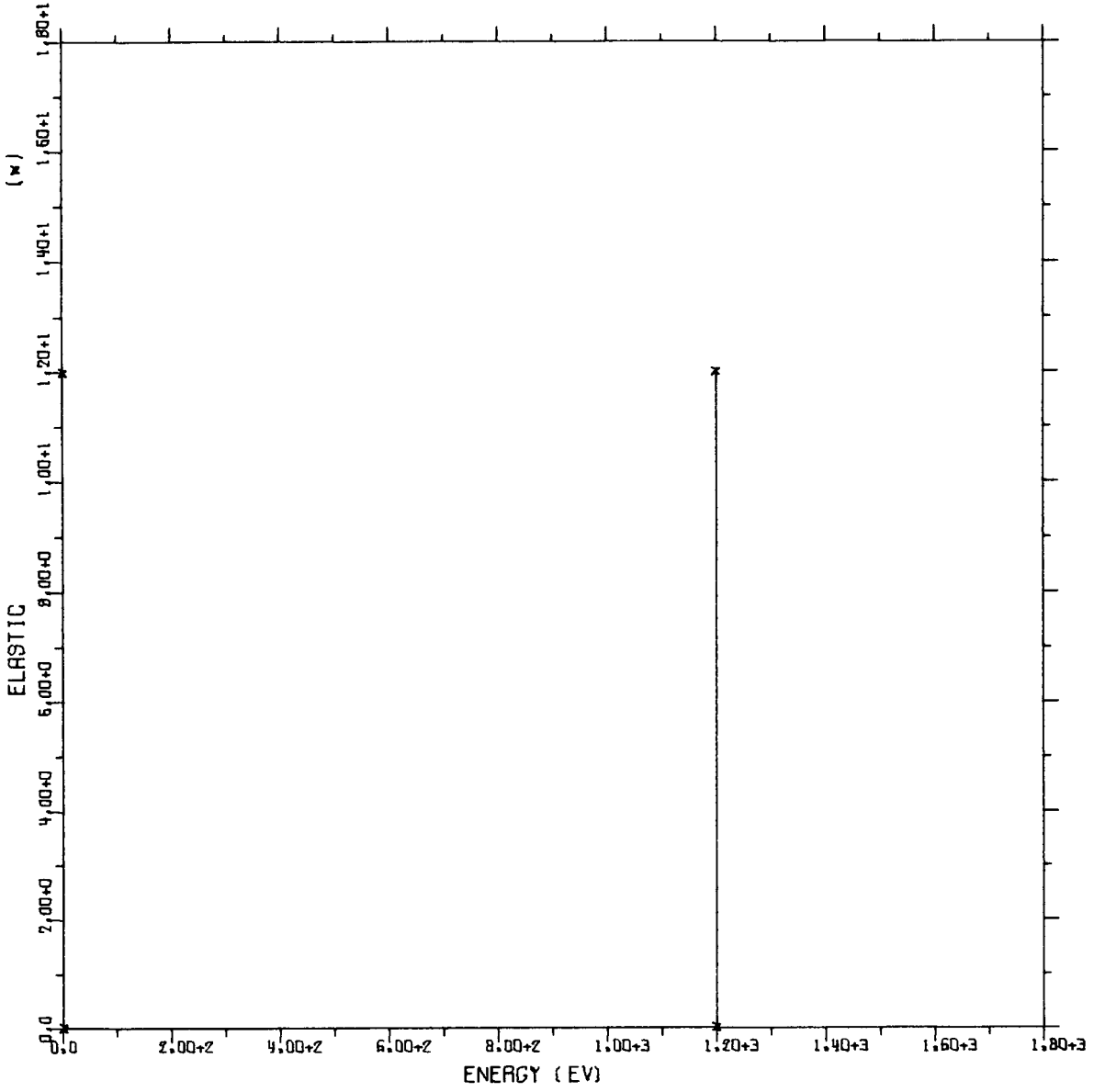
NEPTUNIUM 237 EVALUATED BY IDAHO NUCLEAR CORP NRTS



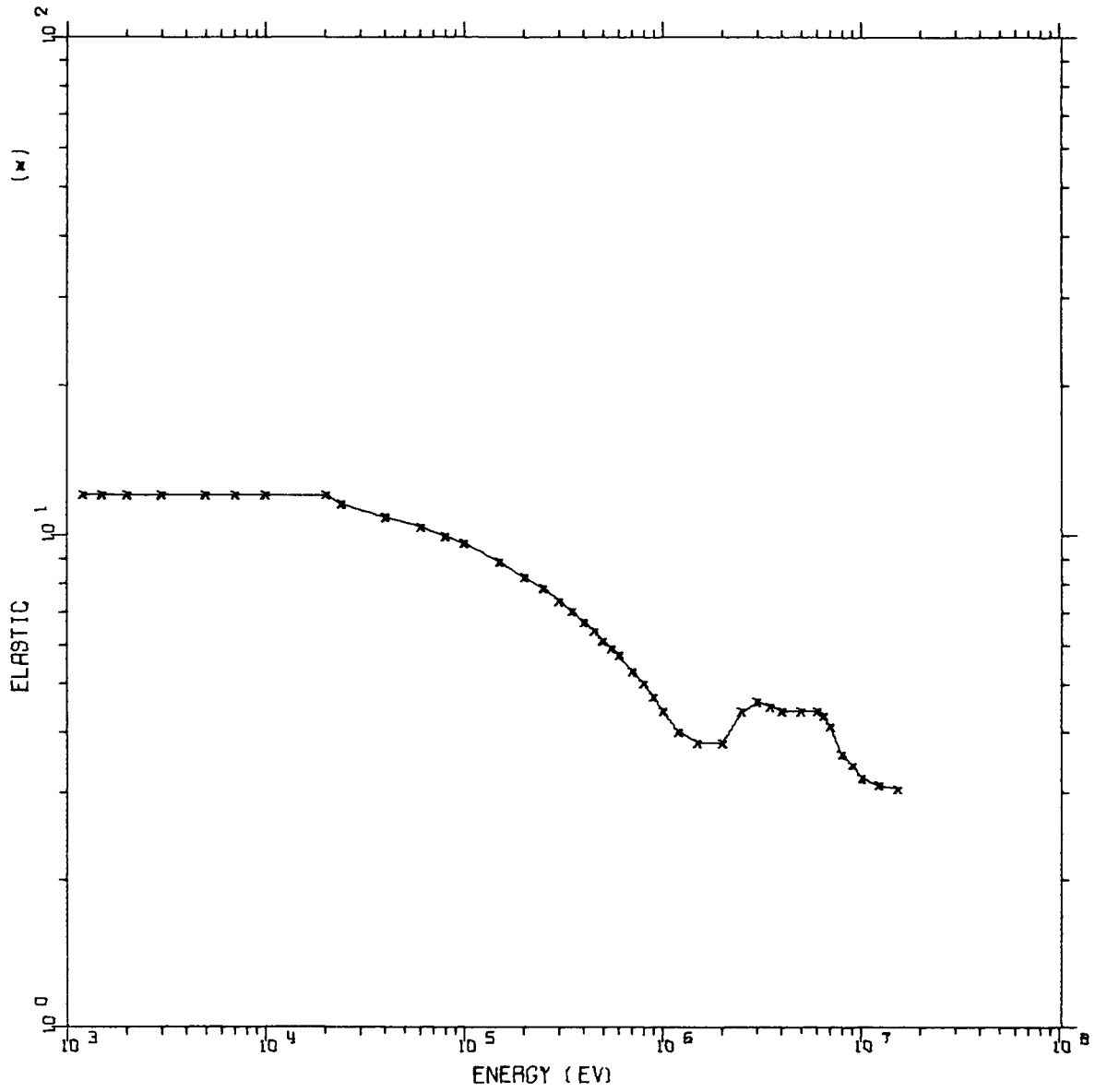
NEPTUNIUM 237 EVALUATED BY IDAHO NUCLEAR CORP NRTS



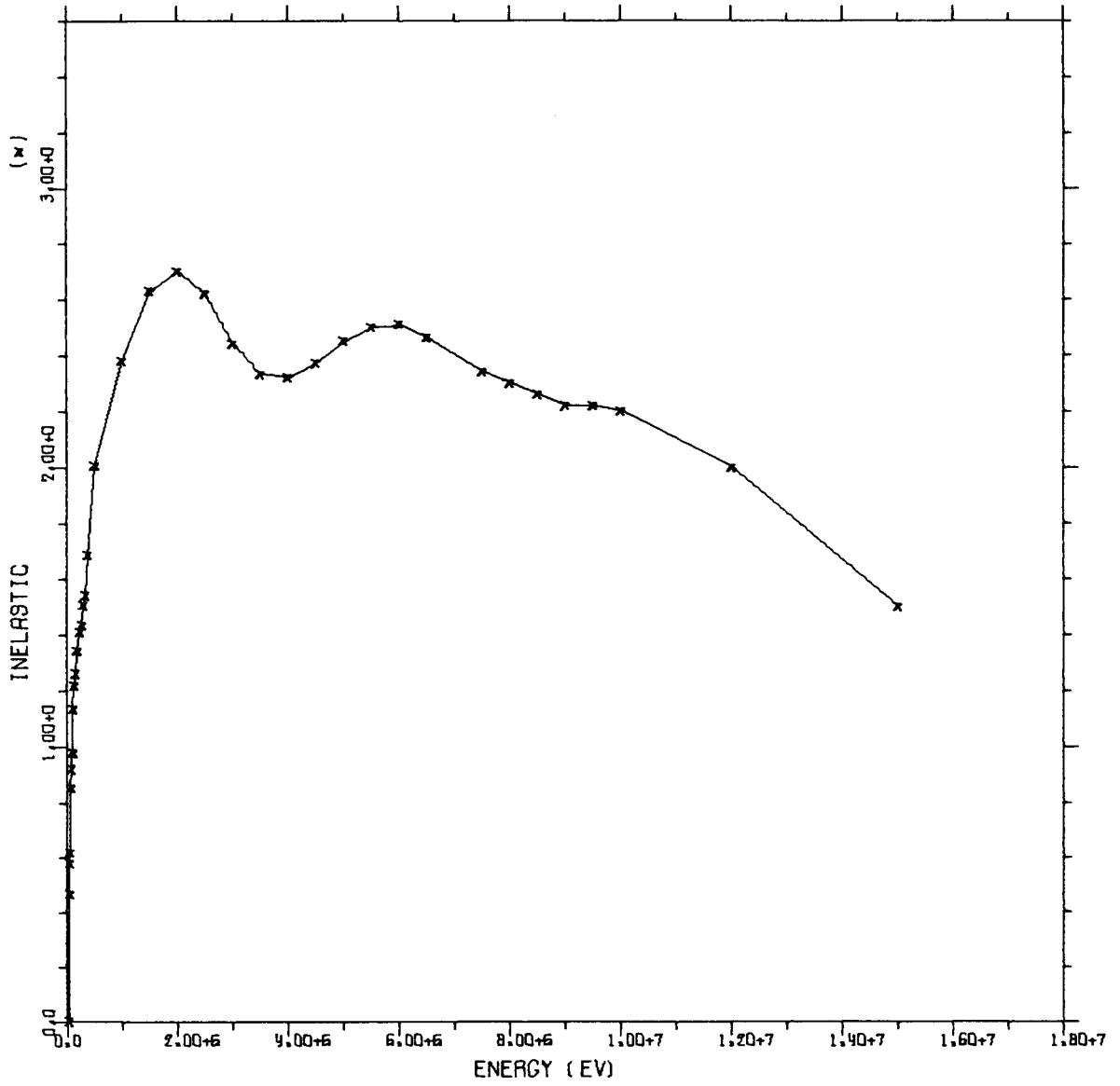
NEPTUNIUM 237 EVALUATED BY IDAHO NUCLEAR CORP NRTS



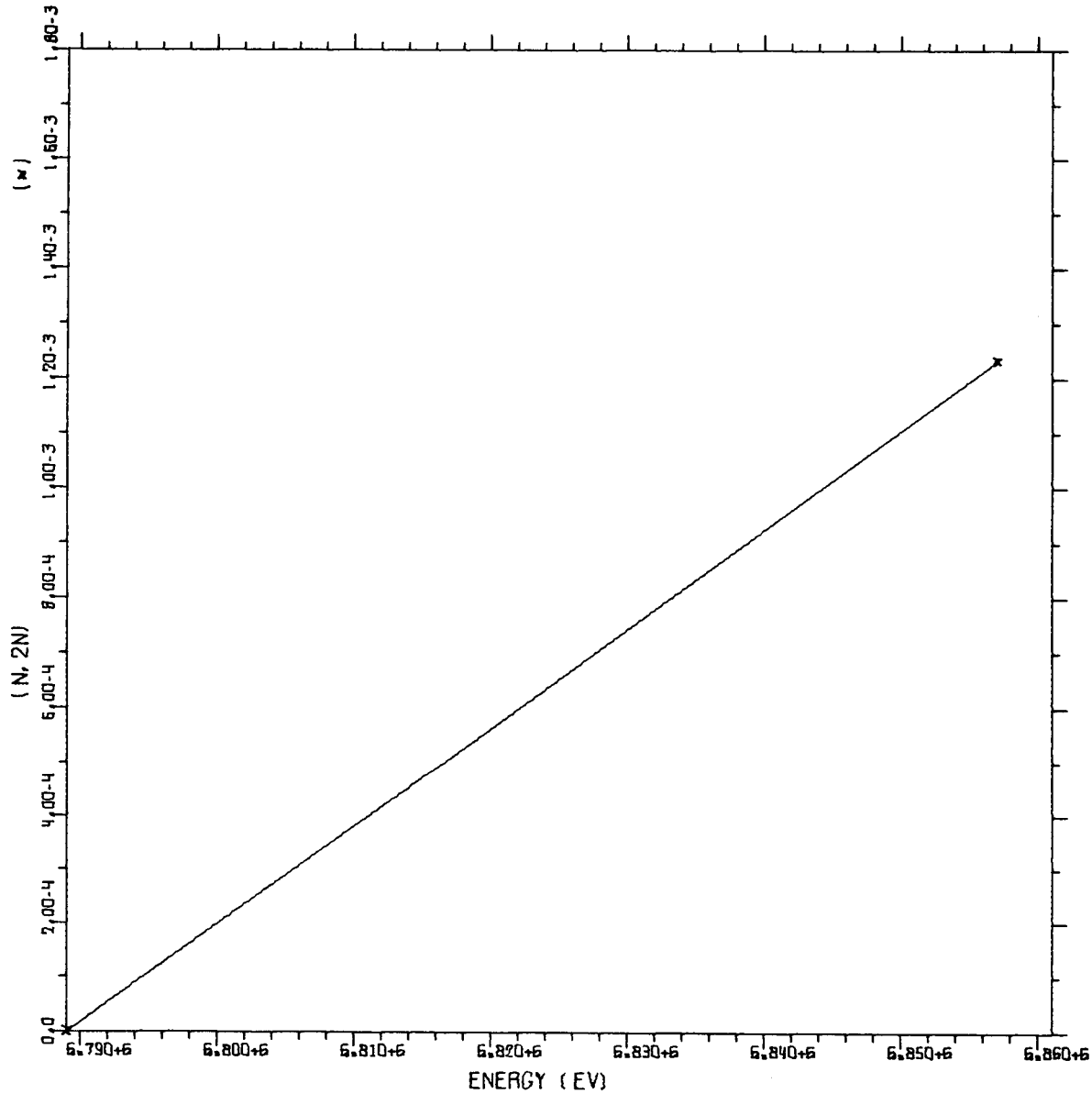
NEPTUNIUM 237 EVALUATED BY IDAHO NUCLEAR CORP NATS



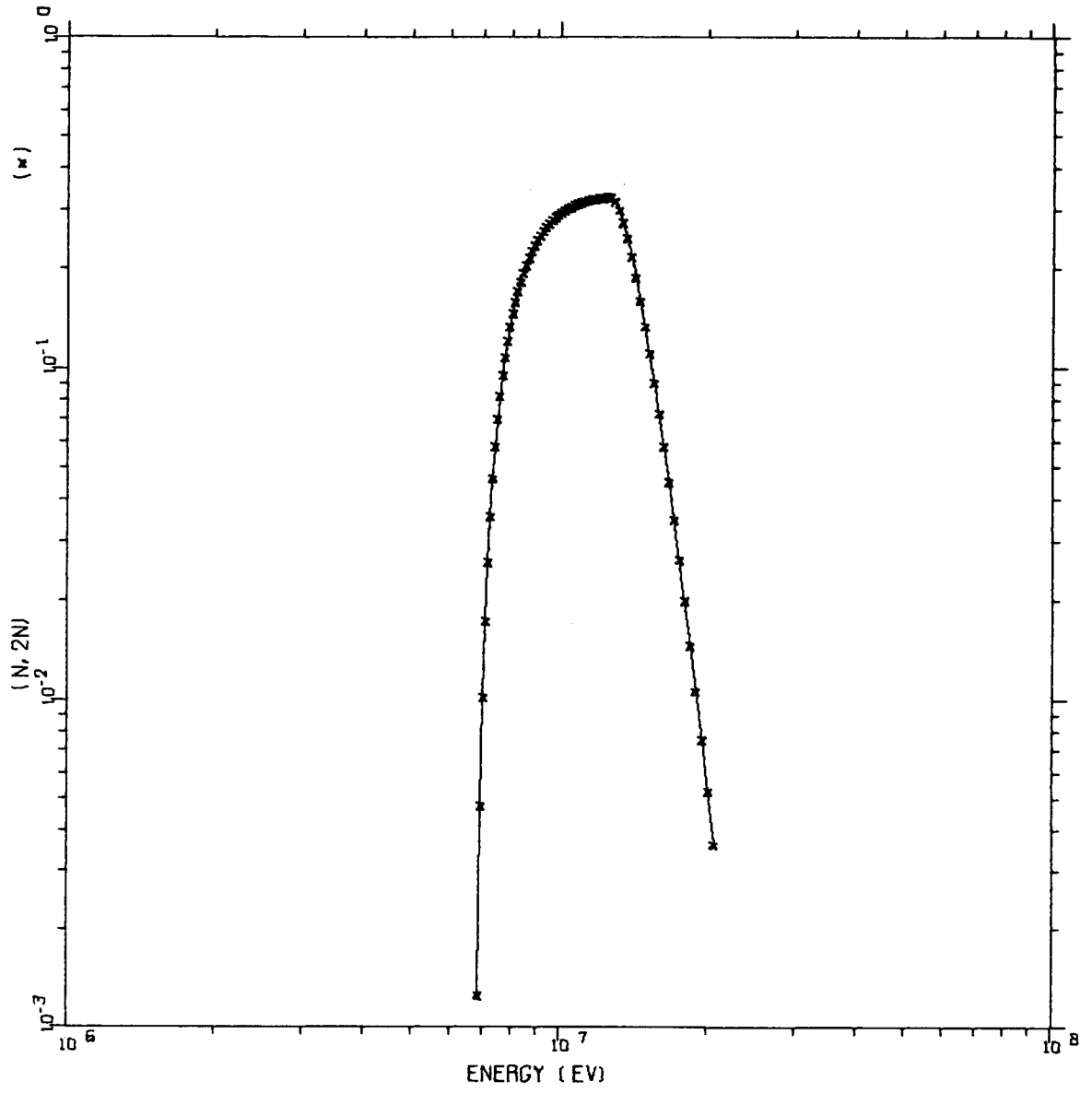
NEPTUNIUM 237 EVALUATED BY IDAHO NUCLEAR CORP NRTS



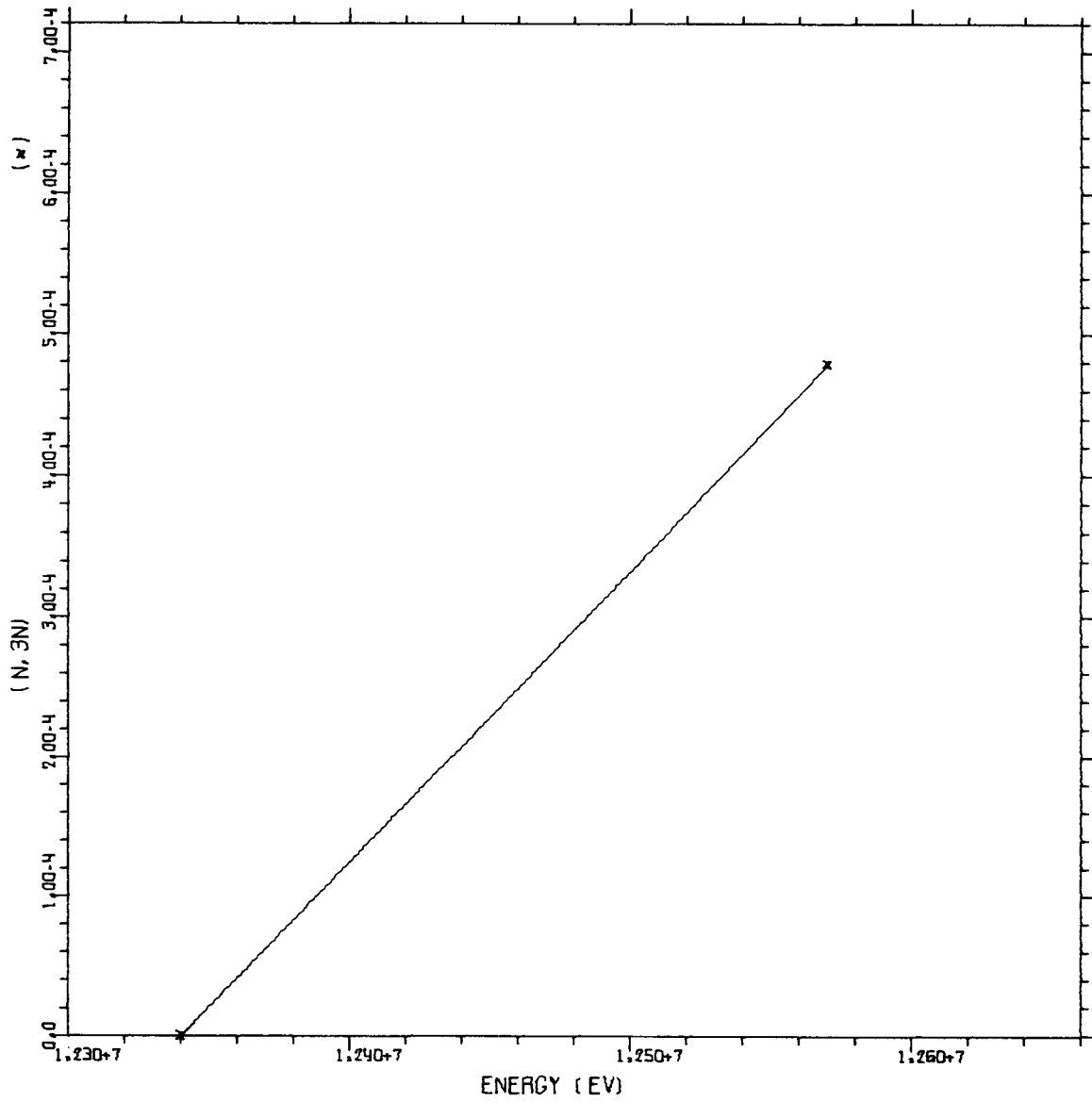
NEPTUNIUM 237 EVALUATED BY IDAHO NUCLEAR CORP NRTS



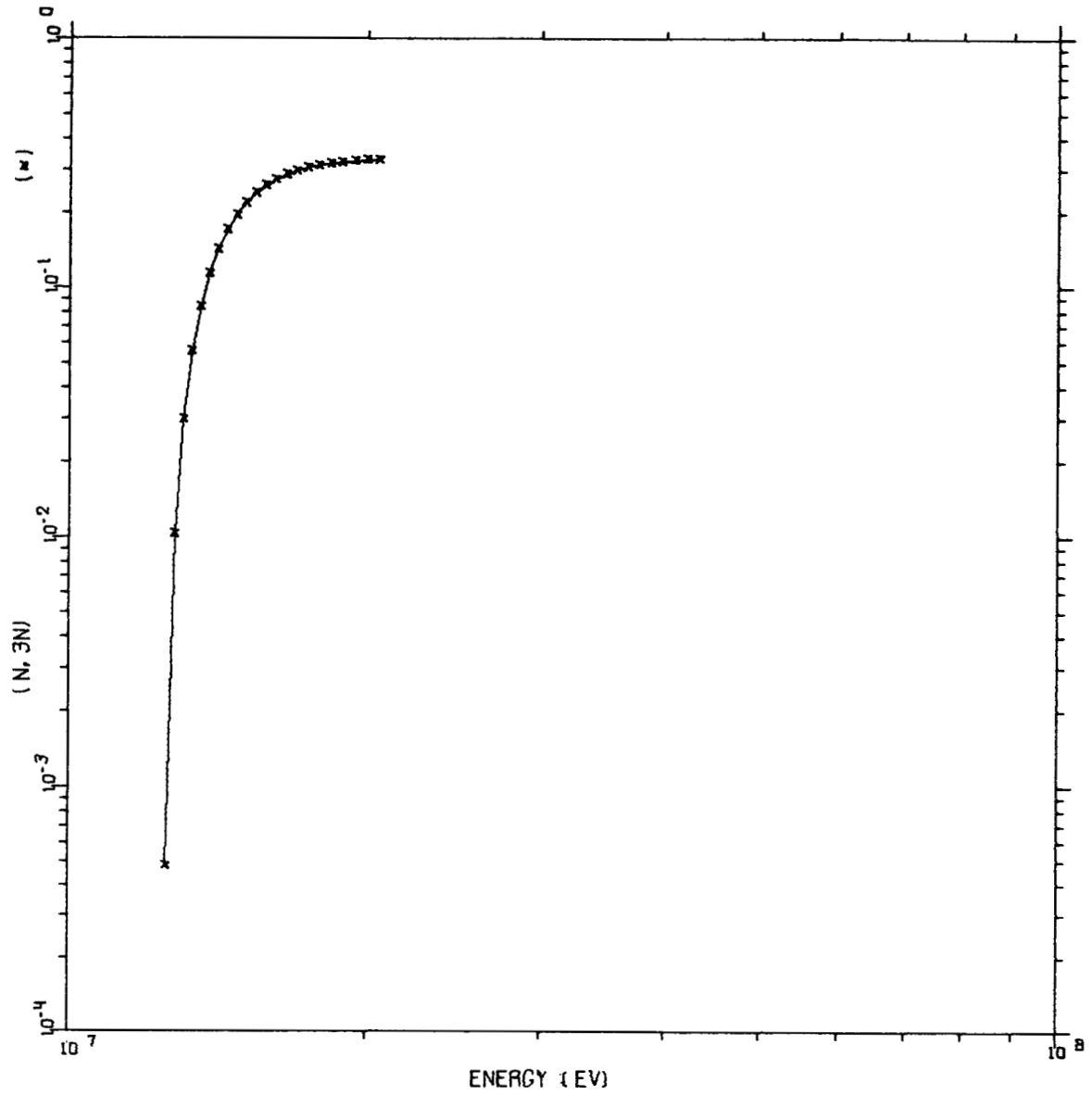
NEPTUNIUM 237 EVALUATED BY IDAHO NUCLEAR CORP NRTS



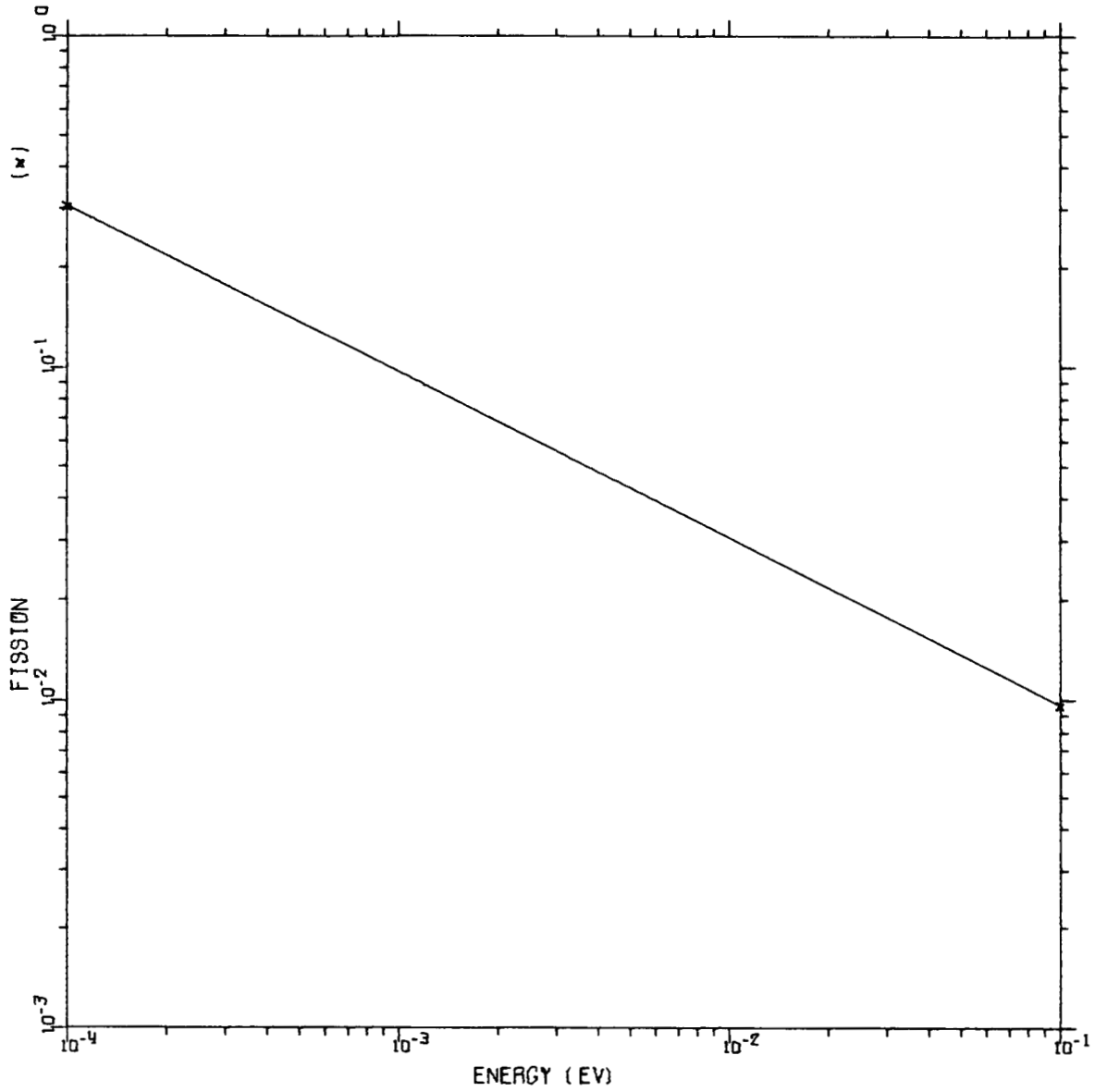
NEPTUNIUM 237 EVALUATED BY IDAHO NUCLEAR CORP NRTS



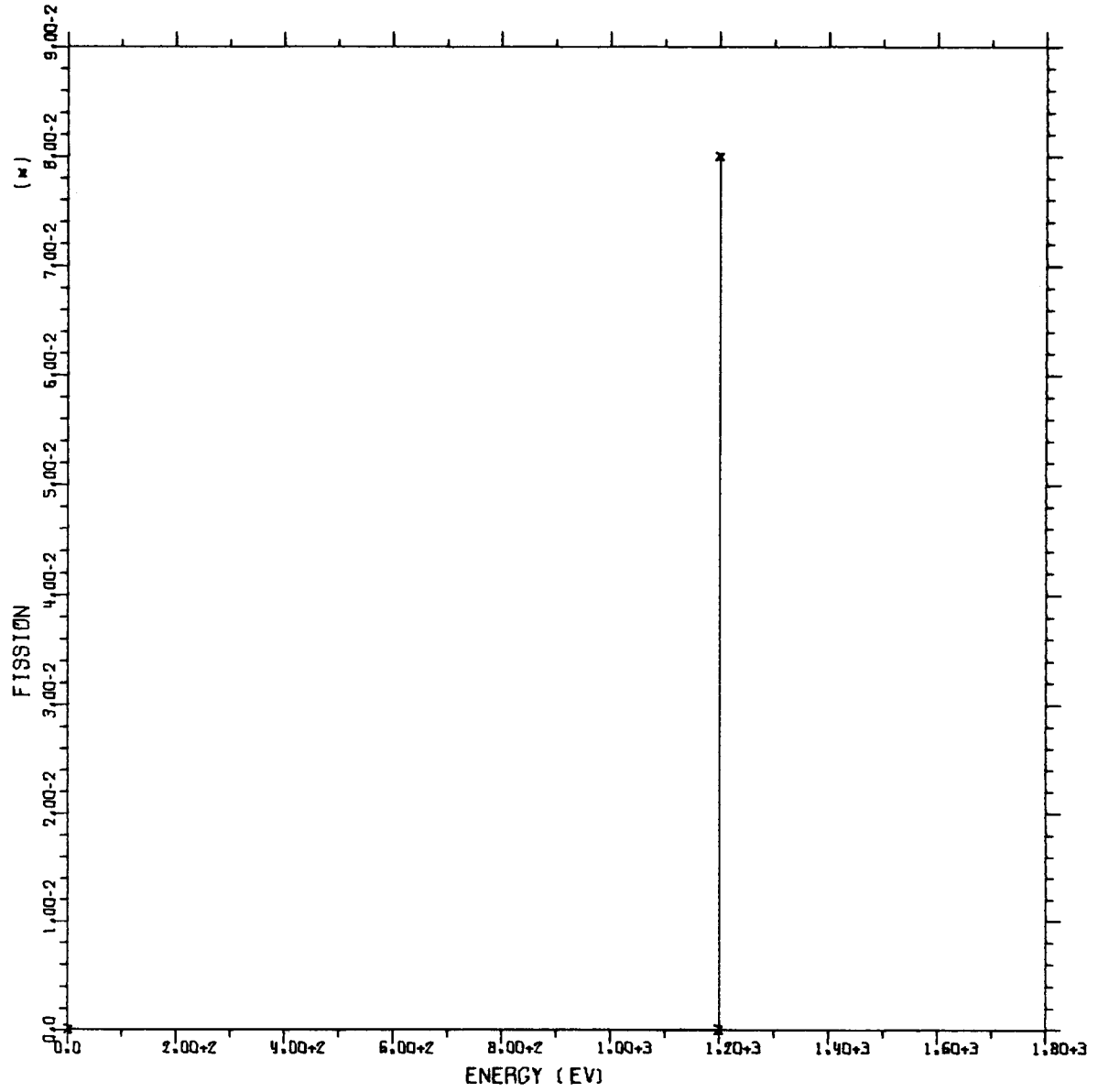
NEPTUNIUM 237 EVALUATED BY IDAHO NUCLEAR CORP NRTS



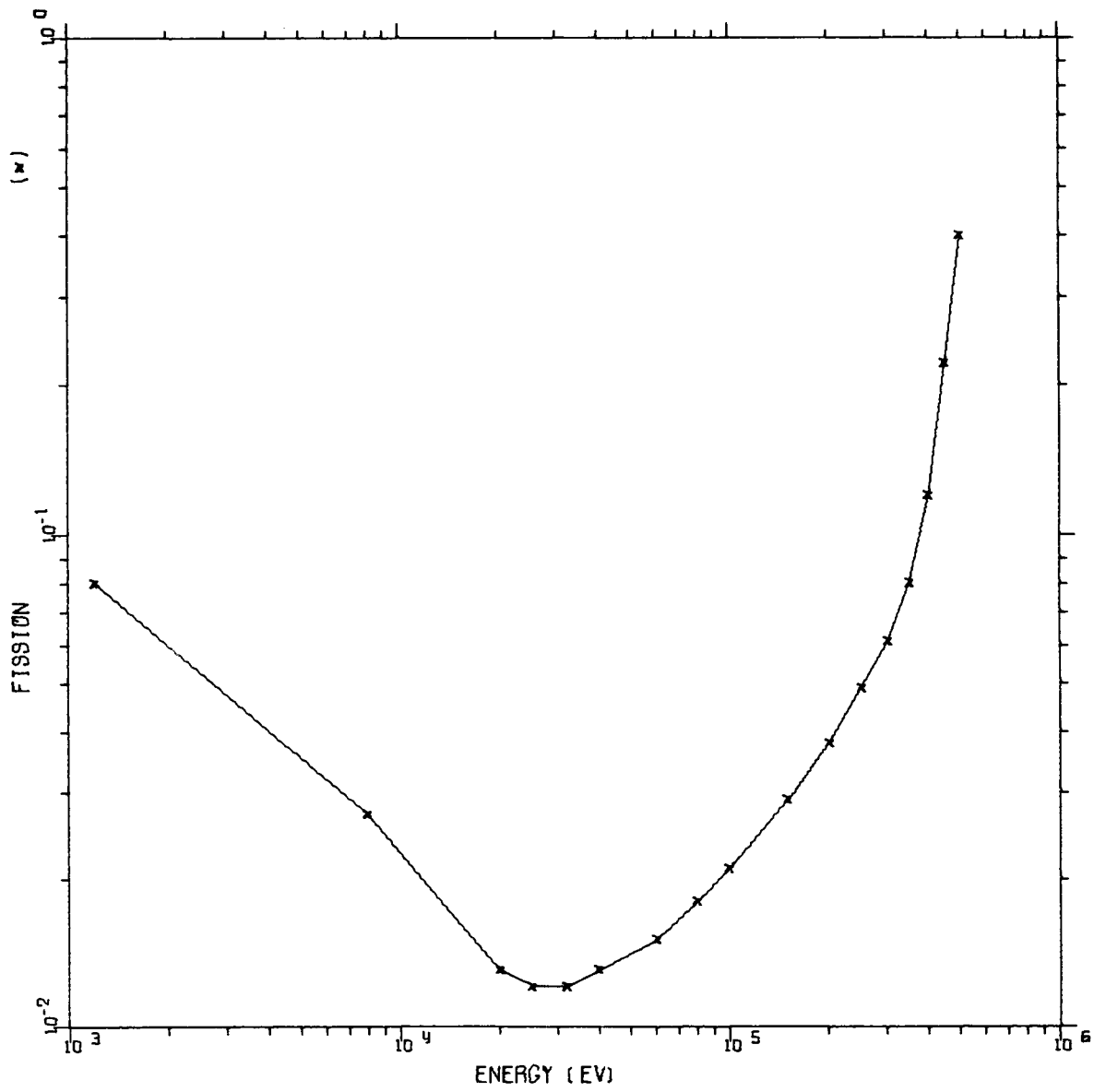
NEPTUNIUM 237 EVALUATED BY IDAHO NUCLEAR CORP NRTS



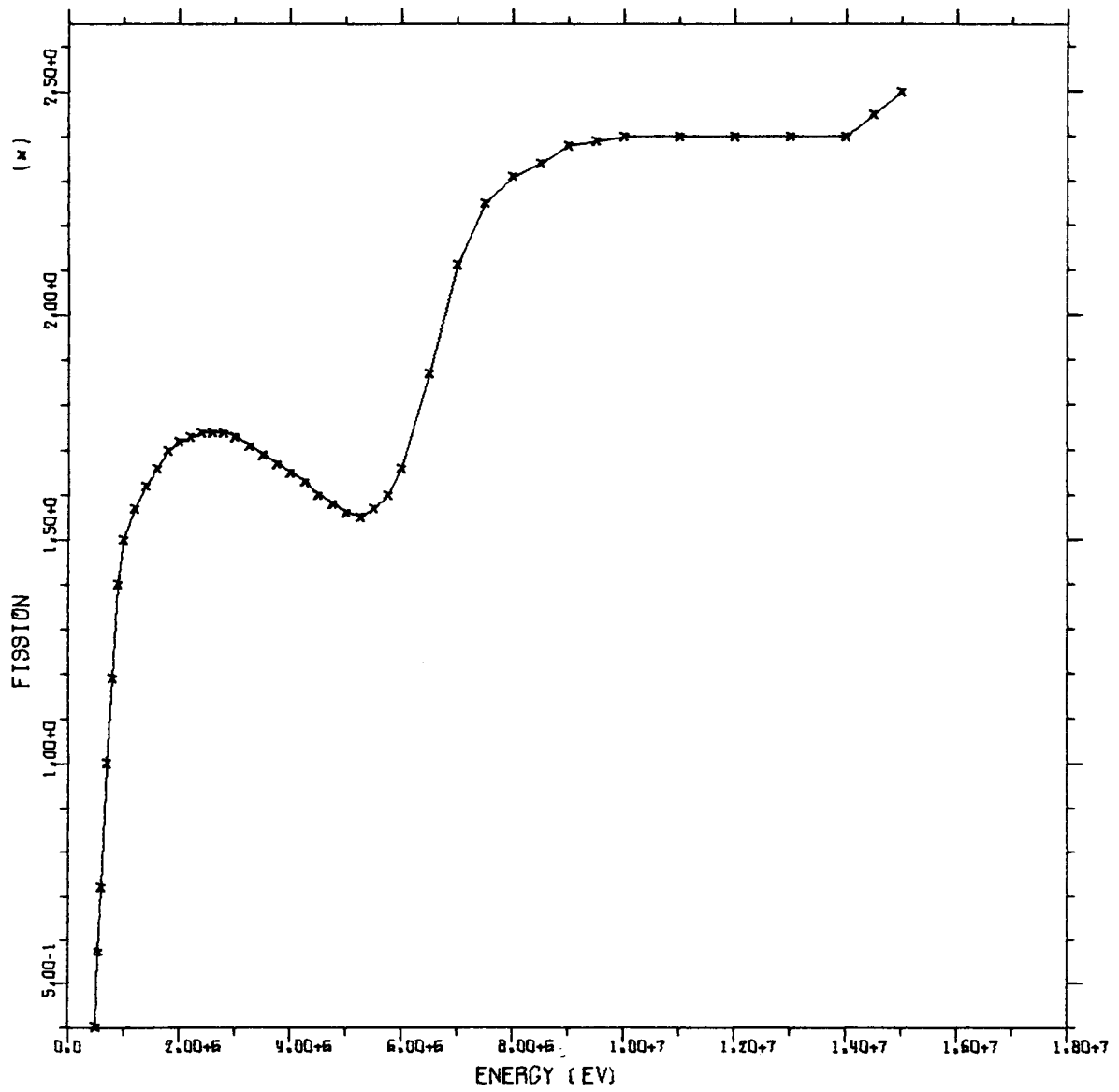
NEPTUNIUM 237 EVALUATED BY IDAHO NUCLEAR CORP NRTS



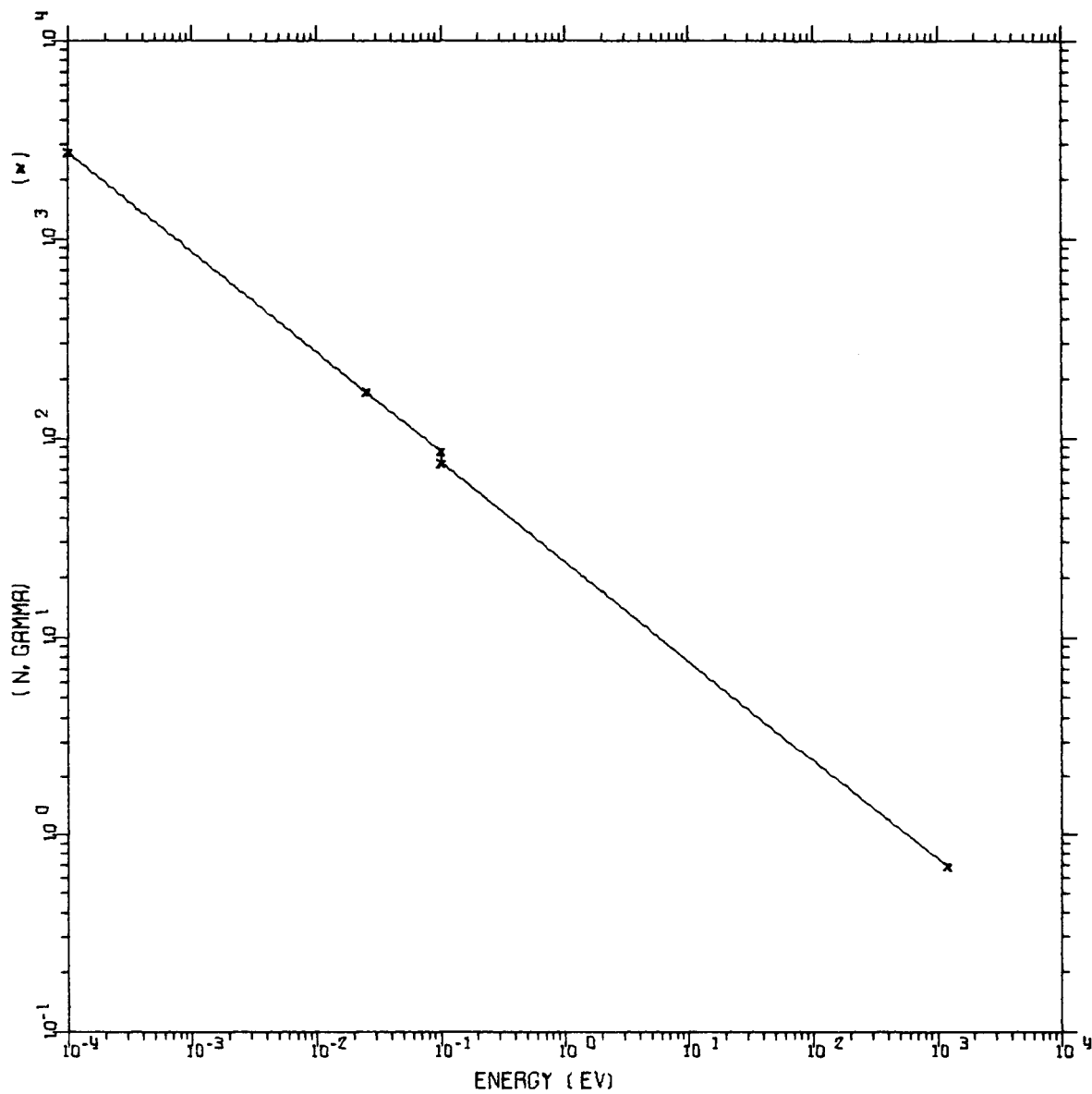
NEPTUNIUM 237 EVALUTED BY IDAHO NUCLEAR CORP NRTS



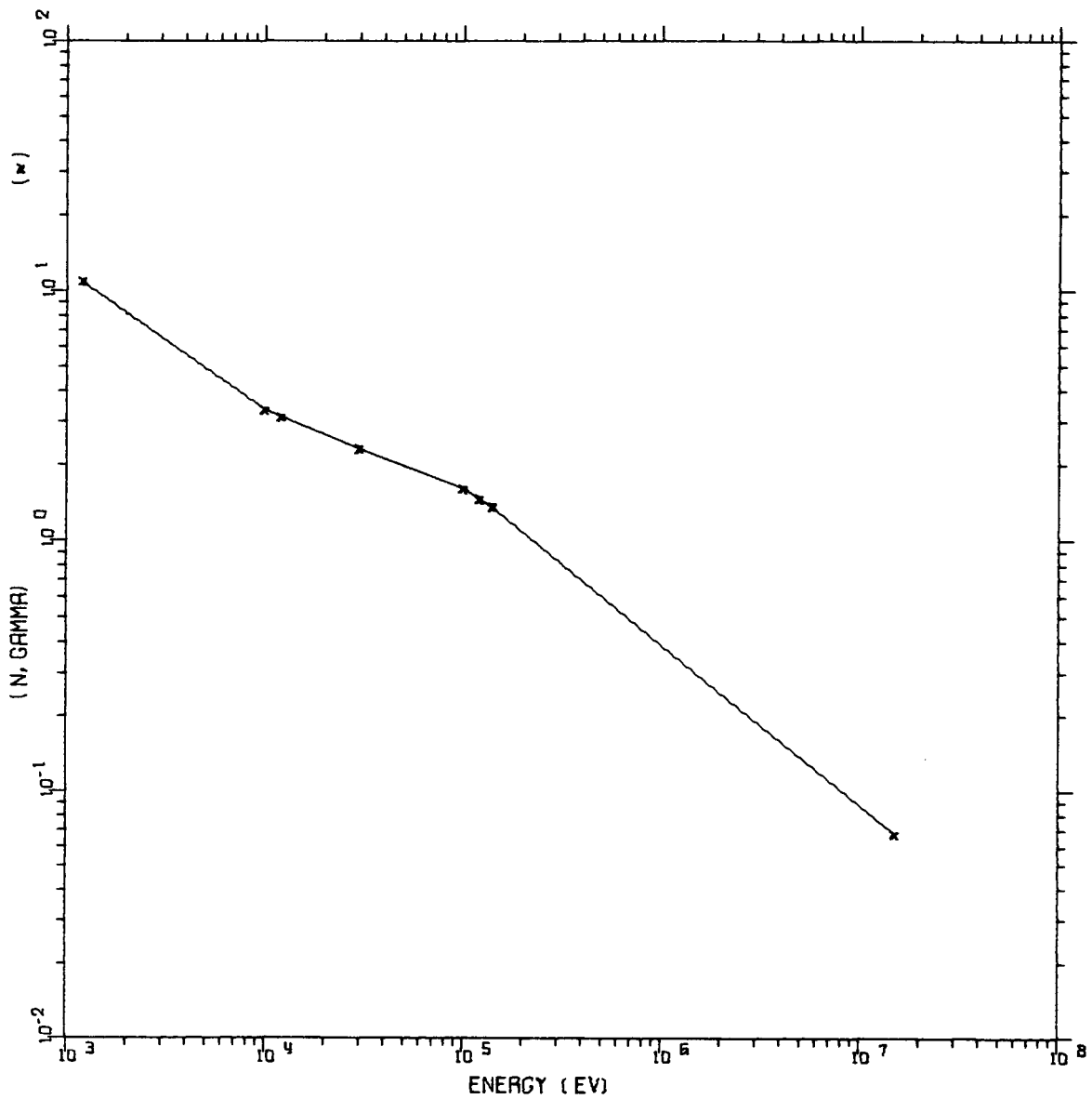
NEPTUNIUM 237 EVALUATED BY IDAHO NUCLEAR CORP NRTS



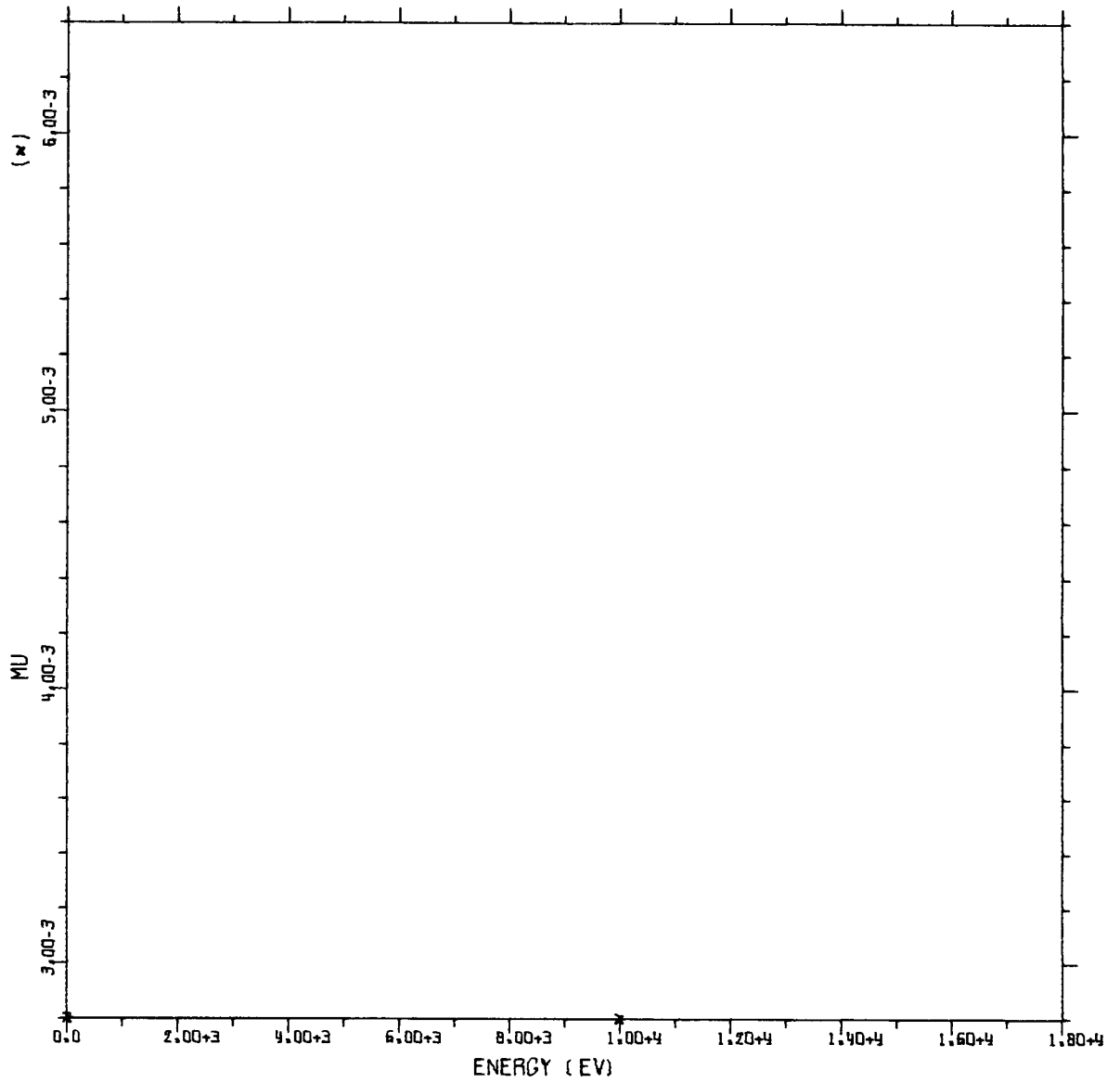
NEPTUNIUM 237 EVALUATED BY IDAHO NUCLEAR CORP NRTS



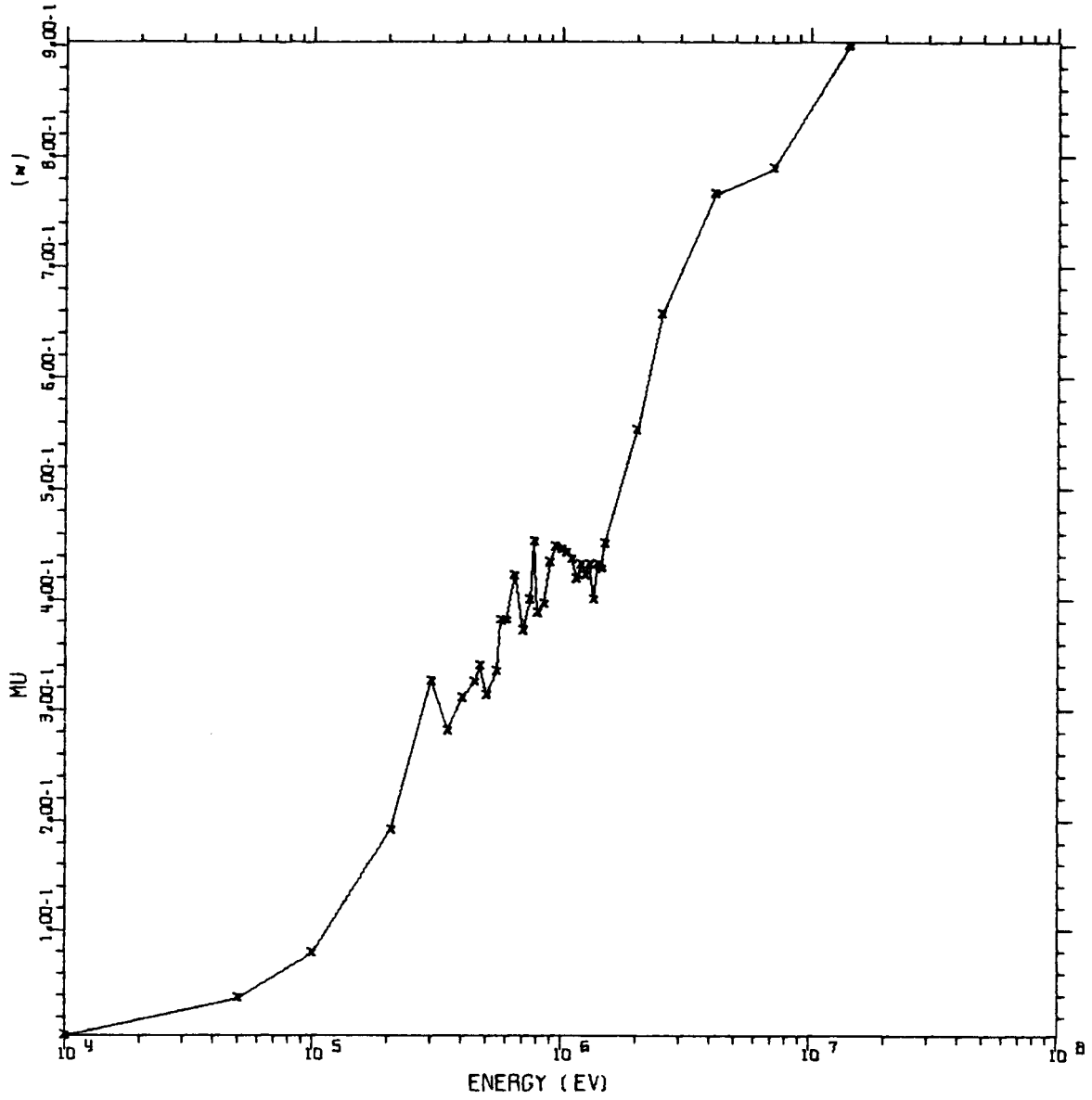
NEPTUNIUM 237 EVALUATED BY IDAHO NUCLEAR CORP NATS



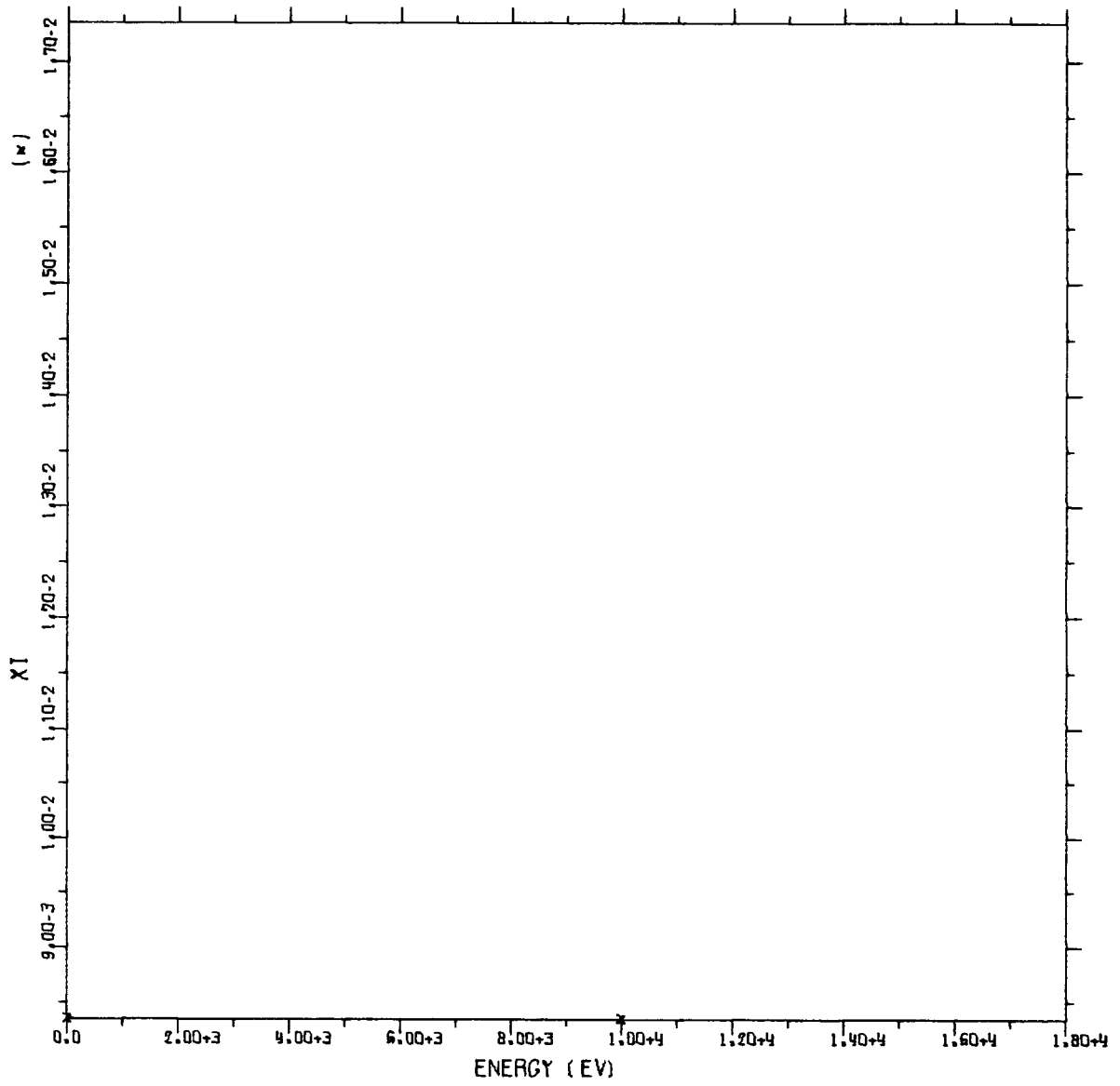
NEPTUNIUM 237 EVALUATED BY IDAHO NUCLEAR CORP NRS



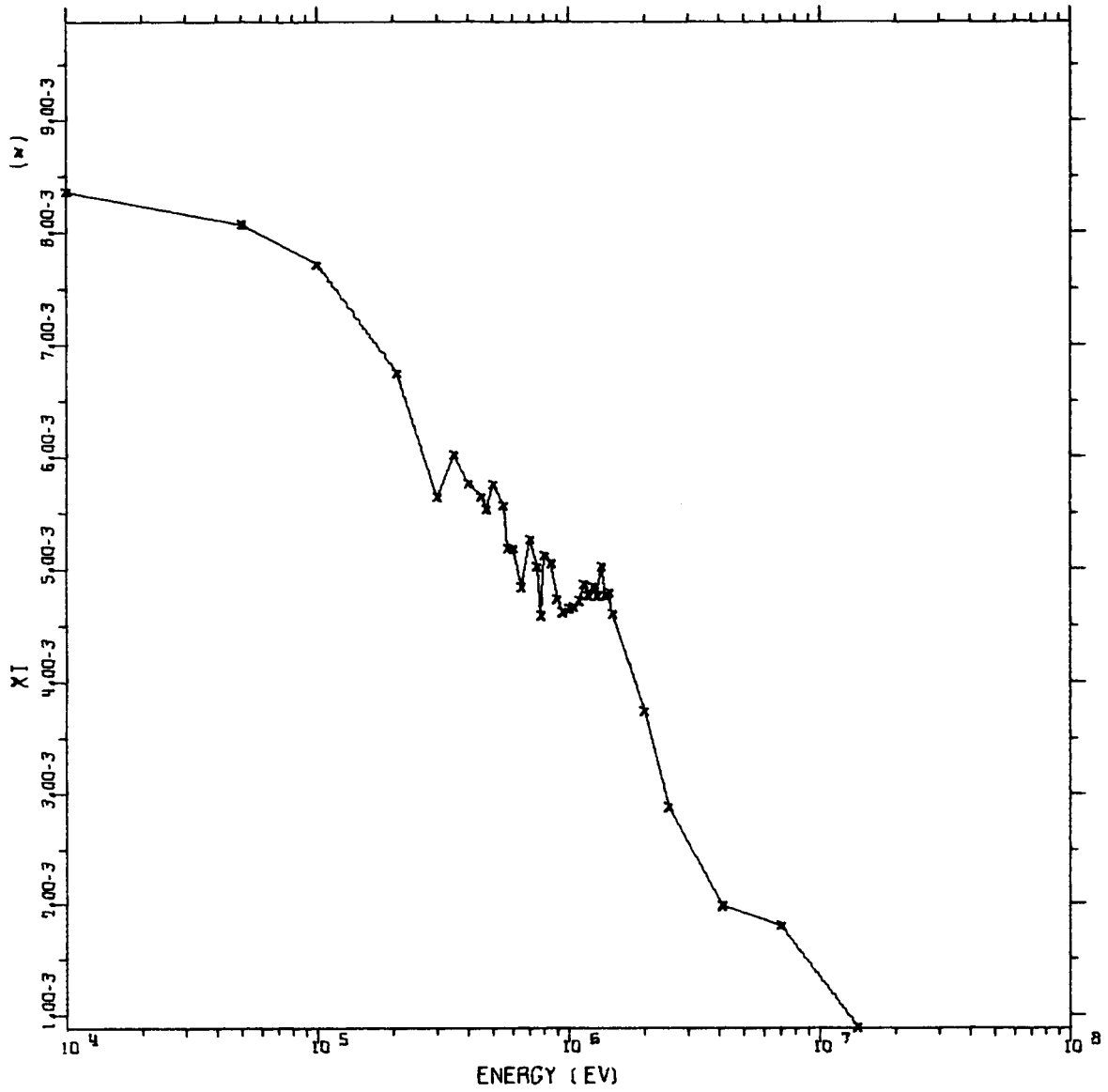
NEPTUNIUM 237 EVALUATED BY IDAHO NUCLEAR CORP NRTS



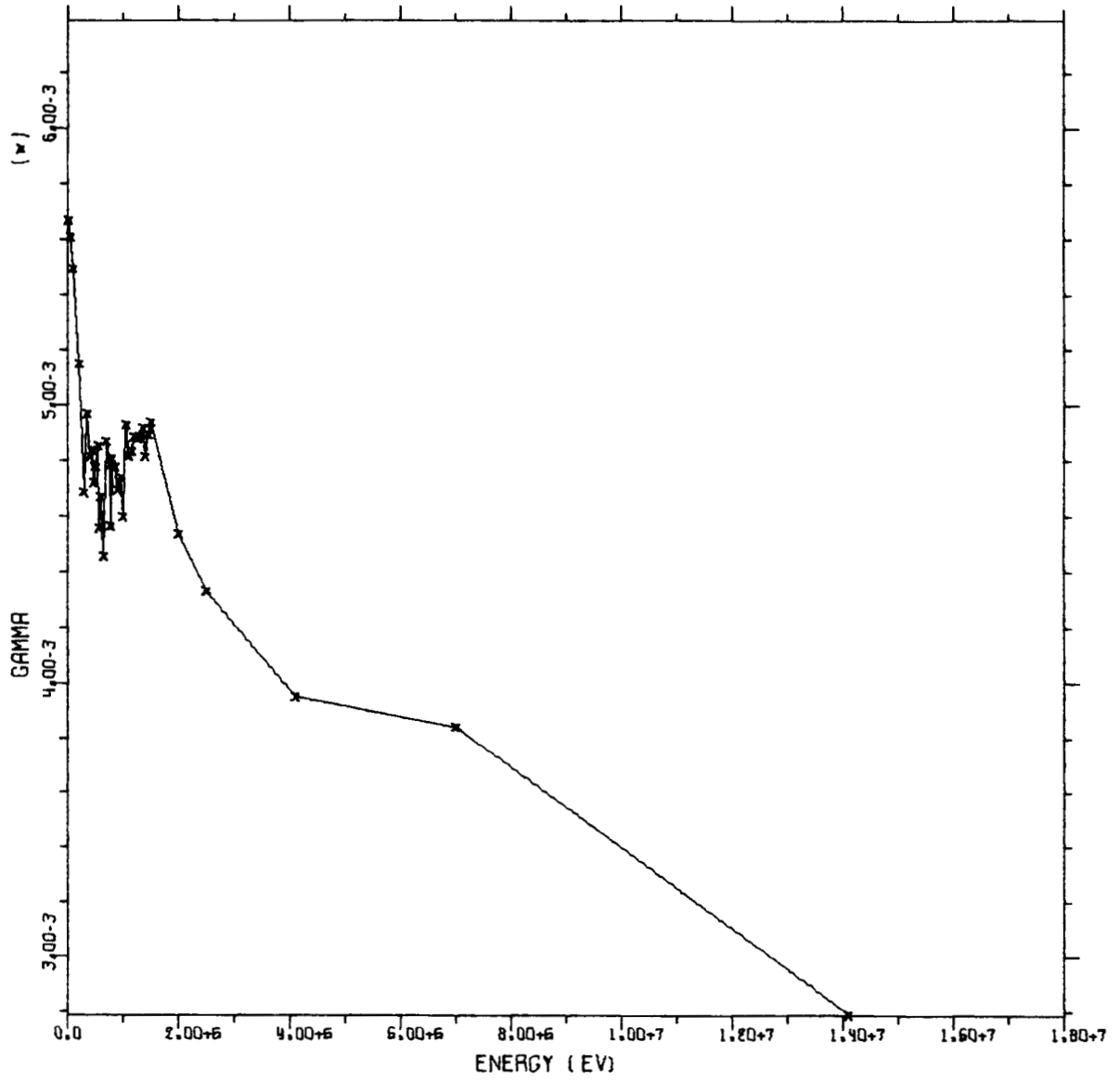
NEPTUNIUM 237 EVALUATED BY IDAHO NUCLEAR CORP NATS



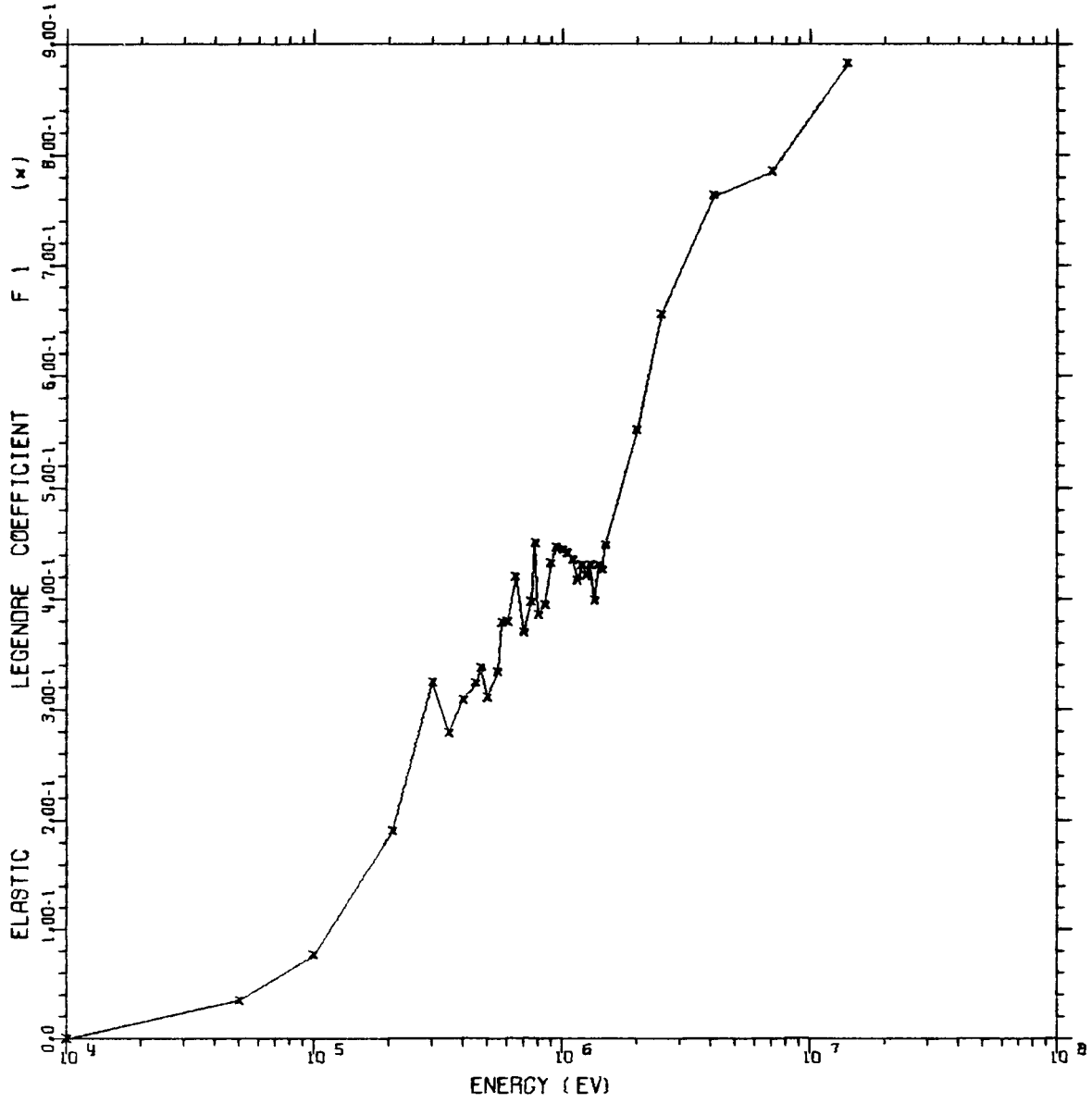
NEPTUNIUM 237 EVALUATED BY IDAHO NUCLEAR CORP NRTS



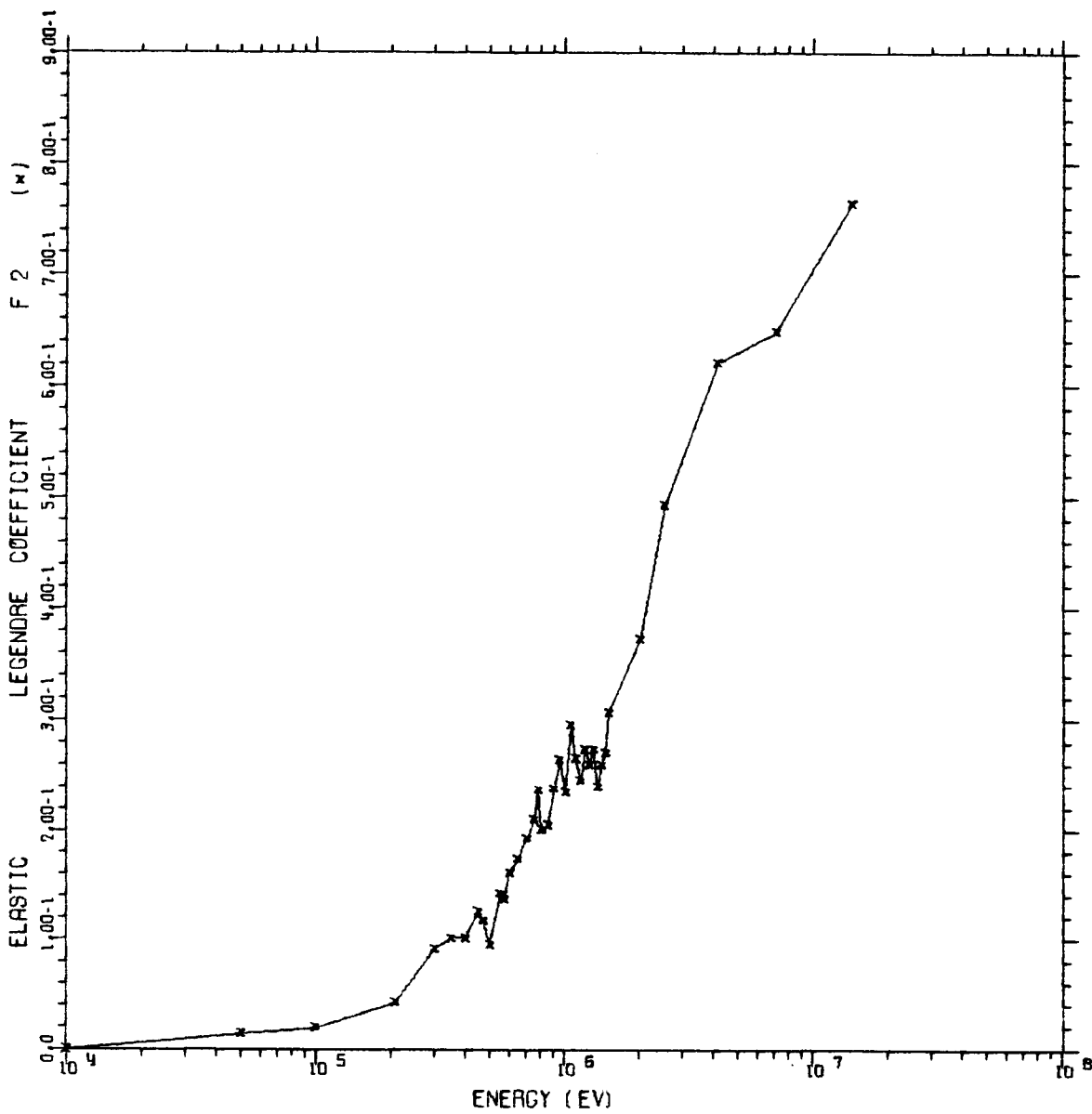
NEPTUNIUM 237 EVALUATED BY IDAHO NUCLEAR CORP NRS



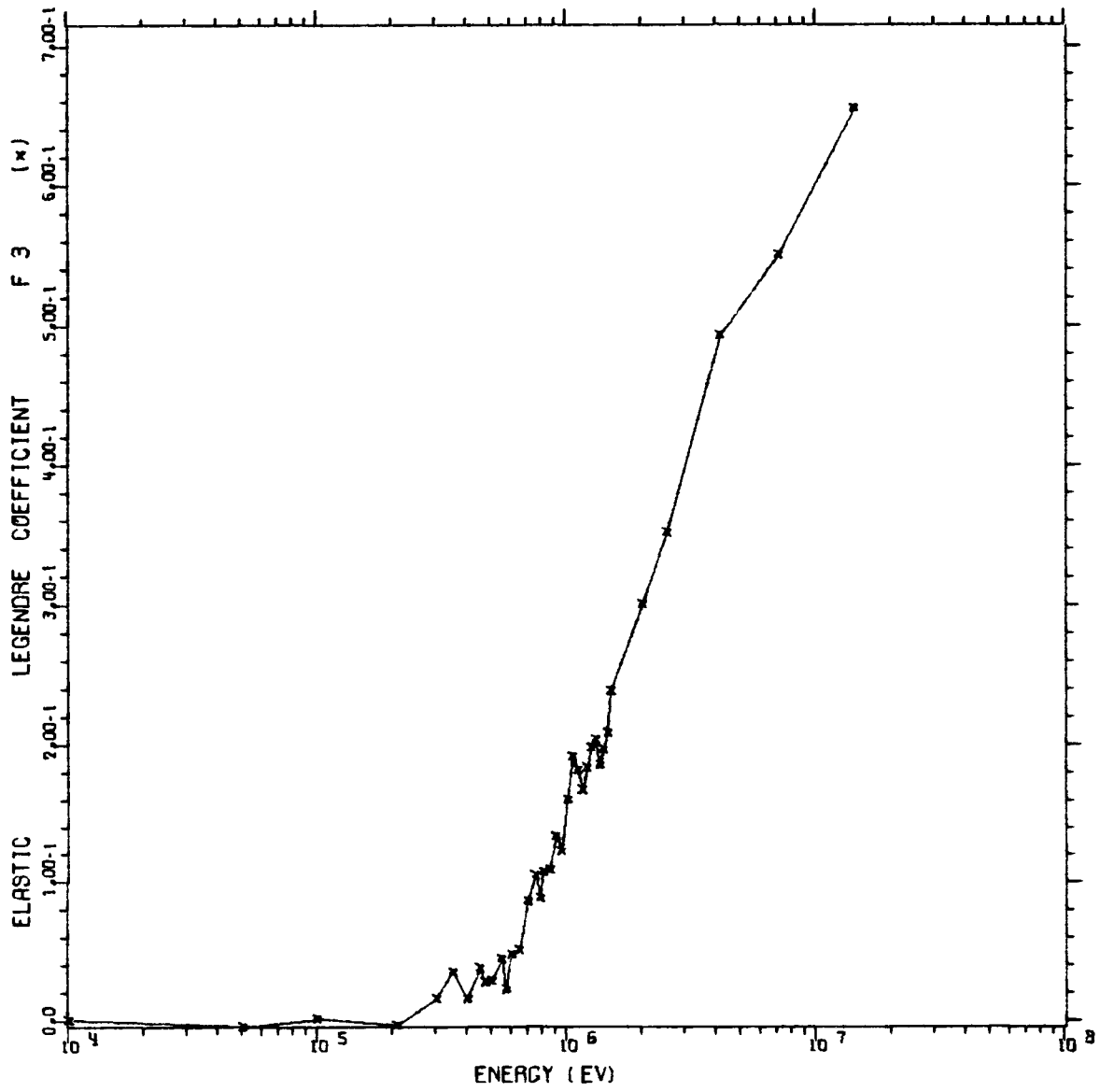
NEPTUNIUM 237 EVALUATED BY IDAHO NUCLEAR CORP NRTS



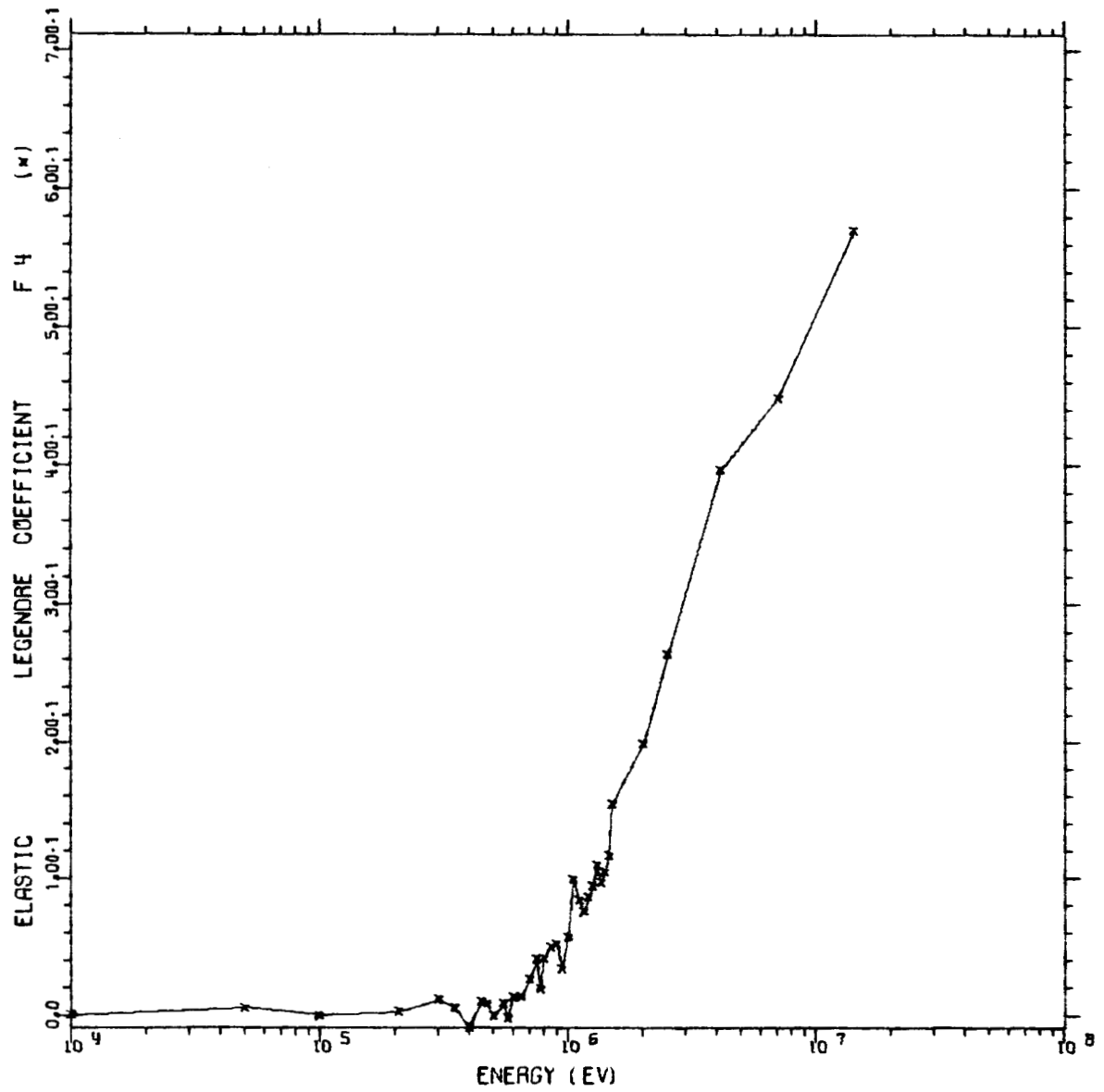
NEPTUNIUM 237 EVALUATED BY IDAHO NUCLEAR CORP NATS



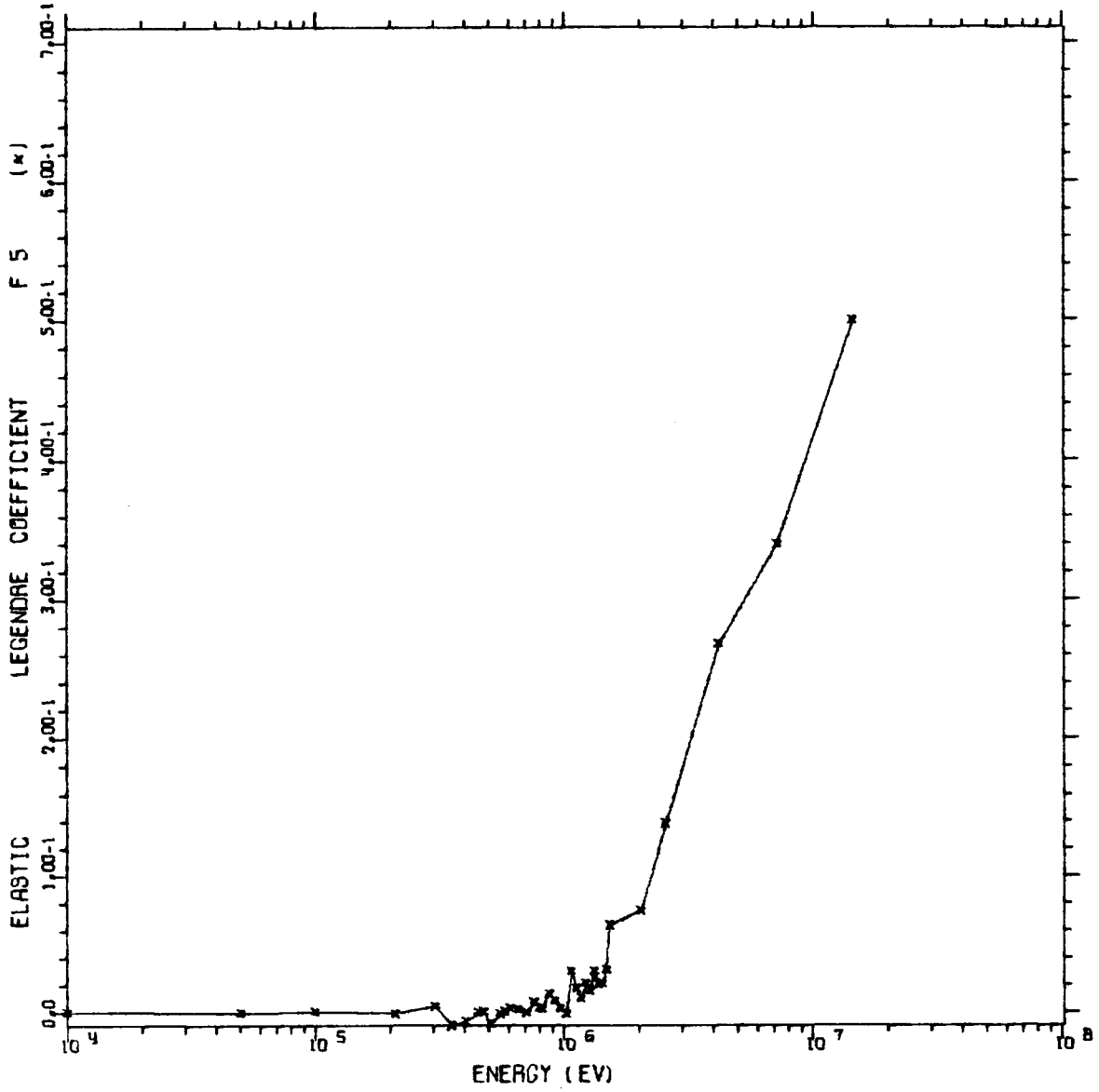
NEPTUNIUM 237 EVALUATED BY IDAHO NUCLEAR CORP NRS



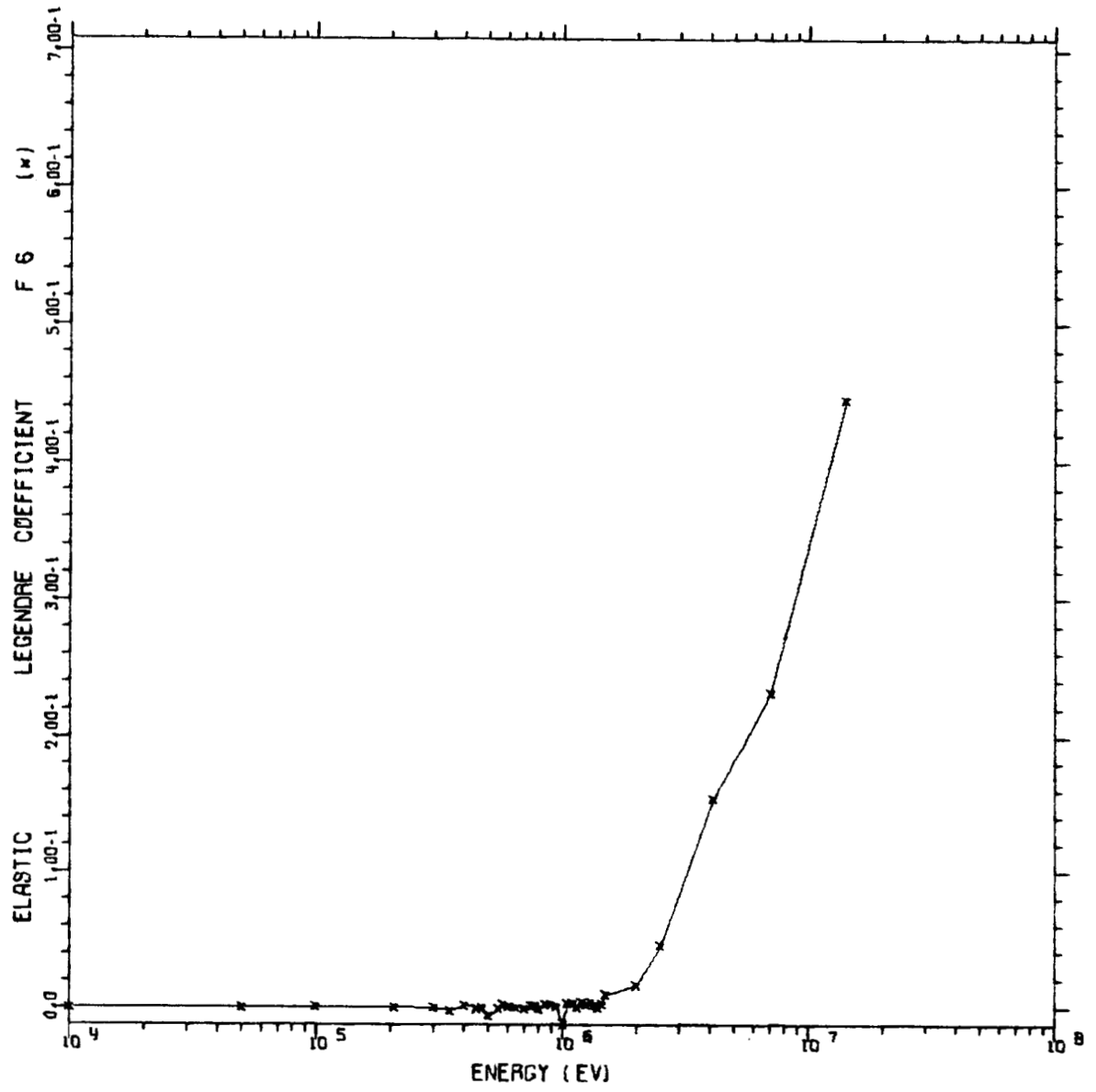
NEPTUNIUM 237 EVALUATED BY IDAHO NUCLEAR CORP NRTS



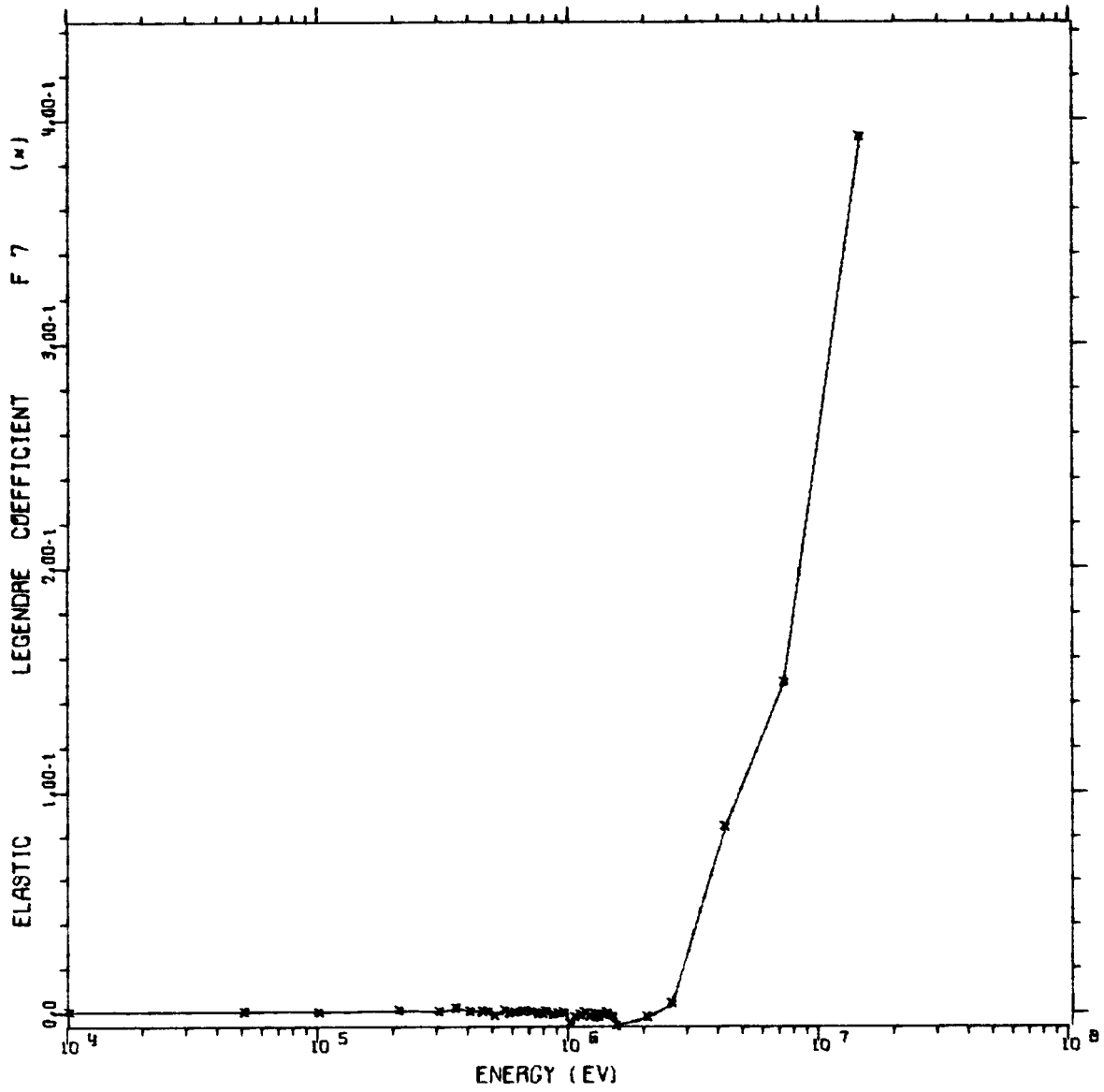
NEPTUNIUM 237 EVALUATED BY IDAHO NUCLEAR CORP NRTS



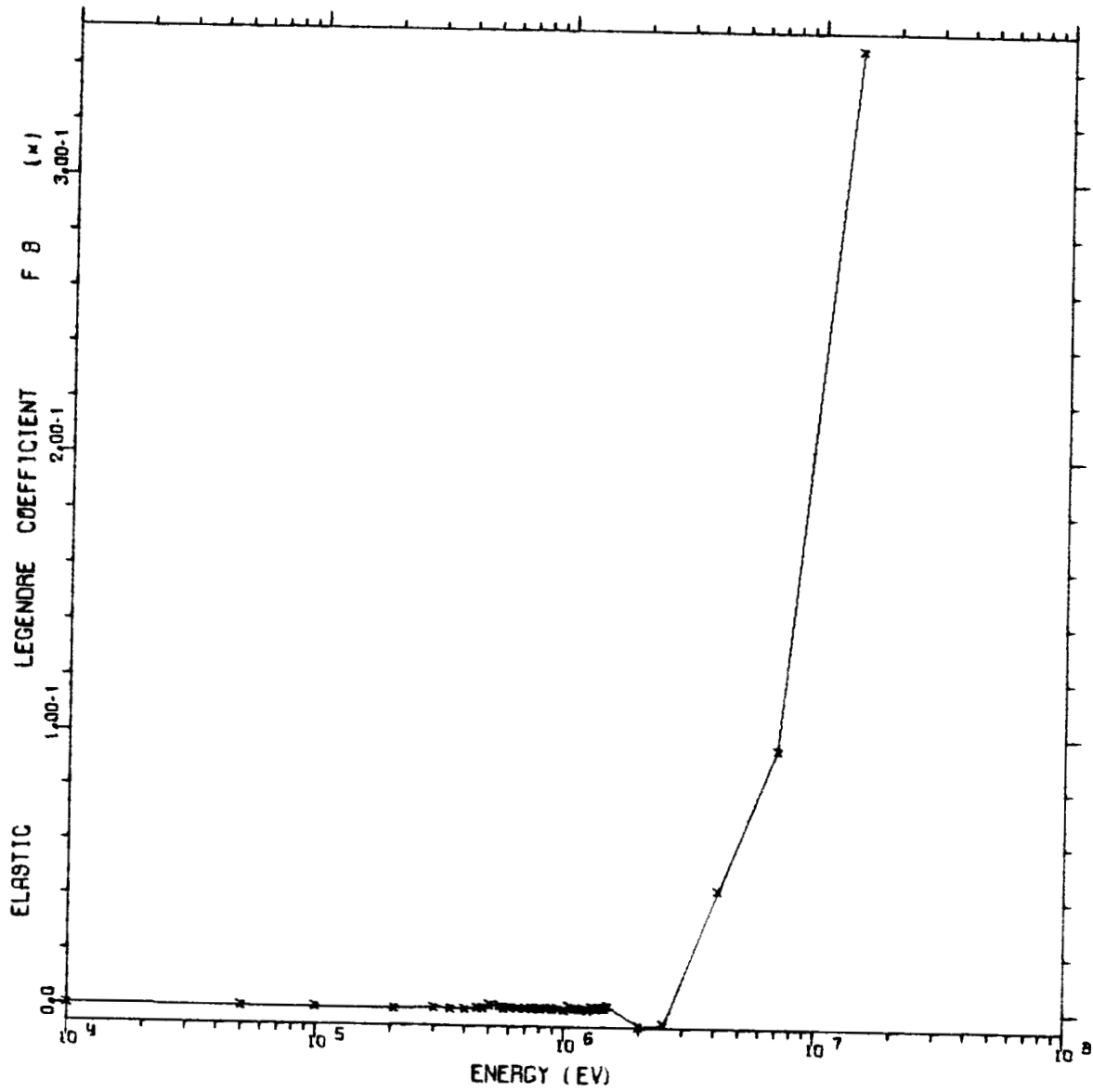
NEPTUNIUM 237 EVALUATED BY IDAHO NUCLEAR CORP NRTS



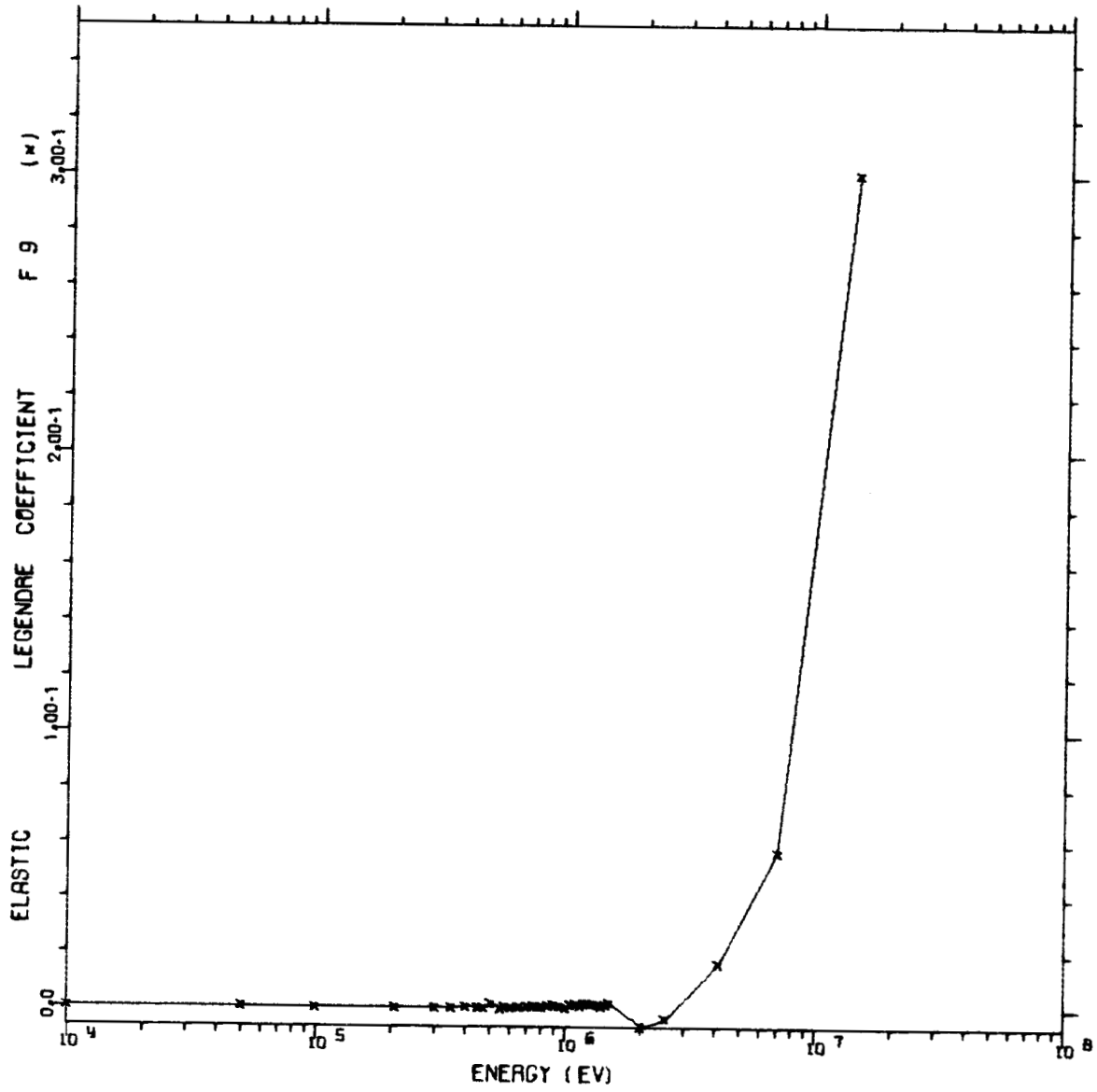
NEPTUNIUM 237 EVALUATED BY IDAHO NUCLEAR CORP NRTS



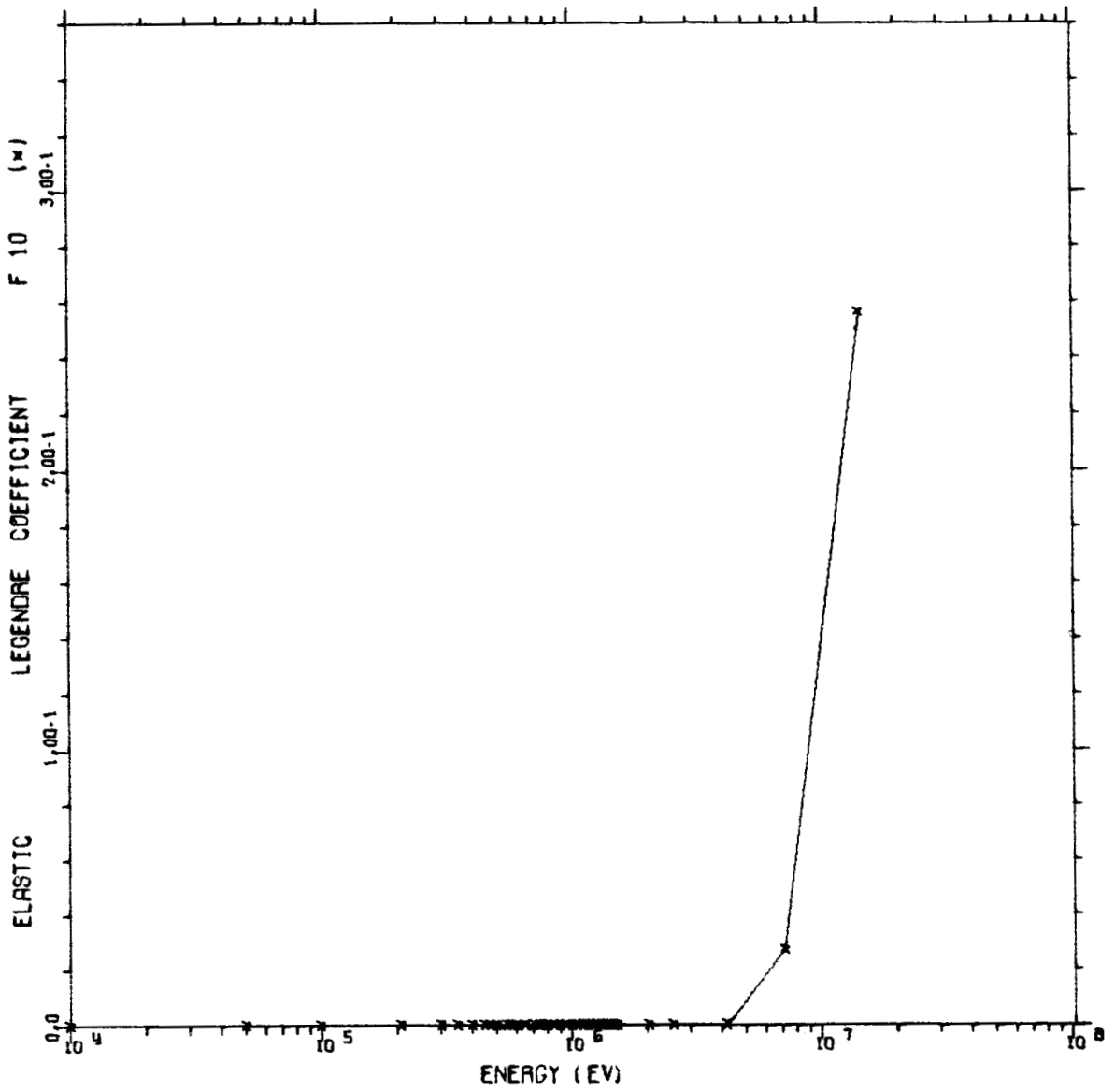
NEPTUNIUM 237 EVALUATED BY IDAHO NUCLEAR CORP NRTS



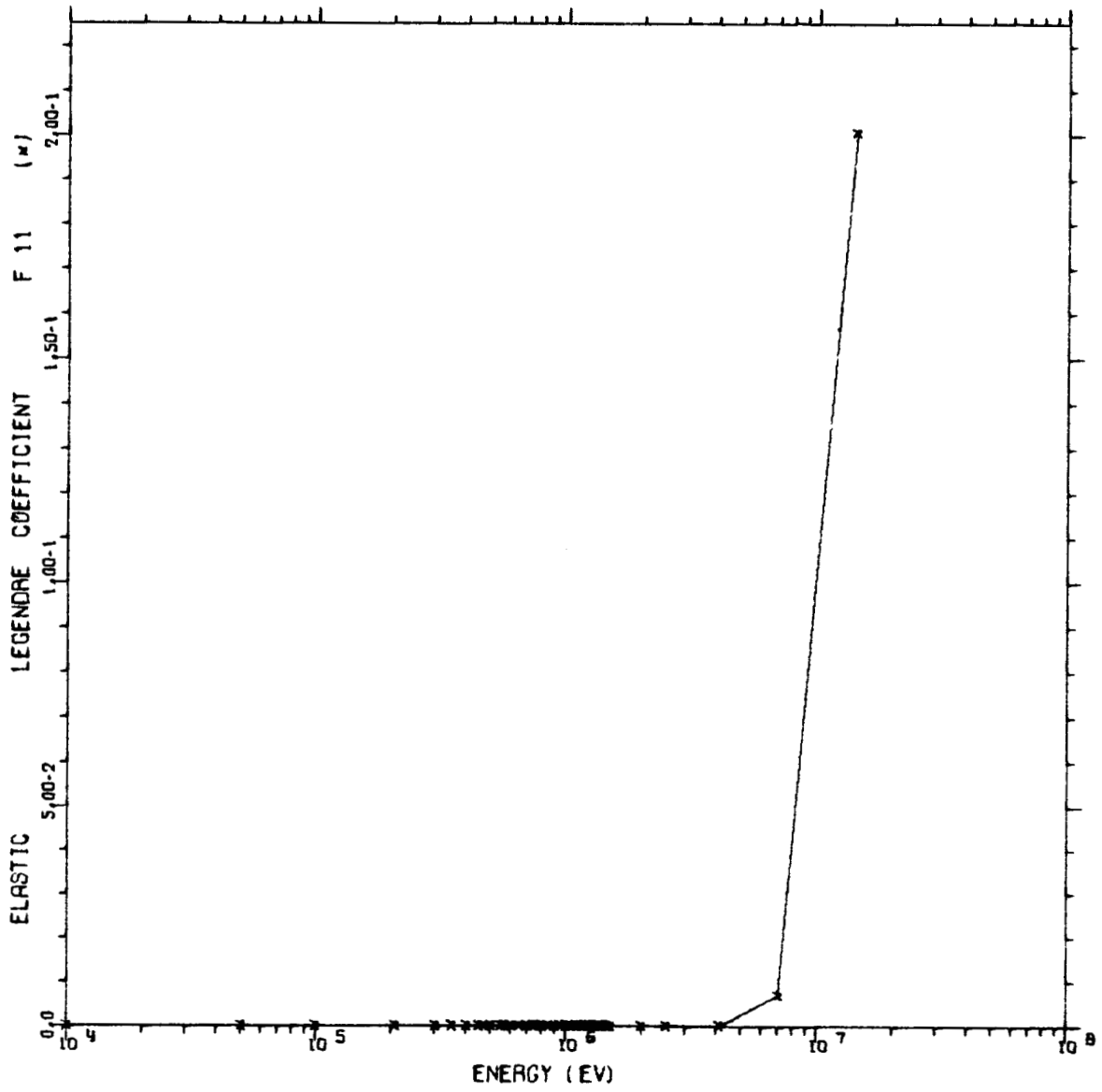
NEPTUNIUM 237 EVALUATED BY IDAHO NUCLEAR CORP NRTS



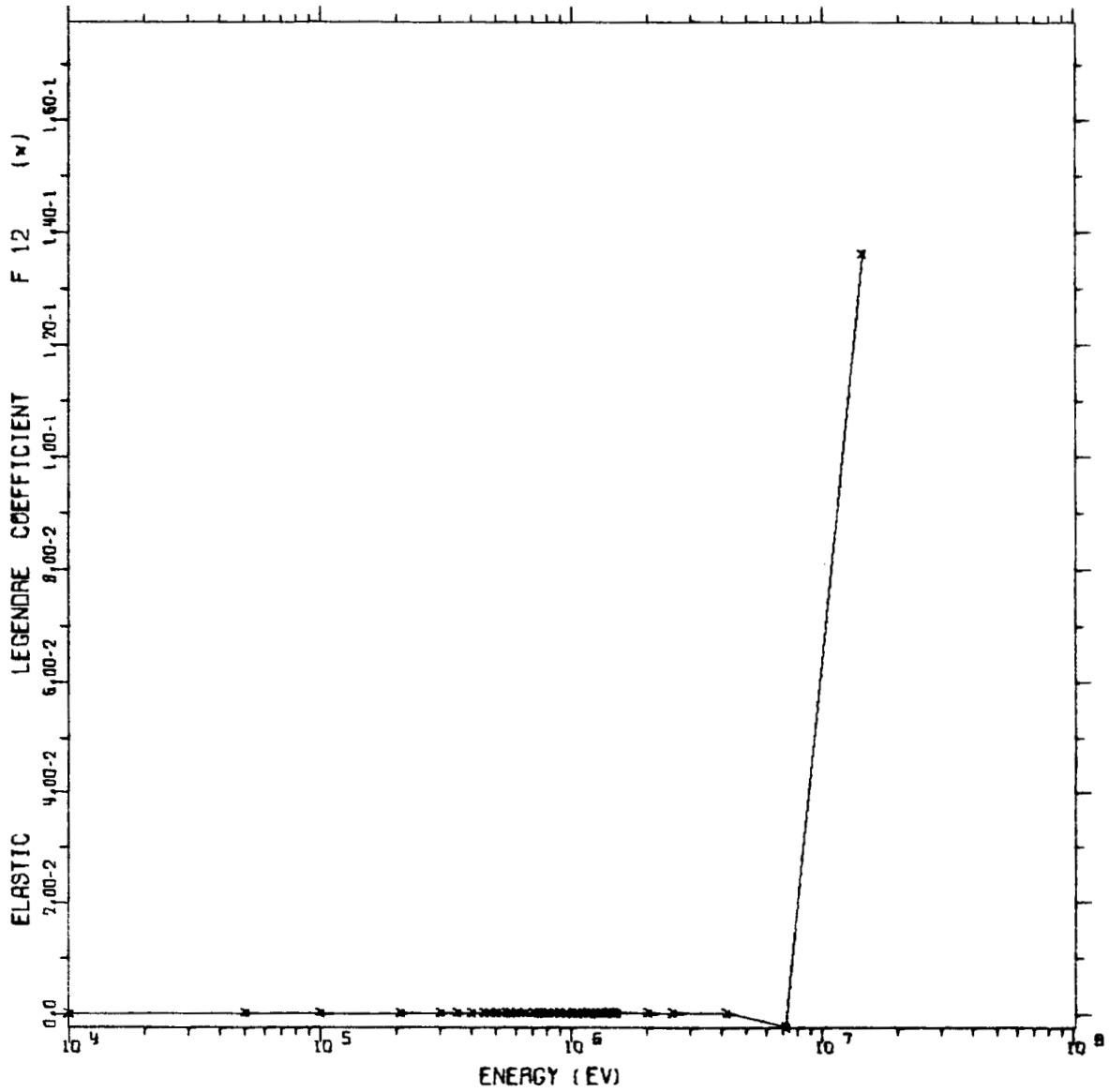
NEPTUNIUM 237 EVALUATED BY IDAMO NUCLEAR CORP NATS



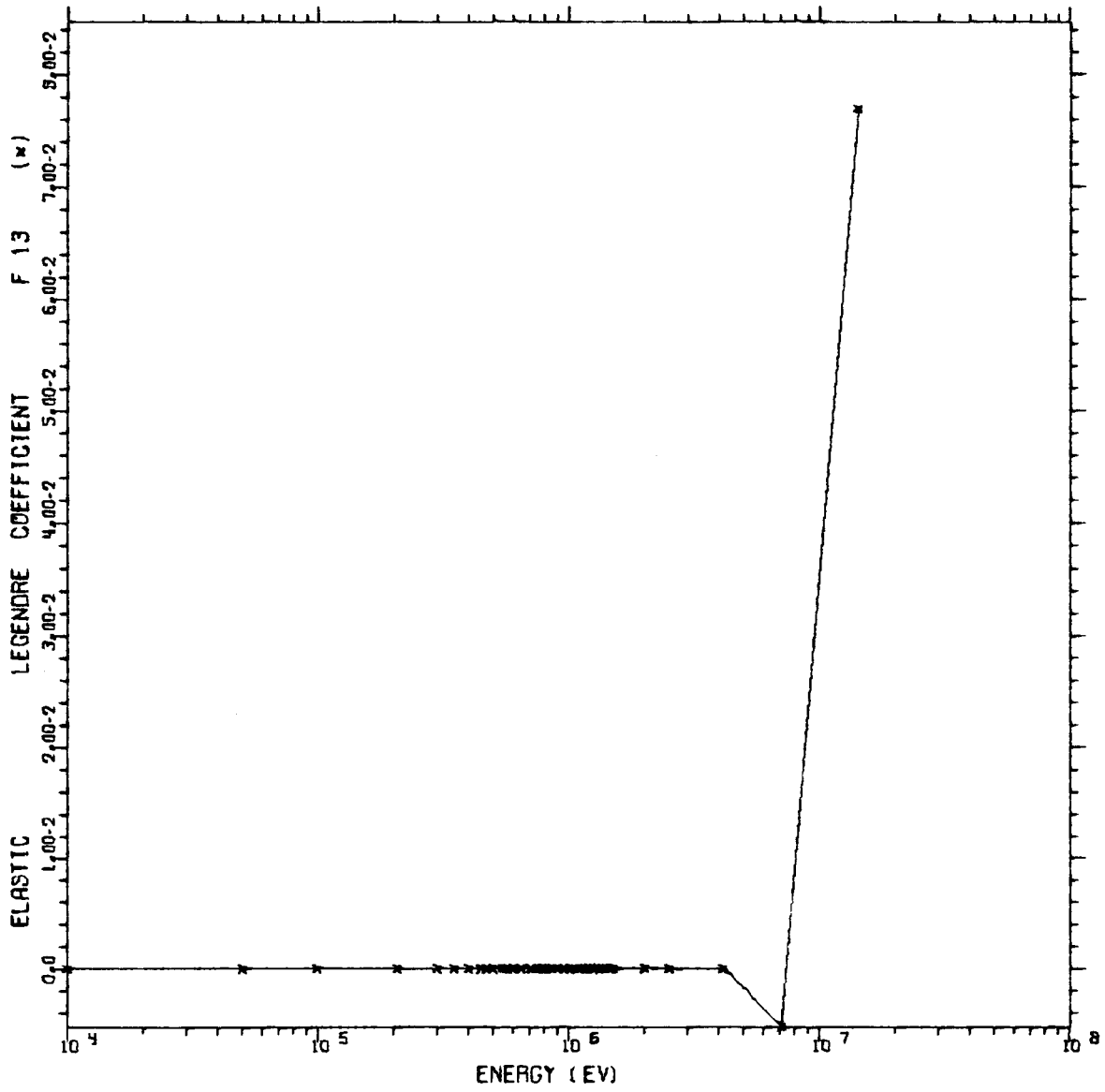
NEPTUNIUM 237 EVALUATED BY IDAHO NUCLEAR CORP NATS



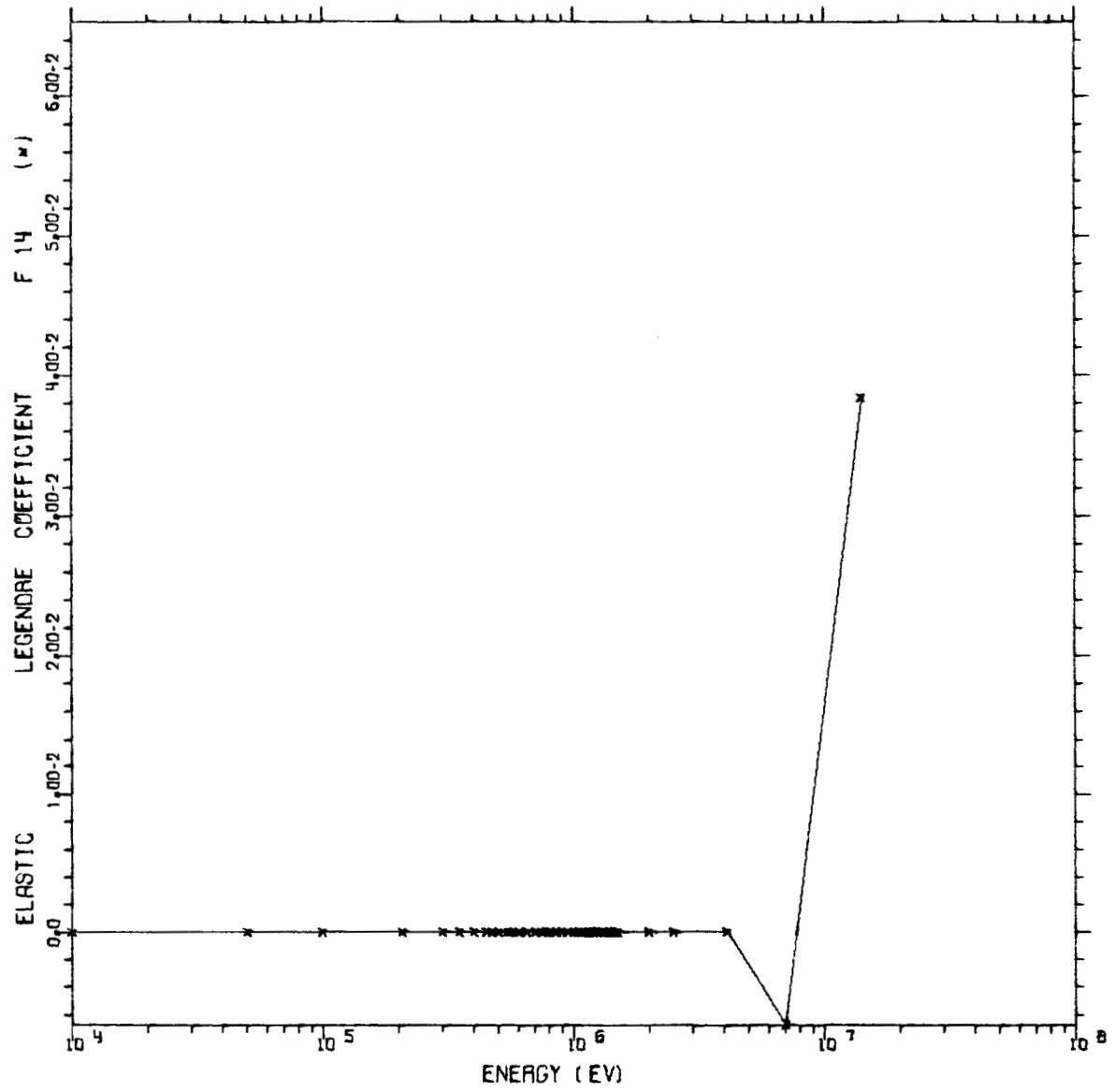
NEPTUNIUM 237 EVALUATED BY IDAHO NUCLEAR CORP NRTS



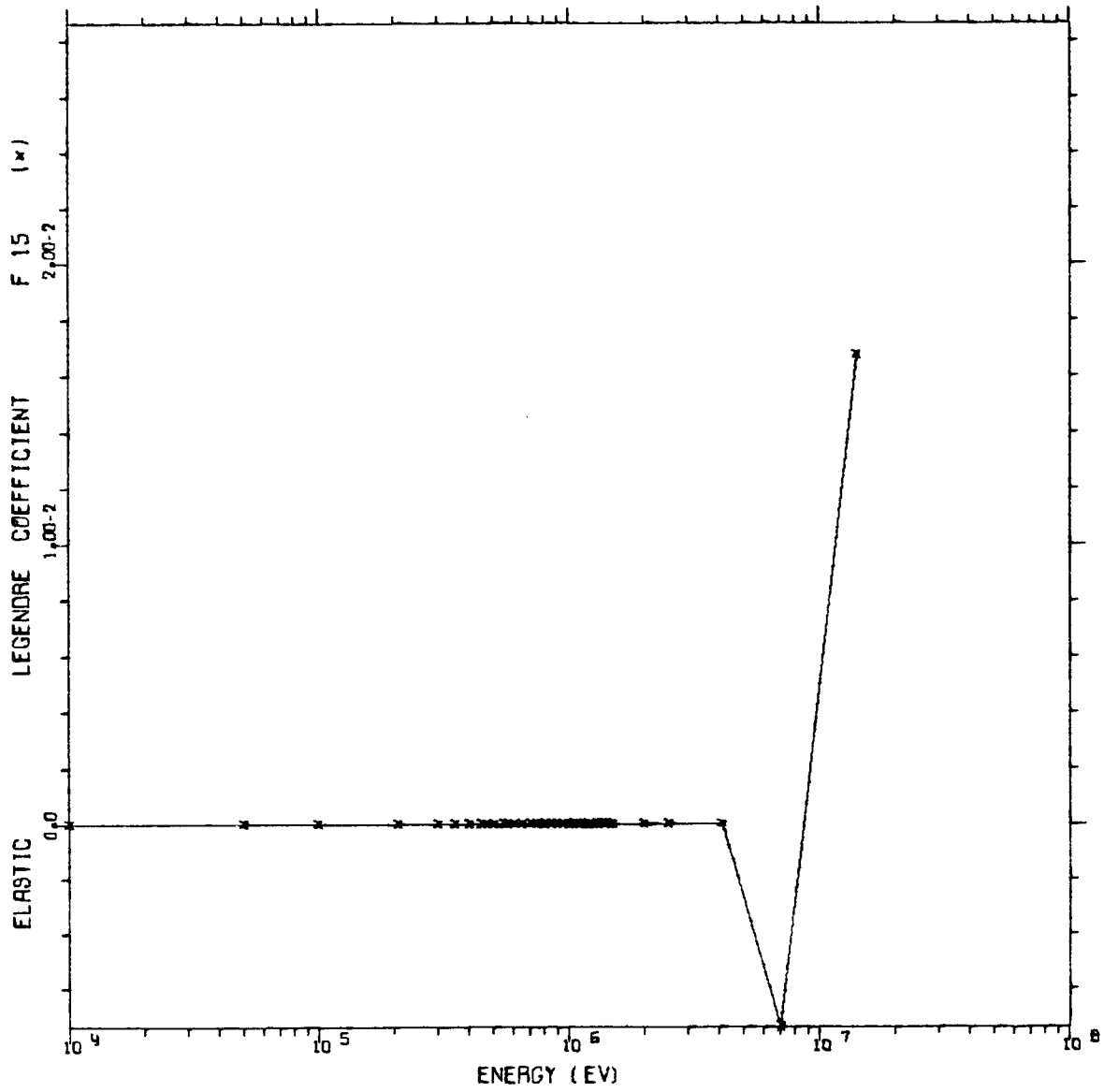
NEPTUNIUM 237 EVALUATED BY IDAHO NUCLEAR CORP NRTS



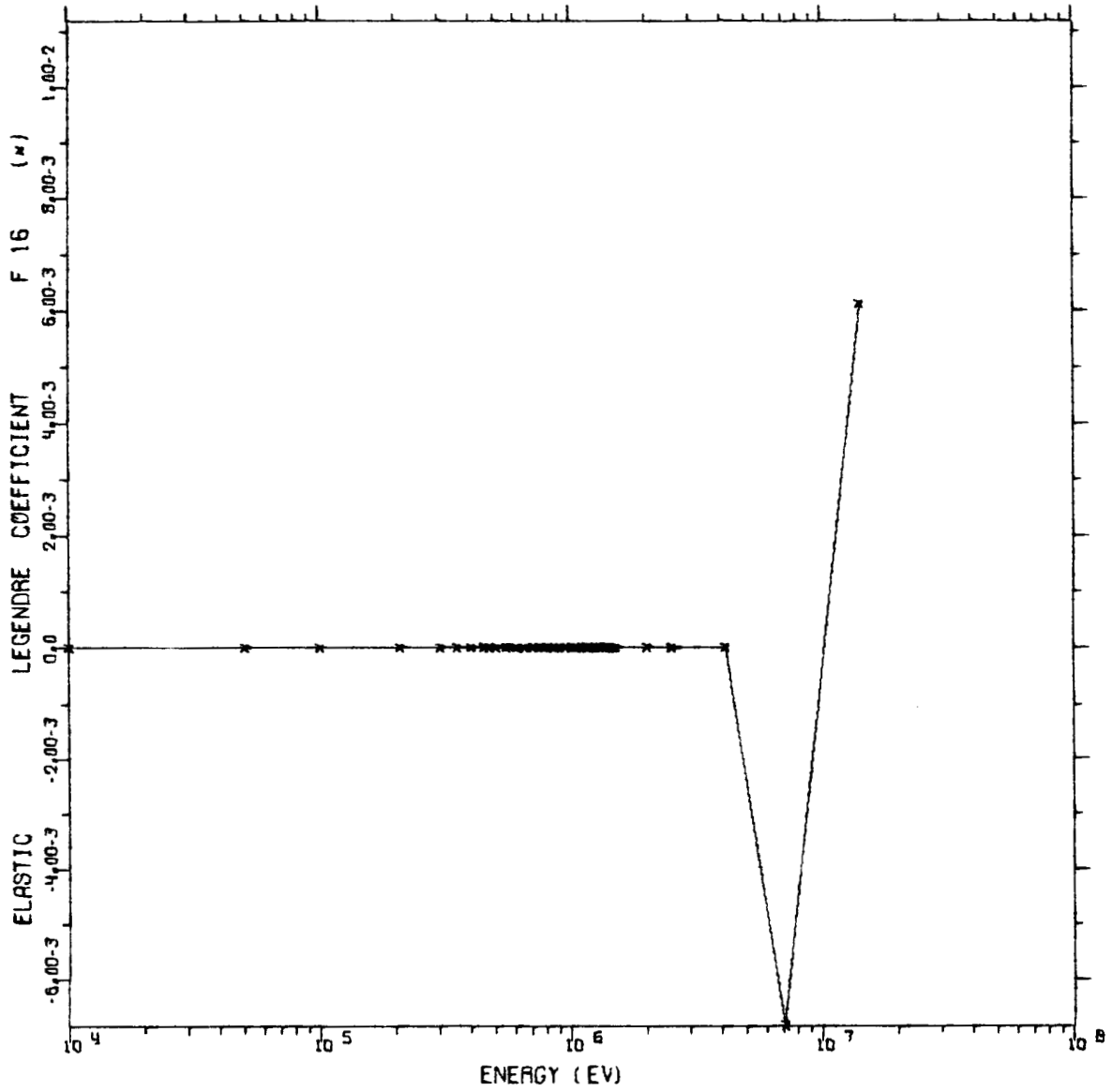
NEPTUNIUM 237 EVALUATED BY IDAHO NUCLEAR CORP NATS



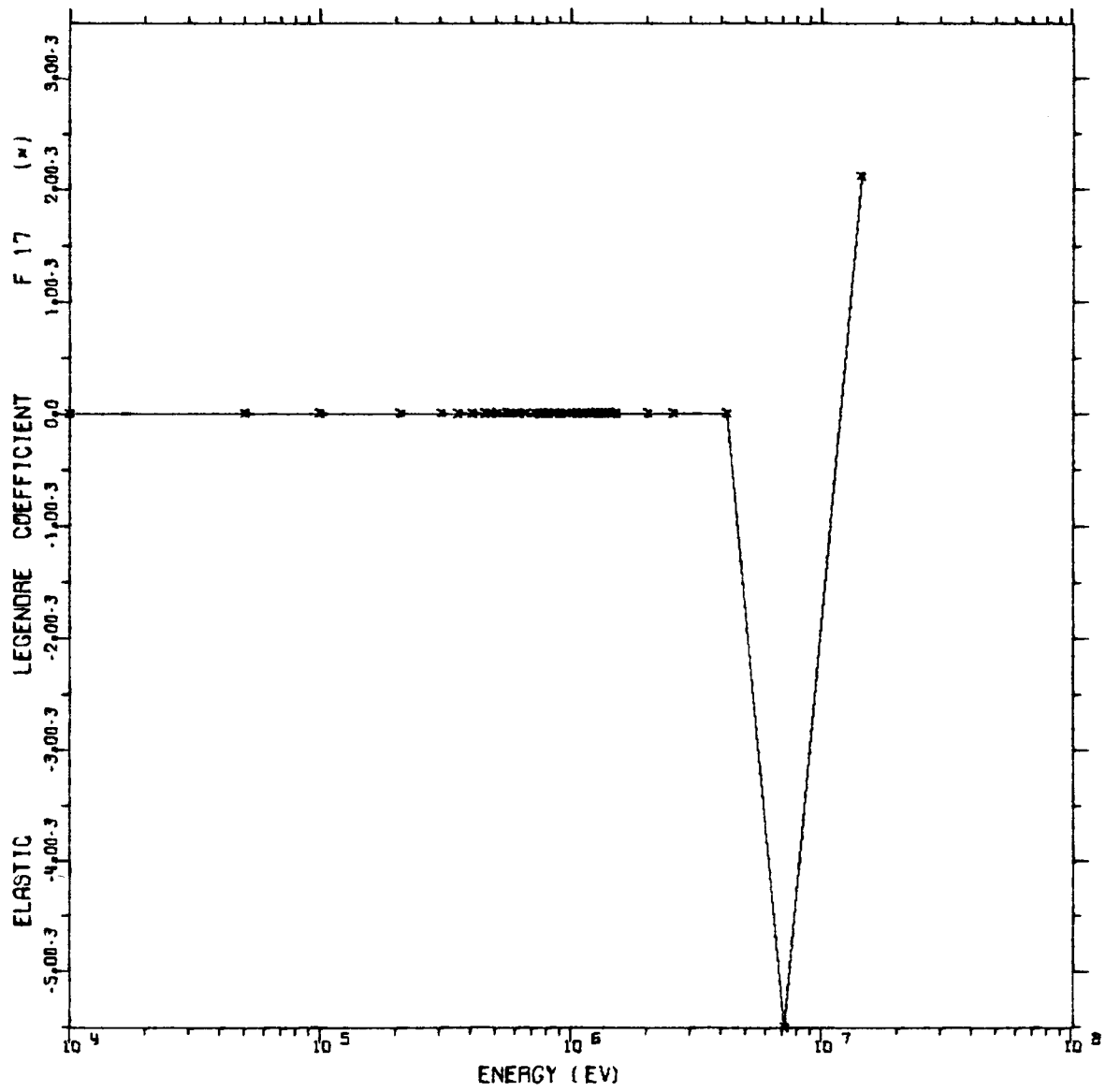
NEPTUNIUM 237 EVALUATED BY IDAHO NUCLEAR CORP NATS



NEPTUNIUM 237 EVALUATED BY IDAHO NUCLEAR CORP NATS

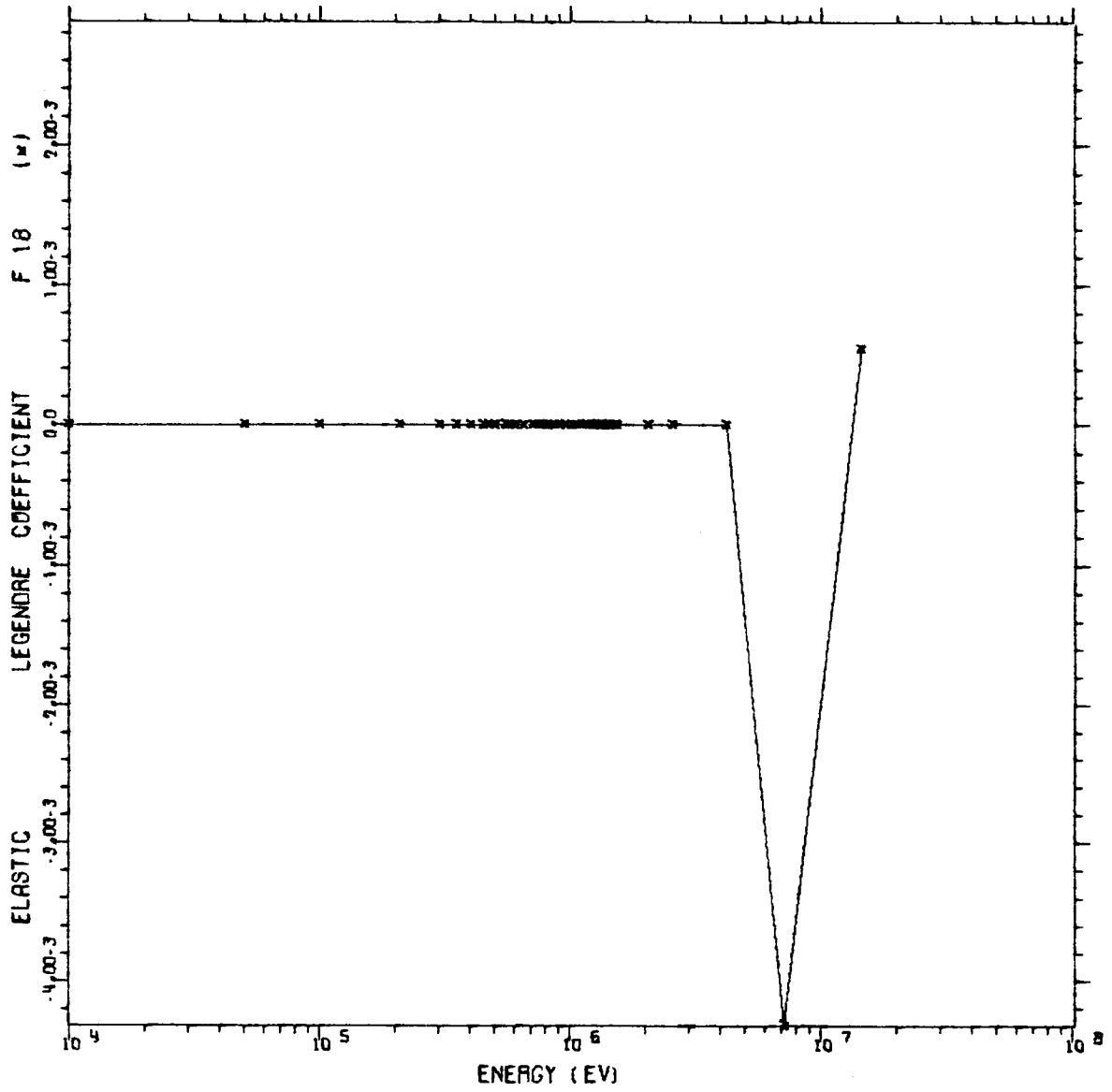


NEPTUNIUM 237 EVALUATED BY IDAHO NUCLEAR CORP NRTS

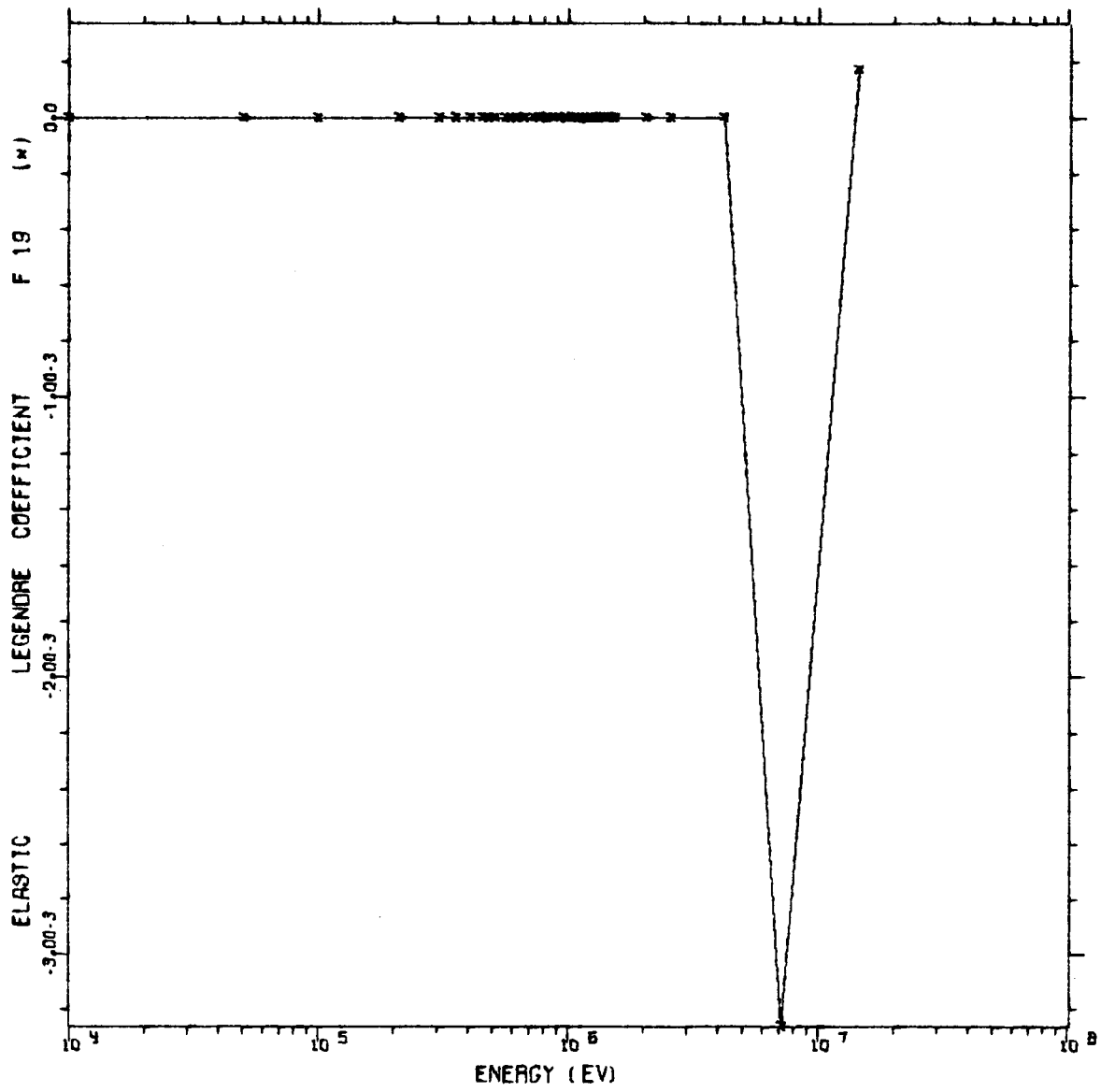


A-37

NEPTUNIUM 237 EVALUATED BY IDAHO NUCLEAR CORP NRS



NEPTUNIUM 237 EVALUATED BY IDAHO NUCLEAR CORP NRTS



NEPTUNIUM 237 EVALUATED BY IDAHO NUCLEAR CORP NRTS

